ISBN 978-82-326-3992-2 (printed version)
ISBN 978-82-326-3993-9 (electronic version)
ISSN 1503-8181

Doctoral thesis at NTNU, 2019:198

Daniela Myland

Experimental and Theoretical Investigations on the Ship Resistance in Level Ice

NTNU
Norwegian University of
Science and Technology
Faculty of Engineering
Department of MarineTechnology

NTNU
Norwegian University of
Science and Technology

Doctoral thesis at NTNU, 2019:198

NTNU

NTNU
Norwegian University of
Science and Technology

Daniela Myland

Experimental and Theoretical Investigations on the Ship Resistance in Level Ice

Thesis for the degree of Philosophiae Doctor

Hamburg, May 2019

Norwegian University of Science and Technology
Faculty of Engineering
Department of MarineTechnology

NTNU
Norwegian University of
Science and Technology

NTNU
Norwegian University of Science and Technology

Thesis for the degree of Philosophiae Doctor

Faculty of Engineering
Department of MarineTechnology

ISBN 978-82-326-3992-2 (printed version)
ISBN 978-82-326-3993-9 (electronic version)
ISSN 1503-8181

Doctoral thesis at NTNU, 2019:198

Printed by Skipnes Kommunikasjon as

To my family

This page is intentionally left blank.

Abstract

The growing interest in Arctic transportation and field logistics leads to an increasing demand for ships with good ice breaking performance. The ice breaking performance of ships is usually defined by their ability to proceed in uniform level ice, where good performance means low ice resistance, high propulsion efficiency and continuous ice breaking. In order to assess the ice breaking performance in an early design stage, several theoretical methods may be applied to predict the ice resistance. However, every theoretical method necessarily makes use of simplifications and assumptions what in turn affects its precision and its reliability. Due to the physical nature of model tests, all processes, and thus, all forces contributing to the ice resistance are considered. As a result, model tests are still the most reliable method to predict the total resistance in ice. But with regard to the high costs of model tests there is a continued demand to gain knowledge on the reliability of theoretical prediction methods and to improve their accuracy.

In the course of this thesis a systematic comparison of existing ice resistance prediction methods is carried out which represent the current state of the art. On this basis an assessment of the assumptions and simplifications of these different methods is outlined and the semi-empirical method of Lindqvist is found to be the most suitable method for further improvement.

In order to achieve a valuable improvement, model test results are used to update the empirical basis of the prediction method with respect to an ice breaking ship type, i.e. ice breaking offshore supply vessels, anchor handling tugs and rescue and salvage vessels. Furthermore, ice model tests are conducted with newly developed testing equipment and techniques as well as a newly developed post-processing procedure to gain new insight on the ice breaking process. Thus, assumptions made by Lindqvist can be verified or corrected with regard to the investigated ship type. In particular, the creation of ice floes in the bow area of the ship and the resulting bottom ice coverage is evaluated by application of an underwater image analysis methodology. Furthermore, the ice floe characteristics are correlated to hull shape parameters, ice properties and finally the ice resistance.

A refined version of Lindqvist's method is then subjected to a numerical optimization algorithm. Thereby, the newly gained insights and a current empirical data set comprising the investigated ship type of ice breaking offshore supply vessels, anchor handling tugs and rescue and salvage vessels are used.

During the optimization process, four variables are applied to the refined version of the semi-empirical prediction method of Lindqvist. By means of a computer algorithm these variables are optimized within specific boundary limits with regard to a minimization of the deviation to the total resistance in ice determined by model tests. Eventually, this process provides an optimized prediction method, with which the total resistance in ice can be predicted with a higher accuracy and reliability for the aforementioned ice breaking ship type.

This page is intentionally left blank.

Preface

This thesis is submitted to the Norwegian University of Science and Technology (NTNU) for partial fulfilment of the requirements for the degree of philosophiae doctor.

This thesis is based on work done at the Hamburg Ship Model Basin, HSVA, from 2013 to 2018. During the thesis process I was financed by the Norwegian University of Science and Technology, NTNU, by HSVA and by the German national funded research project ProEis (03SX391A). This financial help is gratefully acknowledged.

I wish to thank my supervisor Professor Sören Ehlers for his extensive support, his motivation and valuable discussions during the thesis process.

Thanks to Peter Jochmann and Nils Reimer, who provided the opportunity to carry out the present experimental and theoretical investigation as well as good working conditions at HSVA. I would also like to thank Quentin Hisette, whose support and help with daily problems is recognized.

I would like to thank the tank crew and the measurement engineers of the Artic Technology department at HSVA - Björn von Frieling, Nis Schnoor, Mohammed Toure, Roman Krywald, Mario Dalley, Roland Koch and Steve Gehrisch - for their helpfulness, their professional work within the experimental testing and the pleasant working atmosphere.

Special thanks to Dr. Petri Valanto for his interest in my research work, his helpfulness and valuable discussions.

I also want to express my gratitude to all reviewers of this paper-based thesis for their interest in my research work, their willingness for assessment and the resulting valuable comments and suggestions.

Finally, I am very grateful for the encouragement of my husband Johannes and his extensive support during the thesis process.

Hamburg, May 2019 Daniela Myland

This page is intentionally left blank.

Table of Contents

List of Figures

List of Tables

List of publications and author's contribution

This thesis comprises an introductory report and the following six publications:

[PI] Myland, D., Ehlers, S. (2014). Theoretical Investigation on Ice Resistance Prediction Methods for Ships in Level Ice. Proceedings of the 33rd International Conference on Ocean, Offshore and Arctic Engineering, OMAE 2014-23304, June 8-13, 2014, San Francisco, USA.
The author prepared the theoretical investigations on the ice breaking process, performed the analysis of the ice resistance prediction methods and wrote the manuscript.
Ehlers contributed with valuable comments and suggestions.

[PII] Myland D., Ehlers S. (2016). Influence of Bow Design on Ice Breaking Resistance. Journal of Ocean Engineering, 119 (2016), p. 217-232.
The author selected suitable ice model tests from HSVA's data base and prepared the review of Lindqvist's approach including the analysis of the number of cusps and the corresponding influence on the total resistance in ice. Furthermore, the author developed the subdivision of hull shapes into breaking pattern classes, evaluated the corresponding dependencies and wrote the manuscript. The refinement of Lindqvist's approach by means of consideration of hull shape parameters at four longitudinal sections has already been HSVA standard before. Its benefits have been verified for the investigated ship type by the author.
Ehlers contributed with valuable comments and suggestions.

[PIII] Myland D., Ehlers S. (2017). Methodology to Assess the Floe Size and Distribution Along a Ship Hull during Model Scale Ice Tests for a Self-Propelled Ship Sailing Ahead in Level Ice. Journal of Ships and Offshore Structures, 12:sup1, p.100-p.108.
The author developed the entire methodology including the concept of the underwater video carriage, preparation of the semi-automatic Matlab scripts and the size correction of tilted ice floes in the bow area. Furthermore, the author planned and coordinated an ice model test with application of the newly developed methodology as a case study and wrote the manuscript.
Ehlers contributed with valuable comments and suggestions.

[PIV] Myland D., Ehlers S. (2019). Model Scale Investigation of Aspects Influencing the Ice Resistance of Ships Sailing Ahead in Level Ice. Journal of Ship Technology Research, DOI: 10.1080/09377255.2019.1576390.
The author developed the principle of the instrumented skeg and the procedure for preparation of the pre-sawn ice. Furthermore, the author planned, coordinated and evaluated all ice model tests described in this publication including application of the underwater image analysis methodology and wrote the manuscript.
Ehlers contributed with valuable comments and suggestions.

[PV] Myland D., Ehlers S. (2019). Investigation on Semi-Empirical Coefficients and Exponents of a Resistance Prediction Method for Ships Sailing Ahead in Level Ice. Journal of Ships and Offshore Structures, DOI: 10.1080/17445302.2018.1564535.
Ehlers provided the basis for the PSO optimization algorithm and contributed with valuable comments and suggestions.
The author adapted the algorithm to the specific application comprising the definition of the design objective and the underlying method, the variables, the boundary values and the constraints. Furthermore, the author evaluated the results including cross-check cases and wrote the manuscript.

[PVI] Myland D. (2019). Experimental and Theoretical Investigations on the Characteristics of Ice Floes Broken by Ships Sailing Ahead in Level Ice. 38th International Conference on Ocean, Offshore and Arctic Engineering, OMAE 2019-95936, June 4-19, 2019, Glasgow, Scotland (final paper submitted).
The author is the only contributor to this paper.

Notations

Roman symbols

B	Ship breadth
E	Modulus of Elasticity
g	Gravitational acceleration
h_{ice}	Level ice thickness
L_{pp}	Ship length between perpendiculars
n	Number of broken cusps
R_B	Bending resistance
R_{Bi}	Bending resistance at i-th longitudinal section
R_{Br}	Breaking resistance
R_C	Crushing resistance
R_f	Frictional resistance
R_{ice}	Ice resistance in general
RIT	Total resistance in ice
R_p	Potential resistance
R_S	Submersion resistance
T	Ship draught
THDF	Thrust deduction fraction
v	Ship speed

Greek symbols

α	Waterline (entrance) angle
α_i	Average waterline angle at i-th longitudinal section
β	Flare angle
$\Delta\rho$	Density difference (between ice and water)
φ_i	Average buttock angle at i-th longitudinal section
ϕ	Stem angle

λ Scaling factor

μ Friction coefficient between ship hull and ice

σ_{flex} Flexural strength

ψ Normal angle – angle between normal vector to the bow plate and vertical vector

ψ_i Average normal angle at i-th longitudinal section

Abbreviations

BEM Boundary Element Method

CFD Computational Fluid Dynamics

FEM Finite Element Method

HD High Definition

HSVA Hamburgische Schiffbau-Versuchsanstalt, Hamburg Ship Model Basin

ITTC International Towing Tank Conference

PI to PVI Publication I to Publication VI

PSO Particle Swarm Optimization

R&D Research and Development

ROI Region of Interest

Definition of hull shape angles (Lindqvist 1989, adapted)

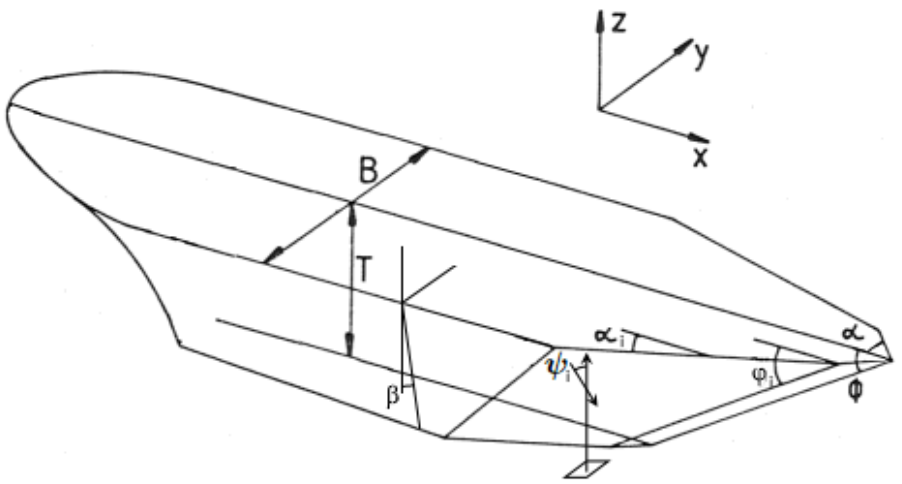

Original features

This thesis focuses on one presently common ice breaking ship type, namely ice breaking offshore supply vessels, anchor handling tugs and rescue and salvage vessels. The following features with respect to this ship type are believed to be original:

1. A systematic comparison of state of the art ice resistance prediction methods is carried out. All evaluated methods consider a different amount of ice properties and bow shape parameters to predict different ice resistance portions. Thereby, the method of Lindqvist considers the most parameters and resistance components. (PI and PII)
2. Model tests in pre-sawn ice reveal that the pre-sawn resistance comprising rotative, submersion and sliding forces for the investigated ship type at typical, i.e. significant forward speed values amounts to 40 to 70 percent of the total resistance in level ice. Thus, the breaking resistance amounts to 30 to 60 percent of the total resistance in level ice. (PIV)
3. Model tests with an instrumented forward skeg reveal that the resistance portion caused by the skeg is 7 to 11 percent of the total resistance in ice. (PIV)
4. To gain insight on the ice breaking process, on the ice floe characteristics and on the extent of the bottom ice coverage, an image acquisition and analysis procedure is developed using underwater video records of ice model tests. (PIII)
5. Application of the image acquisition and analysis procedure confirms findings of towed propulsion tests in ice: A bow breaking pattern consisting of smaller ice floes correlates to a higher total resistance in ice compared to a bow breaking pattern consisting of larger ice floes. (PII and PVI)
6. The results of the image acquisition and analysis procedure further reveal that
    a. ice of smaller thickness can be better cleared off the hull compared to ice of higher thickness. (PVI)
    b. the bottom ice coverage of the investigated ship type amounts to approximately 33 percent. (PIV)
7. A numerical approach is developed to adapt the ice resistance prediction method by Lindqvist to a different empirical data set of ice model tests by optimizing coefficients and exponents related to the influence of ice thickness and ship speed onto the total resistance in ice. (PV)

This page is intentionally left blank.

Part I – Main Report

This page is intentionally left blank.

1 Introduction

1.1 Background

The major requirement for ice breaking ships is a good performance in level ice (Valanto 2015). Good performance means low ice resistance, high propulsive efficiency and guaranteed continuity in ice breaking (Riska 2006a).

Breaking of level ice by a ship is a complex process consisting of several physical phenomena resulting in the ice resistance (Uemura et al. 1997). To simplify the problem, the resistance of a ship in level ice can be subdivided into sequential components in the time domain according to the creation and advance of ice floes caused by the ship hull proceeding through the ice sheet. The following force categories are the result of this subdivision: Breaking, rotary, submersion and sliding forces (Valanto 1989, Puntigliano 1995a, Kämäräinen 2007). In order to investigate the phenomena of the ice breaking process, one ice breaking cycle can be considered as follows (Poznyak and Ionov 1981, Valanto 1989):

- The ice breaking process starts when the ship bow comes into contact with the intact ice sheet.
- With an increase in contact force small ice pieces are extruded from the contact zone. This crushing process continues until the normal and tangential force components are sufficient to induce bending failure of the ice further away from the contact zone.
- The bending ice failure leads to generation of half-moon shaped ice pieces, called cusps.
- Due to the forward motion of the ship the broken ice floes are forced to rotate until they are tangential to the ship's hull surface. The turning process ends when the top surface of the floe is pressed abruptly against the ship hull.
- The forward motion of the ship pushes the broken ice downwards and sideways. The ice floes are submerged along the ship hull to a certain depth as a result of the continuous forming of new ice floes at the waterline, which displace the adjacent ones. Thereby, breaking of ice floes into smaller pieces can take place.
- After the sliding phase the ice floes move laterally either to the sides beneath the intact ice sheet or into the open channel in the wake of the ship. Interaction of the ice with the propeller(s) or other appendages may occur.

In practical ship design, empirical or semi-empirical formulas are used to approximate the resistance in the early design stage. After one or more promising designs have been

developed, a numerical resistance prediction method based on CFD or other advanced numerical methods, such as FEM or BEM may be used (Kaminski and Rigo 2018). But up to now the available numerical methods for ice resistance prediction are not complete enough to give a valuable contribution to the design process. Thus, in a later design stage model tests have to be used to evaluate one or few specific designs (Valanto 2015).

The analytical methods, which often form the basis for general hull design decisions in the early design stage, necessarily make use of simplifying assumptions. Furthermore, coefficients and exponents are often based on empirical knowledge and thus, on a selection of model test or full scale data. Thereby, each analytical method focuses on the ship type and usual dimensions which are common at the time, when the method is developed (Lindqvist 1989, Keinonen 1991 and 1996). Over the time, the common ice breaking ship type may change and so do the usual dimensions and hull shapes. As a consequence, the empirical basis for analytical resistance prediction methods and the resulting coefficients as well as exponents may lose their validity.

In order to save costs and time during the design process it is of great advantage to be able to evaluate the ice breaking resistance of a vessel in an early design stage as precisely as possible. Thus, the availability of an engineering tool for the prediction of the total resistance in level ice in the early design stage is of general interest.

1.2 State of the art

1.2.1 Level ice resistance prediction methods for ice breaking in continuous mode

Runeberg proposed the first formula for predicting the ice resistance of a ship sailing in level ice in 1888/89 (Runeberg 1888/89). The formula was related to ice breaking ships operating in the Baltic Sea in continuous movement. Runeberg included mean angles of the bow shape and thus, considered that the entire waterline in the bow region influences the breaking process. Similar to Runeberg Shimansky (1939) presented a semi-empirical method for predicting the ice breaking resistance based on the assumption that the forces induced by the entire bow dominate the ice breaking process. Therefore, he further investigated the effect of the bow geometry on the ice resistance.

Other early works (Kari 1921, Simonson 1936, White 1970, Crago et al. 1971) which are also limited to the breaking component induced by the bow are based on the assumption that the ice is broken by the stem only. Tarshis (1959) included the sides of the vessel in addition to the stem.

In 1956 Jansson (1956) proposed a very simple formula in which the ice resistance is divided into a speed and a breaking component. The latter one is mainly a function of ice thickness and the ship breadth at the waterline. For solving the formula two empirical coefficients are used. Similar approaches comprising a speed and a breaking component are used by Segal and Levit (1972), Maksutov (1973) and Segal (1982).

The next milestone in theoretical ice resistance prediction was reached by Kashtelyan et al. (1968). They established an ice resistance prediction method based on four components which are the resistance due to ice breaking, the resistance due to submersion, the speed related resistance as well as the resistance due to open water. The formula was developed from model tests and full scale ice trials. Kashtelyan et al. took into account the ice strength, the ship breadth as well as other form parameters, the ice thickness, the ship speed and the friction between ice and hull. Thereafter, a number of further ice resistance prediction methods were published following the same subdivision of resistance contributions (Elisejev 1968, Lewis and Edwards 1970, Lewis et al. 1982, Vance 1980, Poznyak and Ionov 1981, Zahn and Phillips 1987, Cho and Lee 2015).

In the 1970s and 1980s a lot of shipping activities took place in the Arctic Sea. Thereby, new hull forms for ice breaking ships were introduced and numerous researchers started to analyze the problem of ice resistance on the basis of model tests, analytical and numerical methods as well as full scale ice trails (Jones 2004, Valanto 2015, Kämäräinen 1993).

Enkvist (1972) presented a semi-empirical formula comprising a component for ice breaking, a component for ice floe turning and a component for the submersion of the broken ice floes. The increase of resistance with increasing speed was mainly included in the turning component. By conduction of model tests at small and at normal speed, he was able to separate the speed related term. The submersion component was derived from pre-sawn ice tests. Later the approaches of Naegle (1980), Luk (1986 and 1988), Kotras et al. (1983), Lindström (1990), Kämäräinen (1993) and Jeong et al. (2010) were based on mainly the same subdivision. Contrary to Enkvist, some of them assumed that the speed-dependent component has to be related to the mass forces.

Milano (1973) introduced the first attempt for an entire physical model by summarizing the energy loss due to ship motion in level ice. He described the individual energy-based components by usage of analytical expressions and analyzed the influence of ice and ship parameters on his method (Milano 1975, 1980, 1982). Another energy-based approach was proposed by Carter (1983) who did not consider inertia and buoyancy forces within his approach.

One of the most established semi-empirical ice resistance prediction methods was published in 1989 by Lindqvist (1989). Similar to other methods which are based on the principle of superposition, Lindqvist divided the ice resistance into components, i.e.

breaking and submersion components. He described the effects of these components by simple, but physically sound formulas and further divided the breaking component into a crushing and a bending term. The two main components are supplemented by empirical based speed terms.

The theoretical method of Spencer (1992) and Spencer and Jones (2001) comprises four resistance components similar to Kashtelyan et al (1968), but the components are defined as follows: resistance due to open water, resistance due to ice breaking, resistance due to ice buoyancy and resistance due to ice clearing. Thus, the method presented by Spencer is also inspired by Enkvist (1972). Cho et al. 2014 and 2015 reviewed and refined the formula of Spencer and Jones (2001) by usage of model test and full scale data. The aim was to address the need for a better prediction method for large commercial ice breaking vessels.

Riska et al. (1997) developed a simple ice resistance formula based on the approaches of Ionov (1988), Lindqvist (1989) and Kämäräinen (1993) and validated it with full scale data of ten ships. Riska et al. divided the ice resistance into a speed-dependent and a speed-independent term. They considered only very few parameters in their formula, which are the stem angle and the ice thickness. Further ice parameters are kept constant.

Keinonen (1991, 1996) carried out one of the most comprehensive studies of ship resistance up to date. For development of his formula he analyzed full scale data as well as operators' interviews of 18 ice breakers. Keinonen's formulation comprises three components: the resistance due to open water, the resistance at a speed of 1 m/s and the resistance at speeds higher than 1 m/s. The latter component can be considered as a speed-dependent term.

Jeong (2017) proposed a method based on the approach of Lindqvist (1989) and Milano (1973). In the course of his approach the crushing and bending forces during ship-ice interaction are determined by a concept of energy consideration and the forces due to submersion of the ice floes are calculated according to the Lindqvist (1989) approach.

Most of the presented ice resistance prediction formulas assume that the ice resistance can be subdivided into components. The mathematical expressions of these components are based on further assumptions and their dependencies on environmental parameters are often determined with regression analyses. The advantage of the component-based approach is that it gives a possibility to limit the effects of single parameters to individual components. Thereby, the regression analysis for determination of the coefficients of the components is simplified (Valanto 2015).

However, since the effects of speed cannot be separated from breaking the intact ice sheet and submersion of the ice floes afterwards, Valanto emphasized the need to get insight on

all physical phenomena involved for a ship that sails in continuous mode in level ice (Valanto 1989). Consequently, he started to investigate the consecutive phases of the ice breaking process separately in the time domain. Based on the new gained knowledge by execution of systematic ice model tests, Valanto (2001) developed a 3D numerical model of the ice breaking process at the waterline. He combined his numerical model with the formula of the submersion component according to Lindqvist (1989) resulting in a newly semi-numerical ice resistance prediction method.

Due to the major advances made in computer technology, the number of proposed numerical methods noticeably increased within the last decades. Efforts have been made to review or to further enhance available prediction methods or to propose new approaches and to implement them in numerical models such as Lindström (1990), Puntigliano (1995a and 2003), Kämäräinen (2007), Su (2011), Sawamura (2012), Tan et al. (2013), Zhou and Peng (2014), Zhou et al. (2016). As the focus of this thesis lies on a semi-empirical method only three numerical ice resistance prediction methods are described briefly in the following for the reason of completeness:

Lindström (1990) presented a numerical estimation for the calculation of dynamic loads and average ice forces on sloping structures and ships in level ice. The method contained the determination of a normal force including viscosity related terms, a frictional force and stresses in the ice sheet. Before generalizing the method for the entire hull, the effects linked to one individual ice floe were considered. The normal contact force resulting from the collision between an inclined structure and an ice sheet was given by the average ice pressure multiplied with the contact area.

Puntigliano (1995a and 2003) developed a theory and a numerical model to predict a path of the ice floes sliding along the hull. Therefore, he performed model tests with a segmented hull and pressure transducers to measure the low pressure phenomenon between the model hull and the layer of submerged ice floes. These measurements were confirmed by data gained during full scale trials. By use of the numerical model, the clearing ability of ships as well as the amount of ice reaching the propeller plane can be determined.

Zhou et al. (2016) presented a solution in the time domain by a combined method comprising a numerical part and semi-empirical formulas. The process of a ship breaking through a level ice sheet is modeled numerically based on the work of Zhou and Peng (2014), Hirano (1981) and others. It was simulated by a 2D method involving the discretization of ice edges and the ship's waterline. The contact loads were calculated, compared with the bending capacity of the ice and then used to determine the possibility of ice breaking. The equations of ship motions were solved and the ice information updated. The forces acting below the waterline were calculated based on Spencer and Jones (2001).

1.2.2 The ice breaking process

This chapter is limited to first-year level ice and continuous mode ice breaking. Furthermore, in this chapter the available knowledge on those aspects of the ice breaking process is summarized which is relevant for the thesis.

Several studies have been published on the influence of the ice properties on the ice resistance as presented in the following:

- The ice resistance is proportional to a power of the ice thickness that varies within a range between 1.1 and 2.2, Enkvist (1972).
- The ice resistance is proportional to a power of the ice thickness of 1.4, Nyman (1986).
- The ice resistance is proportional to a power of the ice thickness of 2.0, Ettema et al. (1989).
- The ice resistance is proportional to a power of the ice thickness of approximately 2.0, Puntigliano (1995b).
- The ice resistance is proportional to a power of the ice thickness which varies within a range of 1.0 and 2.0, ITTC (2002).
- The ice resistance is proportional to a power of the ice thickness of around 2 and of the ship speed of 2, Zahn et al. (1987).
- The ice breaking resistance is proportional to a power of the ice thickness of 2 times the flexural ice strength, Yamaguchi et al. (1997).
- The ice resistance, i.e. average and peak values increase with increasing ship speed, von Bock und Polach and Ehlers (2011).
- The ice breaking resistance is independent of the ship speed, Enkvist (1972), Milano (1973), Kotras et al. (1983).
- The ice breaking resistance is dependent on the ship speed, Yamaguchi and Kato (1994).

The influence of the ship design on the ice breaking process has been analyzed by many researchers. The partly contradicting findings are listed in the following:

- The stem angle should be as low as possible, Runeberg (1888/89).
- A reduction of the stem angle from 82 to 20 degree decreases the ice resistance by approximately 60 percent, Johansson and Mäkinen (1973).
- In low speed range, the ice breaking resistance is small for small stem and large waterline angles, i.e. spoon shaped bows, Yamaguchi et al. (1997).
- Generally, the ice resistance decreases with decreasing stem and normal angles, Nozawa (2009).
- An increase in ship length of 38 percent increases the ice resistance by approximately 30 percent, Johansson and Mäkinen (1973).
- A decrease in ship length of 38 percent decreases the ice resistance by approximately 10 percent, Johansson and Mäkinen (1973).
- The ice resistance is independent of the ship length, Edwards et al. (1976).
- The ice resistance clearly increases with length, Kitagawa et al. (1982).
- An increase in ship breadth of 33 percent increases the ice resistance by approximately 40 percent, Johansson and Mäkinen (1973).
- A decrease in ship breadth of 27 percent decreases the ice resistance by approximately 36 percent, Johansson and Mäkinen (1973).
- The ice resistance is directly proportional to the ship breadth, Edwards et al. (1976).
- The ice resistance increases with increasing ship breadth, Kitagawa et al., (1982).
- The ship draught does not affect the ice resistance, Virtanen et al. (1975).
- The ice resistance is proportional to the ship draught, Edwards et al. (1976).
- The ice resistance is proportional to the block coefficient, Edwards et al. (1976).
- The avoidance of crushing at the stem leads to decreasing level ice resistance values, Narita and Yamaguchi (1981).
- Model scale tests with the Max Waldeck before and after conversion to a Thyssen-Waas bow form lead to a decrease of the ice resistance of about 25 percent, whereas the speed increases approximately by 100 percent for the same power. Full scale data gave reasonable agreement (Hellmann 1982).
- The progress in the design of ice breaking ship bows over the last two decades has been to decrease normal angles, waterline angles and stem and buttock angles, Sodhi (1995).
- By concave bow frames which are vaulted inwards, the level ice is broken at a relatively small normal angle by bending so that compression of ice in the shoulder area is avoided (Schwarz et al. 1981).
- Soft and rounded shape of the ice waterline leads to a higher ice resistance than a more sharpened shape of the waterline, Lee et al. (2006).

The portions of the level ice resistance have been evaluated so far as follows:

- The resistance below the waterline was considerable, i.e. about 20 percent of the level ice resistance, Milano (1973).
- The length of the parallel mid-body contributed to approximately 33 percent of the level ice resistance, Vance (1980).
- For medium sized ship models the ice breaking component contributed to about 40 percent of the level ice resistance, Poznak and Ionov (1981).
- The level ice breaking component was between 40 and 80 percent of the total creeping speed resistance (determined by full scale measurements), Enkvist (1983).
- The ice breaking component contributed to about 80 percent to the level ice resistance, Poznyak and Ionov (1981) and Nyman (1986).
- For small ships at low speeds in model and full scale, the crushing and shearing at the stem contributed to about 20 to 40 percent of the level ice resistance, Enkvist and Mustamäki (1986).
- For a segmented ship model the contribution measured at the shoulders of the ship model is found to be approximately twice of that in the middle of the bow at waterline level. In total between 77 and 100 percent of the level ice resistance were measured in the bow region. Thus, the stern resistance was mostly negligible. If a relevant contribution below waterline was measured, it was found at the beginning of the flat bottom, Liukkonen and Nortala-Hoikkanen (1992).
- The clearing resistance contributed to about 15 to 30 percent of the level ice resistance even at low draught and to about 35 to 65 percent at normal draught. Thus, a considerable loss of energy is associated with the initial acceleration of the broken ice floes, Colbourne et al. (1992).
- At the beginning of the sliding phase the rotative motion of the floe in model scale and the extreme change from rotative to translative motion contributes significantly to the ice breaking resistance, Puntigliano (1995b) (based on Valanto 1989).
- According to measured and computed level ice resistance contributions, the resistance forces occurring at the waterline (crushing, bending and rotation forces) of the ship seem to be half of the level ice resistance. The other half is caused by the sliding phase, i.e. motion of broken ice floes under the ship (submersion and sliding forces), Valanto (2001).
- For a ship sailing in level ice the resistance in the sliding phase can be up to 65 percent of the level ice resistance, Puntigliano (2003).
- The ice breaking force which is the largest contribution to the level ice resistance at low speeds amounted to about 50 percent, Riska (2006a).

The breaking patterns result from the bow penetrating into the level ice sheet. According to the literature they depend on:

- bow form, ship speed and hull motions, Ettema et al. (1989).
- bow form, ice quality, speed, ice thickness and snow cover, Puntigliano (1995b).
- ship speed and ice thickness. Thereby, higher speeds and thinner ice cause a smaller ice floe width and a higher number of ice floes, Enkvist (1972), Poznyac and Ionov (1981), Ettema et al. (1989), Luikkonen and Nortala-Hoikkanen (1992). According to Enkvist this is due to the increasing mass forces of water and ice.
- ship speed, Valanto (1993). He stated that the length of the ice floes seem to first decrease with increasing speed and then, at moderate speeds, to reach a constant value.
- ship speed, Yamaguchi and Kato (1994). According to Yamaguchi and Kato the ice floe size decreases with increasing ship speed.
- stem angle, Uemura (1997). He reported that the ice floe width decreases with increasing stem angle.
- stem angle and waterline angle, Yamaguchi et al. (1997). They reported that the ice floe width decreases with increasing stem angle. Moreover, ship bows with small stem angles and large waterline angles, i.e. spoon shaped bows, produce wider but shorter ice floes.
- stem angle, Lee et al. (2006). According to Lee et al. a decreasing hull stem angle leads to an increasing width of the broken ice floes.
- ship speed, von Bock und Polach and Ehlers (2011). They stated that with increasing speed the scatter of the ice floe widths becomes smaller as well as the width itself.

This chapter outlined the large variety of existing ice resistance prediction methods based on different data sets, analysis techniques and ship designs. Thereby, the testing techniques as well as the ship designs improved and changed within the time (Ettema 1989, Puntigliano 1995b). However, the found knowledge on the ice breaking process, on ice resistance portions and the influence of ice properties on the level ice resistance is not sufficient to get a consistent overview of the ice breaking process and the resulting level ice resistance. Actually, some of the available references are partly contradictory. Thus, there is a need to get more insight on the ice breaking process and to update the available information with regard to common ice breaking ships. Subsequently, such findings can be used to increase the reliability and accuracy of level ice resistance prediction methods.

1.3 Research question

The main research question of this thesis is to improve a selected prediction method for the resistance of ships sailing ahead in level ice for the early design stage. This improvement shall increase the accuracy and reliability of the chosen method compared to other existing methods. Thereby, new insight shall be gained on the ice breaking process, the ice floe characteristics and the bottom ice coverage by application of new techniques and methodologies in the course of ice model tests. Furthermore, the empirical basis of this prediction method shall be updated with respect to ice breaking offshore supply vessels, anchor handling tugs and rescue and salvage vessels.

1.4 Research methodology

At the beginning of the thesis an analysis of state of the art ice resistance prediction methods is carried out and a method is identified which suits best for improvement (PI+PII).

The selected prediction method, i.e. approach by Lindqvist (1989), is evaluated with respect to influencing factors, uncertainties and assumptions. As a result, a number of aspects bearing potential for improvement are outlined (PII).

By means of model tests in pre-sawn ice at significant forward speed, the range of the resistance portion due to breaking is determined. Furthermore, ice model tests with an instrumented skeg deliver insight on the possible resistance contributions of a skeg in the bow area, which is a typical design feature of the investigated ship type (PIV).

A systematic evaluation of ice model tests is carried out focusing on correlations between the hull shape, the bow breaking pattern and the total resistance in ice (PII).

In order to gain further insight on the creation of ice floes, its characteristics and the bottom ice coverage a methodology is developed for acquisition and analysis of underwater images gained during ice model tests (PIII). Application of the image analysis procedure to ice model tests and an analysis of the corresponding test results, reveals correlations between hull shape parameters, ice floe characteristics, ice properties and the ice resistance (PVI). Moreover, valuable numbers of the bottom ice coverage are determined for the investigated ship type (PIV).

In order to evaluate the influence of the ship speed and the ice thickness on the total resistance in ice, the selected ice resistance prediction method is subjected to a numerical optimization algorithm. Thereby, the empirical basis is adapted to the investigated ice breaking ship type and the insight gained in the aforementioned studies is used during this optimization process. Finally, an enhanced prediction method for the total resistance in level ice for the early design stage of an ice breaking ship of the investigated type is presented (PV).

The thesis is structured according to the descriptions above. Figure 1 shows the connections and dependencies of the different publications.

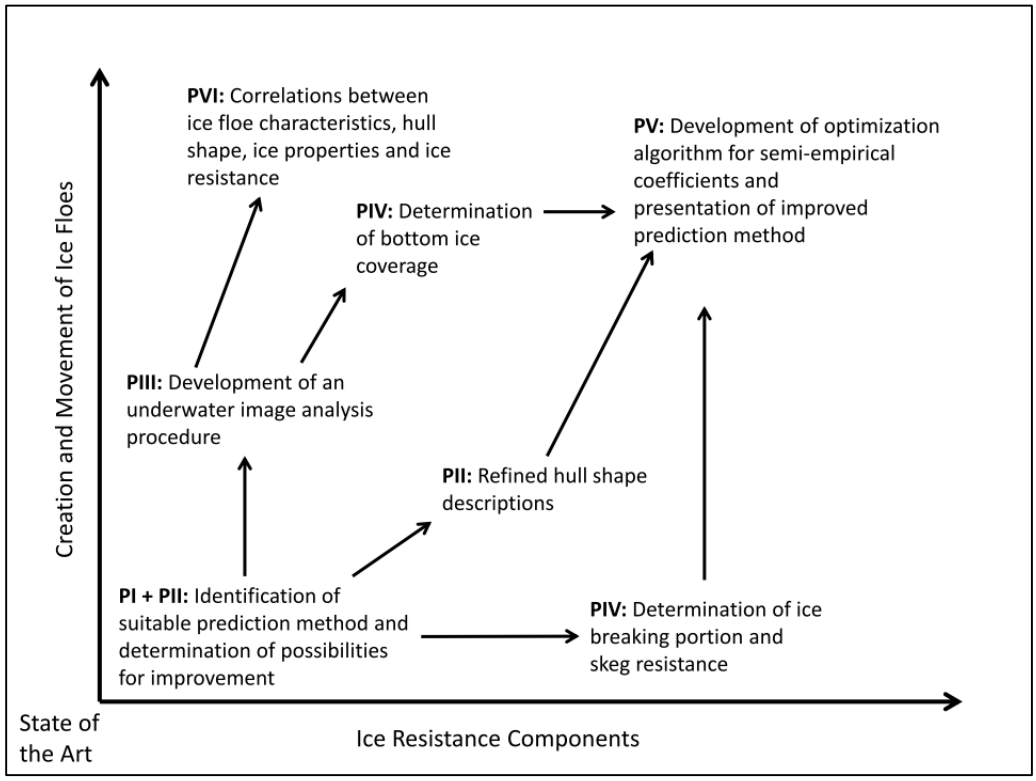

Figure 1: Contributions of the different publications (PI to PVI) as part of this thesis

1.5 Limitations

The thesis focuses on one ice breaking ship type, namely ice breaking offshore supply vessels, anchor handling tugs and rescue and salvage vessels as presented in Table 2. As a consequence, the new insight and the enhanced resistance prediction method presented in this thesis are limited to this ship type.

As all analyses and developments are based on ice model tests carried out in HSVA's large ice model basin, the results of this thesis are limited to model test results gained in model ice comprising a top layer of fine grained ice and a bottom layer of columnar ice. Within this thesis scaling uncertainties are not considered.

The developed prediction method and all gained knowledge are limited to ice breaking offshore supply vessels, anchor handling tugs and rescue and salvage vessels under forward motion in first-year level ice with the investigated range of ice thickness and ship speeds. Nevertheless, the acquisition and analysis procedure as well as the optimization algorithm developed within this thesis can also be applied to other ship types or data sets.

2 Ice model tests

This thesis, the newly gained insights described herein and the enhancement of the ice resistance prediction method are based on ice model tests which are carried out in HSVA's large ice model basin. All of the tests are executed as towed propulsion tests.

For the tests the ice sheets are produced according to HSVA's standard procedure (Evers and Jochmann 1993) taking into consideration the target ice conditions (mainly ice thickness and flexural strength). For production of the ice sheet, water droplets are sprayed into the cold air of the ice tank at about -18°C. The droplets freeze in the air and form small ice crystals which settle onto the water surface. These crystals initiate the growth of a fine-grained ice of primarily columnar crystalline structure. Highly pressure-saturated air in the ice tank water leads to formation of air bubbles embedded in the model ice.

During the towed propulsion tests the ship models are towed at constant speeds and the propeller rate is raised in steps from idling propeller condition up to a rate above the model self-propulsion. Therefore, the ship model is equipped with its own propulsion system and trimmed to its ice draught. During the test the pull force is measured by a load cell mounted at the ship bow and the total thrust is determined by a six component scale located at the top of the propulsor's shaft line. Based on the assumption that for a constant speed the thrust deduction fraction, THDF, is independent of the rate of revolution or the propulsor load, a linear regression is applied to the data of pull force vs. developed propulsor thrust. Using this regression function the towing force for vanishing thrust is determined. The value obtained in equilibrium is the ice resistance, R_{ice}, see Figure 2.

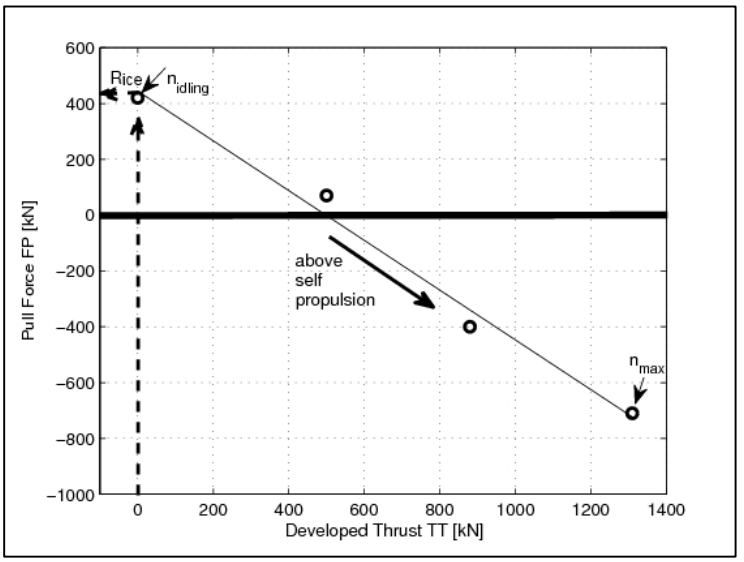

Figure 2: Test analysis of towed propulsion test in ice (HSVA)

The ice model tests which are used in the course of this thesis are listed in Table 1 together with their purpose of analysis.

Table 1: Ice model tests used in the course of this thesis

Test Campaign(s)	Number of Models	Number of Tests	Used for Analysis	Chapter	Publication
HSVA's data base 1996 – 2014	11	11	Breaking pattern dependency	5.1	PII
			Refinement of Lindqvist method	6.1	PII
Ice Model Tests within R&D project "ProEis"	1	4	Skeg Resistance	4.2	PIV
	1	1	Image Analysis Procedure	5.2	PIII
	4	16	Ice Floe Correlations	5.3	PVI
			Bottom Ice Coverage	5.4	PIV
			Breaking Resistance Portion	4.1	PIV
			Optimization of Lindqvist method	6.2	PV

The ice model tests are conducted with different ship models representing the ice breaking ship type of ice breaking offshore supply vessels, anchor handling tugs and rescue and salvage vessels. The main hull data of the investigated ships in full scale are presented in Table 2. Thereby, the average waterline angle is defined as the mean value of the waterline angles at the stem, at 1/8 B, 2/8 B, 3/8 B and near 4/8 B. Each of the ship model bows is equipped with a skeg.

Table 2: Main hull data of investigated ships and scaling factors

Property	Abbreviation [Unit]	Value
Length	Lpp [m]	between 70 and 90
Breadth	B [m]	between 18 and 23
Draught	T [m]	between 6.5 and 8.5
Stem angle	Φ [°]	between 19 and 27
Average waterline angle	α[°]	between 31 and 47
Forward skeg	-	present
Scaling factor	λ [-]	between 17.14 and 26.25

3 Identification of best-suited ice resistance prediction method (PI, PII)

A systematic comparison of existing, representative level ice resistance prediction methods developed by Lindqvist (1989), Su (2011), Sawamura (2012), Lindström (1990) and Valanto (2001) is carried out. These methods can be considered as state of the art and the original publications introducing them contain sufficient information to allow comparison in this thesis. The comparison focuses on the suitability of the existing methods as engineering tools for the prediction of different resistance components as well as the total resistance in ice.

Table 3: Comparison of theoretical ice breaking prediction methods with regard to relevant ship and ice parameters (Myland and Ehlers 2016)

Author / Parameter	Su (2011)	Sawamura (2012)	Lindström (1990)	Valanto (2001)	Lindqvist (1989)
Stem angle ϕ [deg]	no	no	yes	yes	yes
Waterline entrance angle α [deg]	no	no	yes	yes	yes
Buttock angle φ [deg]	no	no	yes	yes	yes
Ship breadth B [m]	yes	yes	yes	yes	yes
Ship speed v [kn]	yes	yes	yes	yes	yes
Ice thickness h_{ice} [m]	yes	yes	yes	yes	yes
Number of broken cusps n [-]	no	no	no	no	yes
Friction coefficient μ [-]	yes	yes	yes	yes	yes
Flexural strength σ_{flex} [kPa]	yes	yes	yes	yes	yes
Density difference of ice and water $\Delta\rho$ [kg/m^3]	no	no	no	yes	yes

From analysis of the presented methods it can be concluded that further research is required to predict the total resistance in ice and its components more precisely. Some of the resistance contributions or individual effects are considered by means of generalizing assumptions and strong simplifications, or are even neglected.

Due to its straightforward character, its clear expressions and its relatively detailed consideration of the bow shape the prediction method by Lindqvist (1989) is found to be the most suitable approach for the development of an enhanced ice resistance prediction method.

Erceg and Ehlers (2017) provided a similar comparison of different prediction methods, also including for example the semi-empirical method of Keinonen et al. (1991, 1996) and the method of Riska et al. (1997). The outcome of the comparison supports the aforementioned decision for the method by Lindqvist for further developments.

Lindqvist approximated the ice resistance by simple but physically sound formulas. The ice resistance was divided into two main components - ice breaking and submersion of the ice floes. The submersion component includes the resistance due to ice floes sliding along the ship hull, whereas the rotation of the ice floes is not taken into account by Lindqvist.

The breaking component is further divided into a bending and a crushing component. Both formulas consider only roughly the mechanical parameters of the ice, the hull geometry of the ship and the ship speed based on empirical coefficients.

The submersion component was estimated by application of full scale experiments and experience gained from model testing. From observations Lindqvist knew that the underwater part of the bow is more or less completely covered by ice pieces. This knowledge led to the calculation of the submersion resistance as the sum of the loss of potential energy and the frictional forces that are acting between the ship hull and the ice floes. Furthermore, also the submersion component includes a speed dependent component based on empirical coefficients.

The formulas of the semi-empirical method by Lindqvist are given in the following (Eq. 1 to 7):

$$R_{ice} = R_{Br} + R_S \tag{1}$$

$$R_{Br} = (R_c + R_B) * \left(1 + 1.4 * \frac{v}{\left(g * h_{ice}\right)^{0.5}}\right) \tag{2}$$

$$R_C = \frac{0.5 \sigma_f h_{ice}^2 \left(tan(\phi) + \mu \frac{cos(\phi)}{cos(\psi)}\right)}{\left(1 - \mu \frac{sin(\phi)}{\cos(\psi)}\right)} \tag{3}$$

$$R_B = \left(\frac{27}{64}\right) \sigma_f \left(\frac{\sigma_f}{\tau}\right) B \frac{h_{ice}^{1.5}}{\left(\frac{E}{12*(1-\nu^2)*g*\rho_W}\right)^{0.5}} \left(tan(\psi) + \mu \frac{cos(\phi)}{cos(\psi)\, sin(\alpha)}\right) \left(1 + \frac{1}{cos(\psi)}\right) \tag{4}$$

$$R_S = (R_p + R_f) * \left(1 + 9.4 * \frac{v}{(g * L_{pp})^{0.5}}\right) \quad (5)$$

$$R_p = \Delta \rho g h_{ice} * B * T * \frac{(B+T)}{(B+2*T)} \quad (6)$$

$$R_f = \Delta \rho g h_{ice} * B * \mu * \left(0.7 * L_{pp} - \frac{T}{tan(\phi)} - 0.25 * \frac{B}{tan(\alpha)} + T * cos(\phi) * cos(\psi) * \left(\frac{1}{sin(\phi)^2} + \frac{1}{tan(\alpha)^2}\right)^{0.5}\right) \quad (7)$$

The normal angle is calculated from the waterline entrance angle and the stem angle according to Eq. 8.

$$\psi = \arctan\left(\frac{\tan \Phi}{sin\alpha}\right) \quad (8)$$

This page is intentionally left blank.

4 Determination of resistance portions

4.1 Breaking resistance (PIV)

The resistance of a ship advancing in level ice can be subdivided into breaking forces, rotative forces, submersion forces and sliding forces. Several publications give estimates of the different contributions. In order to gain information on these contributions related to the considered ship type, a total of 16 towed propulsion tests were conducted in level ice and in pre-sawn ice, made from the same ice sheet, with four different ship models. The tests were executed in ice sheets of about 0.6 and 1.0 m thickness (full scale values) for each of the ship models; the ship model speeds were 2.0 and 3.5 kts (full scale values).

For model tests in pre-sawn ice a breaking pattern for the corresponding ship's bow shape has to be pre-determined. From the level ice tests, an idealized breaking pattern was deducted individually for each of the ship models and for each test condition. Due to only marginal differences between the patterns, the influences of speed and ice thickness were neglected. Thus, for each model only one template for preparation of the pre-sawn ice was produced. By cutting the ice sheet according to the breaking pattern (Figure 3, Figure 4) the breaking forces are basically eliminated. Thus, the resistance in pre-sawn ice consists of the rotative, submersion and sliding forces, only. By subtracting the resistance in pre-sawn ice from the total resistance in level ice with identical test conditions, the breaking forces can be determined.

From the results of these tests it can be seen that the breaking portion decreases with increasing speed for the analyzed speed range, whereas the rotative, submersion and sliding portions increase with increasing ship speed. Furthermore, it can be seen that the ice breaking portion increases with increasing ice thickness values, whereas the rotative, submersion and sliding portion decreases with increasing ice thickness values. However, the dependencies of both resistance portions on the ice thickness and on the ship speed seem to be only weak compared to those between the different models. This means, that the bow shape, even within one ship type, still has a significant influence on the resistance portions. Generally, the ice breaking portion of the investigated ship type amounts to approximately 30 to 60 percent. This corresponds well to the already available literature values which are not related to a specific ship type.

Figure 3: Preparation of the pre-sawn ice sheet

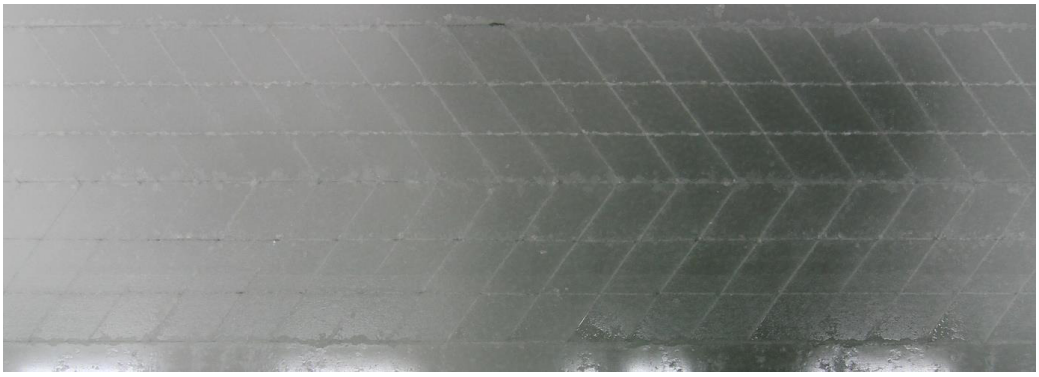

Figure 4: Pre-sawn ice sheet

4.2 Skeg resistance (PIV)

Almost all ships of the analyzed ship type are equipped with a skeg in the bow area to accommodate one or multiple transverse thrusters. A skeg in the bow area can have different impacts on the ice breaking behavior. Depending on the transverse thrusters' dimensions the skeg is often too wide to allow ice floes broken in the bow region to smoothly pass the skeg. In this case, the skeg may increase the resistance significantly. But if the skeg is well-designed in terms of shape and position, it can be an efficient design feature to support the transport of ice floes to the sides under the ice sheet. Therefore - as a mandatory condition - the intact ice sheet has to be broken with a clear center crack at the stem and be separated ahead the forward skeg. Then the ice floes come into contact with

the skeg which pushes the ice floes aside. However, the resistance is increased at least slightly due to floes hitting the forward skeg, even though the skeg reduces the ship bottom area covered by ice floes and thus the sliding forces.

In order to gain knowledge on the potentially additional resistance of a skeg in the bow area, four towed propulsion tests in level ice were conducted with one representative ship model. To measure the forces acting between the hull and the skeg, the skeg of the ship model was instrumented. It was structurally isolated from the model hull and only connected by means of a six component scale. Thereby, the force acting in longitudinal direction, i.e. the portion of ice resistance induced by the skeg, can be directly measured and compared to the total resistance in ice.

It is found that the portion of the skeg resistance for the analyzed ship model amounts to about 7 to 11 percent of the total resistance in ice. Furthermore, the relative portion of the skeg resistance increases for increasing ship speed, whereas the ice thickness seems to have only little effect on the skeg resistance portion for the tested ice thickness values.

This page is intentionally left blank.

5 Analysis of ice floe creation and influence of ice floe parameters on the ice resistance

5.1 Breaking pattern dependency (PII)

One of the main contributions to the total resistance in level ice is the breaking force which is mainly influenced by the bow shape, beside the ice properties and the ship speed. Understanding the influence of the bow shape on the ice breaking resistance is essential for the assessment of the hull form in an early design stage.

As a consequence, a detailed analysis of different bow shapes is carried out for ship models of the investigated ship type which were tested in HSVA's large ice model basin between 1996 and 2014. The analysis focuses in particular on the breaking patterns formed in level ice with regard to relevant hull shape parameters. The ship models chosen for the analysis have similar scaling factors leading to model ice conditions, model speed values and ship model dimensions in the same range. The actual ice property and the ship speed values of the selected towed propulsion tests in ice were measured during the testing and extrapolated to their target values in full scale according to HSVA's standard correction methods, see HSVA (1996). Using the target ice property and ship speed values improves the accuracy of the analysis since the range of considered ice properties is reduced. Thus, the ice property and ship speed values as listed in Table 4 can be kept almost constant throughout the analysis. As a consequence the analysis can be mainly focused on the bow shape. The model test conditions, i.e. ice properties and ship speed, correspond to typical design values of the chosen type of ships. Due to the fact that the selected test data for analysis were taken from towed propulsion tests they provide both, suitable underwater video records to evaluate the bow shapes as well as the total resistance values.

Table 4: Model test parameters of breaking pattern analysis (full scale values)

Property	Abbreviation	Target value	Mean value	Standard deviation
Ice thickness	h_{ice} [m]	between 0.9 and 1.2	1.01	0.08
Ship speed	v [m/s]	between 2.0 and 3.5	2.55	0.58
Ice flexural strength	σ_{flex} [kPa]	500	-	-
Ice-hull friction coefficient	μ [-]	0.1	-	-

Within the analysis frames from underwater video recordings showing the breaking patterns at the bow are subdivided by visual assessment into two breaking pattern classes. Selected geometric parameters of each ship bow are analyzed in order to identify correlations between the ship's hull shape and the total resistance in ice specific for each breaking pattern class.

An example of video frames for different breaking cycles for one ship model within one test run (constant speed and constant ice conditions) is presented in Figure 5. From all of the snapshots belonging to the shown test run only minimal differences between the images can be identified. Since these differences are within the required accuracy for the following analysis all of them are considered to be representative for a certain ship under the given conditions as presented in Table 4. As a consequence, only one characteristic snapshot per test run is used for the analysis.

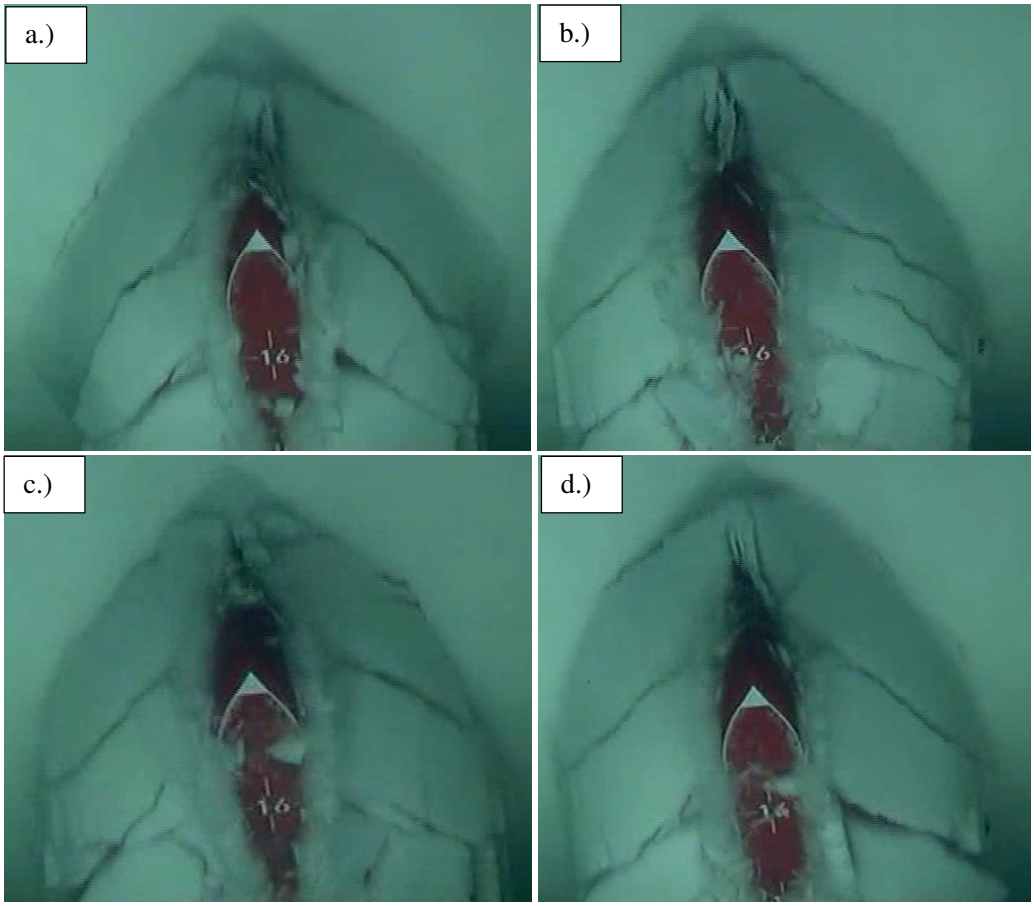

Figure 5: Series of snapshots for different breaking cycles within one test run

Breaking pattern class 1 is characterized by large ice floes covering the ship hull in a regular pattern (Figure 6 left). Mostly, one ice floe covers half of the ship's breadth. Breaking pattern class 2 shows smaller sized floes and consequently an increased amount of floes with different shapes (Figure 6 right). While the ice floes of breaking pattern class 1 are shaped like bars, which are arranged in a regular pattern, the ones of breaking pattern class 2 are shaped and arranged more individually. Nevertheless, the clarity with which the ships of the thesis could be divided into breaking pattern classes based on the initial breaking pattern at the bow has diminished at the beginning of the parallel mid-ship.

Figure 6: Examples for breaking pattern classes - left: breaking pattern class 1; right: breaking pattern class 2

A comparison of the total resistance values in ice to the subdivision of each model into the breaking pattern classes reveal smaller resistance values for breaking pattern class 1 than for breaking pattern class 2. Furthermore, the values indicate a correlation of the bow length, the average buttock angle and the average normal angle to the total resistance in ice and at the same time to the breaking pattern classes. However, these parameters are geometrically related to the stem angle, especially the bow length and the average buttock angle. Thus, their dependency might be a result of this relation. The average normal angle considers additionally the waterline entrance angle.

5.2 Underwater image analysis methodology (PIII)

An image analysis methodology is developed to further evaluate possible correlations between specific ice floe parameters and the total resistance in ice, characteristic values of the ship hull or ice properties during model scale ice tests (Figure 7).

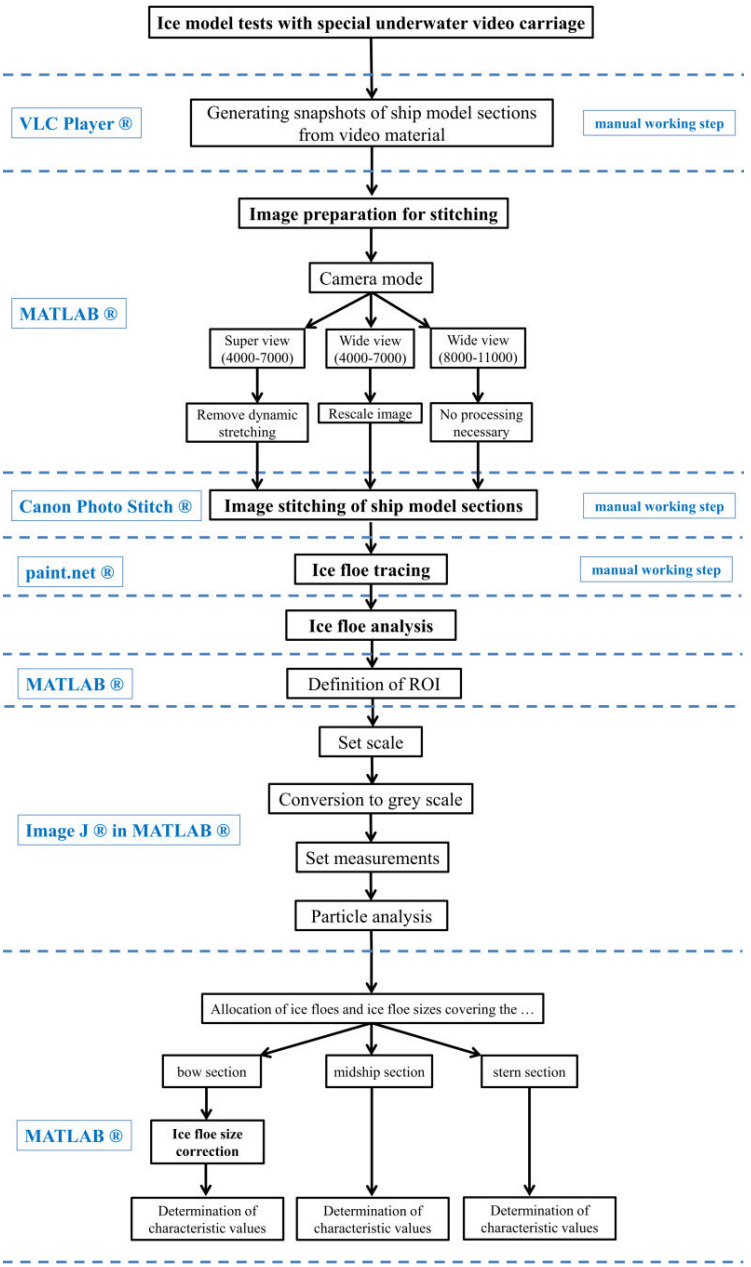

Figure 7: Methodology for assessing the ice floe size and distribution along a ship hull

Assuming that the ice breaking process of a ship advancing in continuous motion in modeled level ice is a quasi-steady process, the ice floe behavior is characterized by the ice floe size and distribution at any given point of time during the test.

The image analysis procedure is developed based on towed propulsion model tests in level ice and can thus ideally be applied to such tests. During the model tests an underwater video carriage is used to continuously record the ice floe motion along the ship hull. The video recording is performed by three video cameras set to full HD quality. These are mounted on a specifically designed underwater video carriage which is guided by rails positioned on the floor of the ice tank. Subsequently, a MATLAB® based image post-processing procedure is applied to the frames of the underwater video recordings to correct the distortion of the recordings, which is produced by the extra wide angle mode of the cameras. After manual tracing of the ice floes in the pictures (Figure 8), they are identified in the image together with their size and location by another MATLAB® script and are assigned a unique identifying number (Figure 9). After further application of a correction method for the tilted ice floes in the bow area, characteristic values like the bottom ice coverage or the average floe size can be calculated.

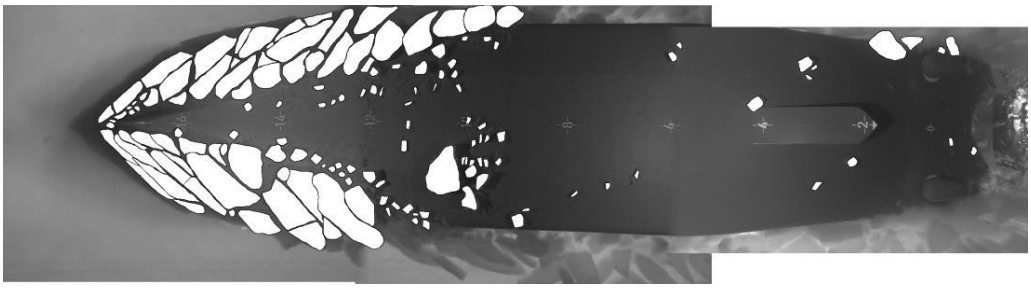

Figure 8: Stitched image with manually traced ice floes

Figure 9: Analyzed image with identified ice floes

The developed methodology is applied to a test case, which is a towed propulsion test in level ice performed in HSVA's large ice model basin. During this model test the required underwater video equipment was used. The results of the methodology as applied to the test case reveal that it is capable to deliver results of the desired amount and quality.

5.3 Ice floe correlations (PVI)

Two aspects of the ice breaking process with regard to ice floe characteristics are analyzed based on results of the image analysis methodology (see chapter 5.2, PIII): First, correlations between ice floe characteristics, hull shape parameters and the level ice resistance and second, dependencies of ice floe characteristics on ice properties. The investigations are mainly based on 16 model tests conducted in level ice of about 0.6 and 1.0 m thickness at two speed values of 2.0 and 3.5 kts (in full scale).

5.3.1 Correlations between ice floe characteristics, hull shape parameters and the level ice resistance

In chapter 5.1 the hypothesis is developed that the ice resistance is generally of smaller amount if larger ice floes are broken in the bow area compared to smaller ice floes. Figure 10 shows the total resistance in level ice, RIT, against the stem angle for the four investigated ship models as well as further total resistance values from towed propulsion tests in level ice for the same ship type from HSVA's data base. The resistance values were scaled by Froude scaling law without application of further correction methods. The different data series represent different test conditions as given in the legend of the figure. The figure indicates that higher stem angles lead to higher values of the total resistance in ice. This indication matches well with, e.g. Johansson and Mäkinen (1973) and Nozawa (2009). The reason for this correlation is that a low stem angle induces a high vertical force and a low horizontal force on the ice sheet and thus, ice breaking in the most efficient way (Riska 2006b).

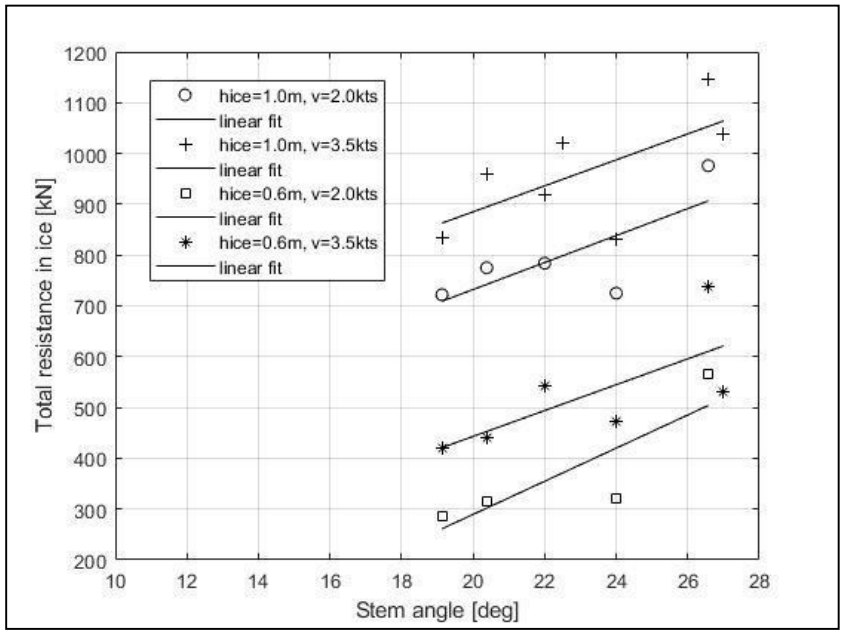

Figure 10: Total resistance in ice from model testing vs. stem angle

Based on the subdivision of the resistance components described in chapter 1.1, the hull shape at the water level affects mainly the ice breaking resistance. Consequently, this relationship is also found when plotting the ice breaking resistance, R_{Br}, derived from the pre-sawn tests (as described in chapter 4.1) against the stem angle for the four investigated ship models, see Figure 11.

In Figure 10 and Figure 11 the ice resistance values of one ship model appear as outliers, i.e. at a stem angle of 24 degree. One reason could be that this ship model has the smallest draught and the smallest breadth of the used ship models.

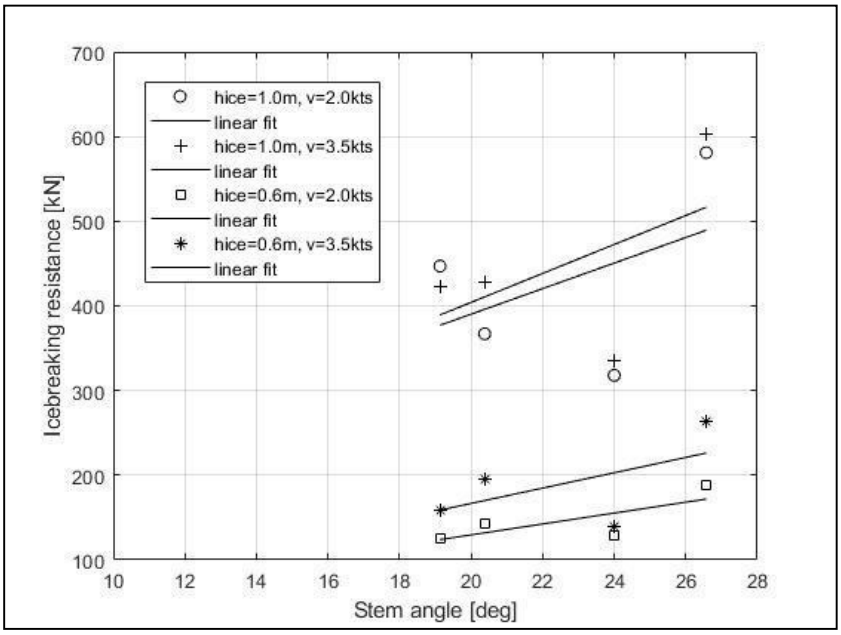

Figure 11: Ice breaking resistance from model testing vs. stem angle

In order to gain insight on the ice floe characteristics and thus to further investigate the aforementioned hypothesis, frames of underwater videos of model tests in level ice are post-processed according to the image analysis methodology described in chapter 5.2 (PIII). For each of the 16 tests frames of three different ice breaking cycles are analyzed with respect to the following ice floe data:

- Number of ice floes covering the bow region of the ship model's underwater hull
- Size of ice floes covering the bow region
- Ice coverage of the bow region, i.e. sum of all individual ice floe areas covering the bow region (hereafter called covered bow area).

For each of the floe parameters the mean value of the three analyzed cycles is used in the following.

Figure 12 presents the mean bow floe size against the stem angle for the four investigated ship models. According to the figure a higher stem angle leads to smaller ice floes broken at the bow. Underwater video records show that the relatively large scatter of the values for the mean ice floe size in 1 m ice thickness mainly results from the different influences of the forward skeg related to each specific design.

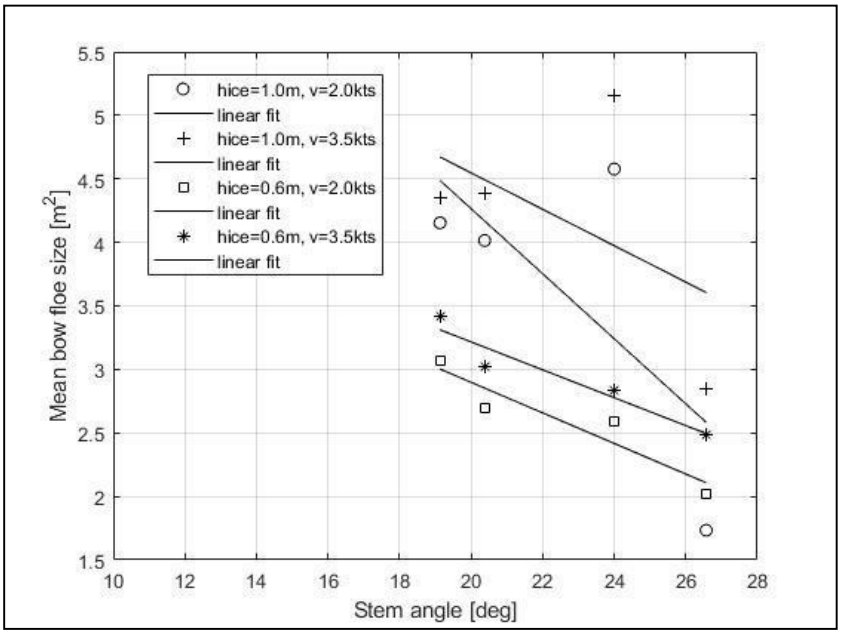

Figure 12: Mean bow floe size from model image analysis vs. stem angle

Figure 13 presents the ice breaking resistance, R_{Br} against the mean ice floe size in the bow region. Therefrom, it can be seen that the ice breaking resistance decreases with increasing ice floe size.

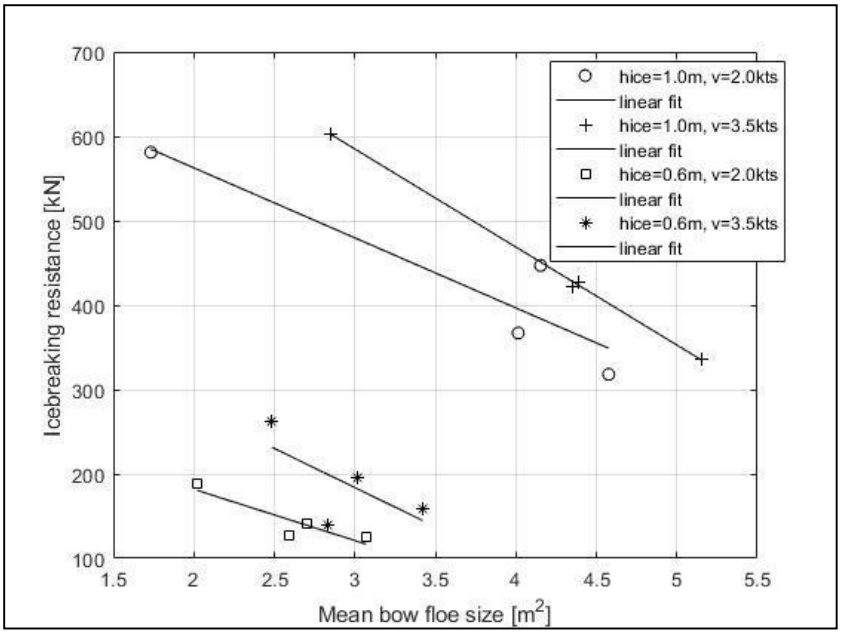

Figure 13: Ice breaking resistance from model testing vs. mean bow floe size from image analysis

From the three aforementioned correlations it can be concluded that a large stem angle leads to small ice floes broken in the bow region what further leads to a high ice resistance.

In order to make the results of the different test conditions comparable to each other and thus, to further evaluate the outlined correlation, the resistance values are normalized with respect to the ship speed and ice thickness. The normalization is done on the basis of chapter 6.2, i.e. the outcome of an optimization algorithm applied to the Lindqvist approach.

However, as h_{ice} cannot be eliminated mathematically correct from the bending resistance, $R_{B,}$ and the crushing resistance, $R_{C,}$ the ice breaking resistance, R_{Br}, is divided by h_{ice}^1 and the speed and ice thickness dependent terms. Thus, the ice breaking resistance values are normalized as follows:

$$R'_{Br} = \frac{R_{Br}}{(-0.212+1.408*h_{ice})*h_{ice}^1*\left(1+1.4*\frac{v}{(g*h_{ice})^{0.5}}\right)^{0.682}} \tag{9}$$

Figure 14 presents the normalized ice breaking resistance values, R'_{Br}, against the mean ice floe size broken in the bow region for the four investigated ship models. It can be seen that the normalized ice breaking resistance decreases with increasing ice floe size, what supports the correlation shown in Figure 13.

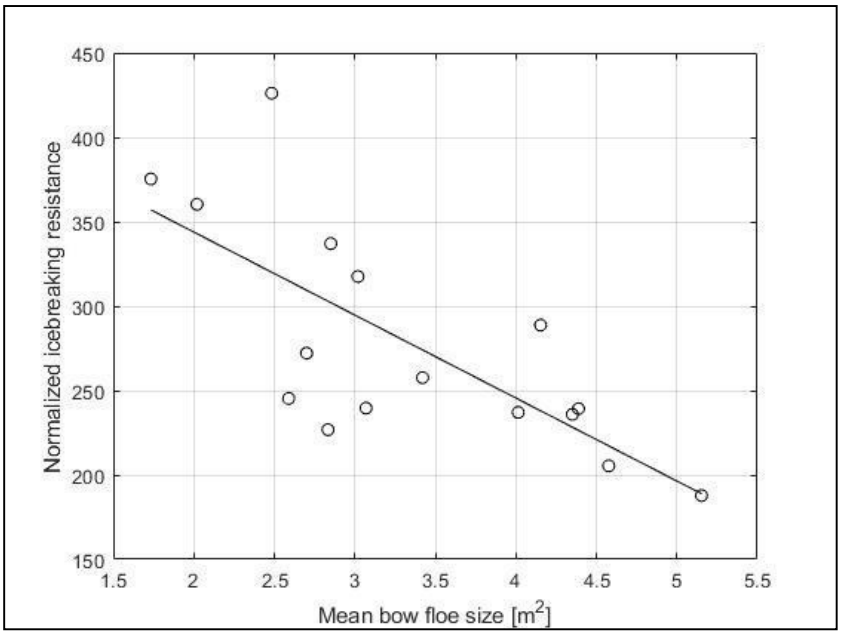

Figure 14: Ice breaking resistance from model testing vs. mean bow floe size from image analysis

Finally, it can be concluded that the data gained from the analysis of the underwater video frames support the hypothesis developed from the results of the analysis related to the bow breaking patterns (chapter 5.1), i.e. the ice resistance is generally of smaller amount if larger ice floes are broken in the bow area compared to smaller ice floes.

5.3.2 Correlations of ice floe characteristics on ice properties

The influence of the ice thickness on the investigated ice floe characteristics at the bow for the investigated ship models and test conditions are presented in Figure 15 to Figure 18. As already stated by Enkvist (1972) and Ettema et al. (1989) the results outline that the bow floe size increases with increasing ice thickness (see Figure 15 and Figure 16). From the results of the present study, i.e. Figure 15 to Figure 18 it can be further concluded that the bow area is covered with less ice floes of larger size at thicker ice compared to thinner ice. The bow coverage is higher at thicker ice. The reason is most probably that thinner ice can be better cleared off the hull compared to thicker ice.

With regard to the ship speed no trends with respect to the investigated ice floe parameters can be outlined. This may be due to the fact that the investigated speed values are in a narrow range.

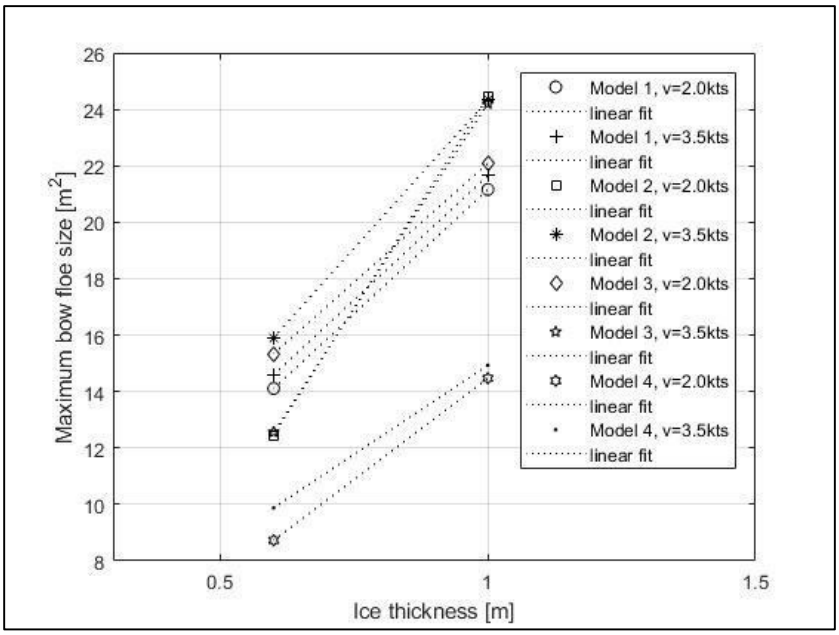

Figure 15: Maximum ice floe size in the bow region vs. ice thickness for four different ship models of the investigated type

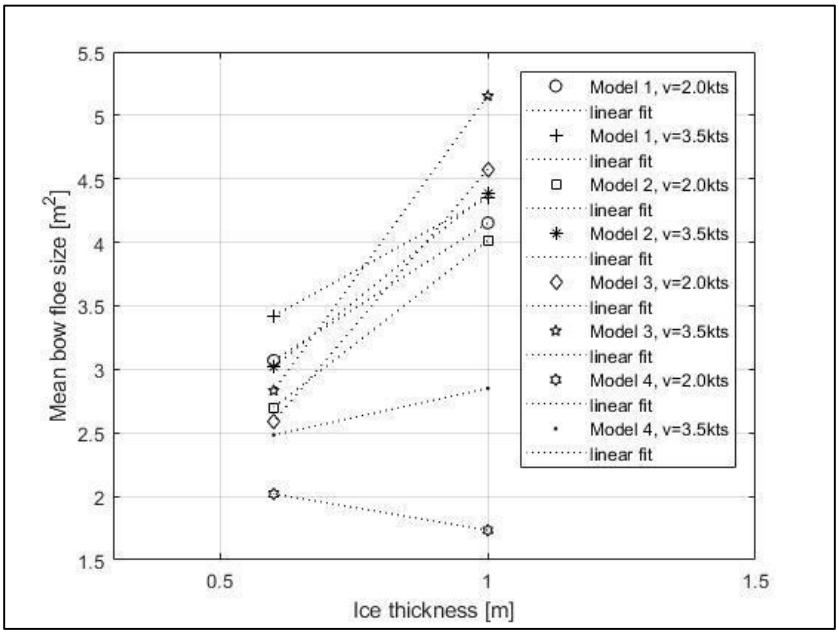

Figure 16: Mean ice floe size in the bow region vs. ice thickness for four different ship models of the investigated type

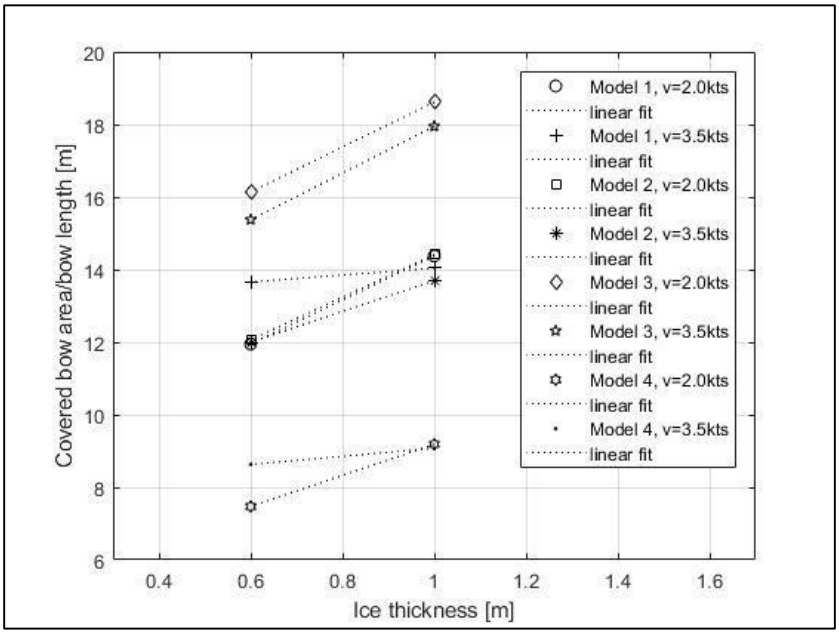

Figure 17: Covered bow area/bow length vs. ice thickness for four different ship models of the investigated type

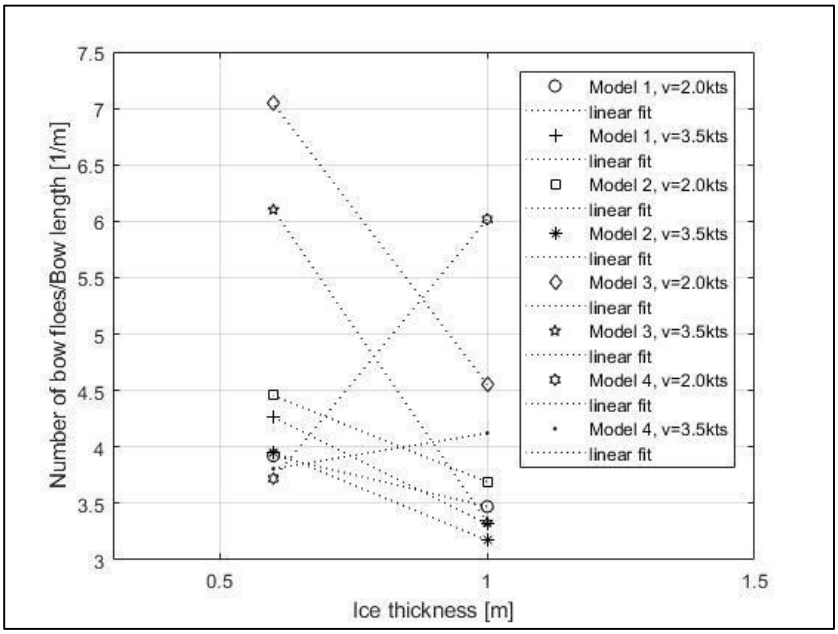

Figure 18: Number of bow floes/bow length vs. ice thickness for four different ship models of the investigated type.

The results presented in this chapter show that common trends can be outlined for all investigated ship models correlating the ice floe characteristics to ship hull parameters, ice properties and the ice resistance. However, the indicative correlations outlined in this chapter do not serve for an improvement of ice resistance prediction methods due to the limited number of underlying model tests.

5.4 Bottom ice coverage (PIV)

The sliding forces acting on a ship advancing ahead in level ice are strongly dependent on the bottom ice coverage. In order to gain information on typical bottom ice coverage values of the ship type which is considered within this thesis, the image analysis methodology described in chapter 5.2 (PIII) is used to analyze the bottom ice coverage of four ship models during a total of 16 towed propulsion tests in level ice. The tests were executed in ice sheets of about 0.6 and 1.0 m thickness (full scale values) for each of the ship models; the ship model speeds were 2.0 and 3.5 kts (full scale values).

The results show that the average bottom ice coverage, i.e. the sum of the projected ice floe area divided by the projected underwater hull area, is 33 percent, with a maximum value of approximately 50 percent and a minimum value of approximately 20 percent. The bottom ice coverage increases with increasing ice thickness. For increasing speed no clear

dependency of the bottom ice coverage could be determined. It seems that the bow shape has a stronger influence on the bottom ice coverage than the ship speed. These determined values of the bottom ice coverage are significantly lower than the 70 percent which are reported by Lindqvist for the ship types investigated in his study.

Figure 19 shows the total resistance in ice versus the bottom ice coverage. It can be seen that the values are scattered around a general trend of increasing total resistance in ice for increasing bottom ice coverage. This trend becomes more pronounced when plotting the resistance values measured in pre-sawn ice tests (see also chapter 4.1), i.e. rotative, submersion and sliding resistance versus the bottom ice coverage as shown in Figure 20. This means that the scatter of the data points is lower for the pre-sawn resistance than for the total resistance in ice, leading to an increased coefficient of determination of $R^2 = 0.3826$ instead of $R^2 = 0.251$. However, the correlation only indicates a dependency.

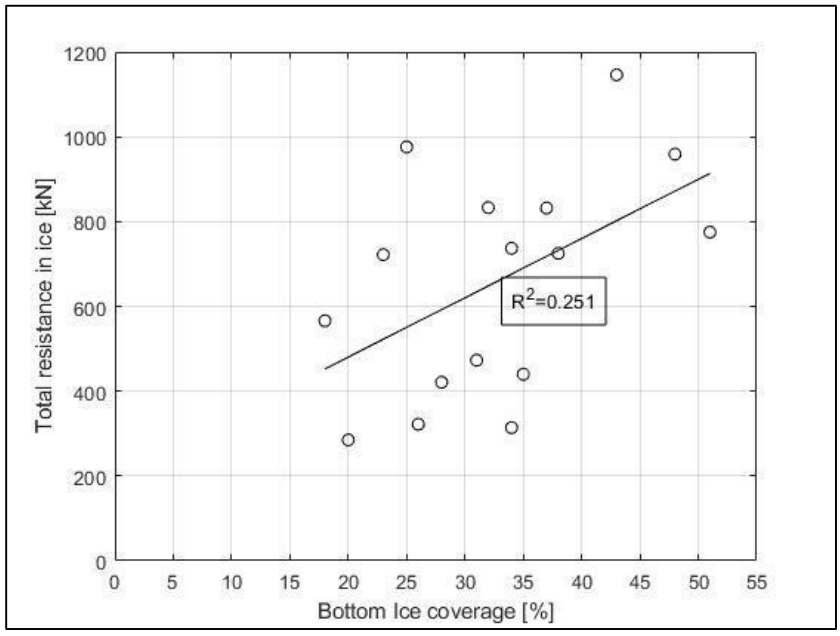

Figure 19: Total resistance in ice vs. bottom ice coverage

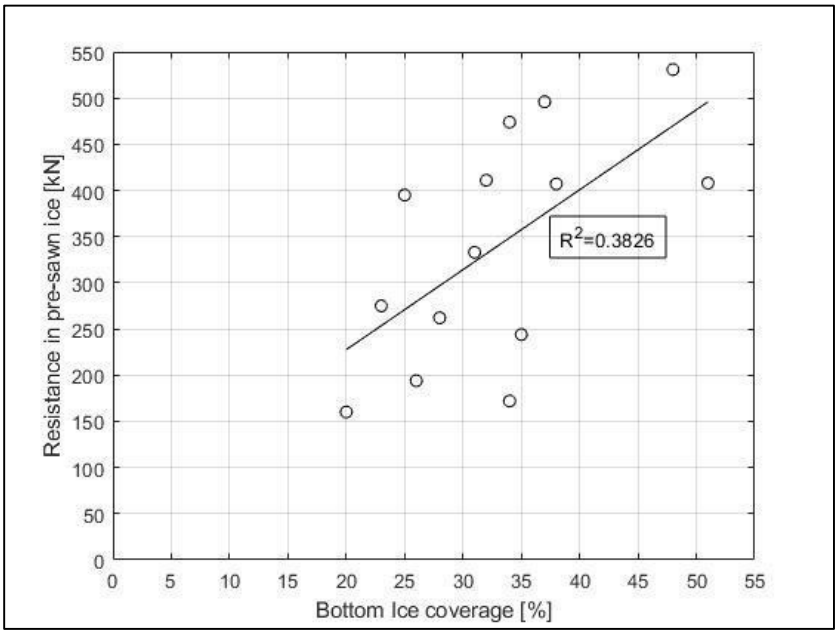

Figure 20: Rotative, submersion and sliding resistance vs. bottom ice coverage

It can be expected that the trend of increasing resistance over increasing ice coverage becomes even more pronounced if only the sliding resistance would be compared to the bottom ice coverage. However, at the time of the model tests, no model testing or post-processing procedure was available to determine the sliding resistance separately from the other resistance components.

This page is intentionally left blank.

6 Enhancement of ice resistance prediction method

6.1 Refinement of Lindqvist method (PII)

Two of the modifications of the Lindqvist approach analyzed by Myland and Ehlers (2016), (PII) lead to significant improvements: First, the determination of the number of cusps by means of video frames taken from underwater records of ice model tests and second, an increased precision with which the hull shape of the ship is considered.

Lindqvist defined the number of cusps as the ice floes broken within one breaking cycle at the waterline at the bow. The submersion part of the total resistance in ice as defined by Lindqvist does not take into account any further breaking within the breaking process. From the underwater videos further breaking of the cusps in the bow region can be identified. Since further breaking induces additional forces at the bow, it can be assumed that this is at least one reason for deviating total resistance values between model tests and Lindqvist.

In order to consider further breaking in the bow region in addition to the initially broken ice floes the number of cusps is determined at the end of the bow region. This is done for 11 ship models on the basis of underwater video recordings of towed propulsion tests in level ice. Finally, the determined number of cusps is compared to the number of cusps resulting from Lindqvist's approach.

Although the number of cusps is strongly affected by the complete bow geometry, Lindqvist considers only a limited number of hull shape parameters for its calculation. For the investigated ship models these parameters are in a very narrow range. In contrast, the model tests consider the complete bow geometry including special design features such as the forward skeg. The number of cusps determined from model tests shows a wider scatter than the number of cusps calculated on the basis of Lindqvist's approach.

Furthermore, the number of cusps determined from model tests is in most cases slightly lower than the number of cusps according to Lindqvist. This is noteworthy especially, when realizing that the number of cusps determined from model tests is considered at the end of the bow region, whereas the Lindqvist approach is supposed to give the number of cusps during the initial breaking process at the waterline.

The majority of the currently available prediction methods, including the method of Lindqvist use only a limited number of characteristic values for the description of the bow shape. Thus, the Lindqvist approach - as well as other methods - does not consider minor changes in the hull shape for prediction of the ice resistance. In order to increase the precision when using Lindqvist's method, HSVA separates the bending resistance into

terms for four longitudinal sections per ship's half. In particular four buttock angles, four waterline angles and four normal angles are used in addition to the originally considered stem, waterline and normal angle at the centerline to calculate average angles for the corresponding sections. The bending resistance terms are expressed as given in Eq. (10) to Eq. (13).

$$R_{B1} = \left(\frac{27}{64}\right)\sigma_f \left(\frac{\sigma_f}{\tau}\right)\frac{B}{4}\,\frac{h_{ice}^{1.5}}{(E/(12*(1-\nu^2)*g*\rho_w))^{0.5}}\left(tan(\psi_1) + \mu\frac{cos(\varphi_1)}{cos(\psi_1)\,sin(\alpha_1)}\right)\left(1+\frac{1}{cos(\psi_1)}\right) \quad (10)$$

$$R_{B2} = \left(\frac{27}{64}\right)\sigma_f \left(\frac{\sigma_f}{\tau}\right)\frac{B}{4}\,\frac{h_{ice}^{1.5}}{(E/(12*(1-\nu^2)*g*\rho_w))^{0.5}}\left(tan(\psi_2) + \mu\frac{cos(\varphi_2)}{cos(\psi_2)\,sin(\alpha_2)}\right)\left(1+\frac{1}{cos(\psi_2)}\right) \quad (11)$$

$$R_{B3} = \left(\frac{27}{64}\right)\sigma_f \left(\frac{\sigma_f}{\tau}\right)\frac{B}{4}\,\frac{h_{ice}^{1.5}}{(E/(12*(1-\nu^2)*g*\rho_w))^{0.5}}\left(tan(\psi_3) + \mu\frac{cos(\varphi_3)}{cos(\psi_3)\,sin(\alpha_3)}\right)\left(1+\frac{1}{cos(\psi_3)}\right) \quad (12)$$

$$R_{B4} = \left(\frac{27}{64}\right)\sigma_f \left(\frac{\sigma_f}{\tau}\right)\frac{B}{4}\,\frac{h_{ice}^{1.5}}{(E/(12*(1-\nu^2)*g*\rho_w))^{0.5}}\left(tan(\psi_4) + \mu\frac{cos(\varphi_4)}{cos(\psi_4)\,sin(\alpha_4)}\right)\left(1+\frac{1}{cos(\psi_4)}\right) \quad (13)$$

Thereby, φ_1 is the average of the stem angle and the buttock angle at 1/8 B, φ_2 is the average of the buttock angle at 1/8 B and the buttock angle at 2/8 B, φ_3 is the average of the buttock angle at 2/8 B and the buttock angle at 3/8 B and φ_4 is the average of the buttock angle at 3/8 B and the buttock angle near 4/8 B. The average waterline and the average normal angles are determined accordingly.

The total bending resistance can then be calculated as given in Eq. (14)

$$R_B = R_{B1} + R_{B2} + R_{B3} + R_{B4} \quad (14)$$

The deviations of the original Lindqvist approach from the model test results can be reduced for most of the investigated ships by application of the refined method.

Since model tests are usually conducted in later design stages, the first of these refinements, i.e. determination of the number of cusps by means of model tests, is not usable for a resistance prediction tool in early design stages. Thus, only the second of the aforementioned refinements, i.e. separate calculation of the bending resistance for four longitudinal sections, which still provides a valuable improvement, is considered in the course of the optimization process in Chapter 6.2.

The prediction method comprising the separate calculation of the bending resistance for four longitudinal sections is referred to within this publication as "refined Lindqvist approach".

6.2 Optimization of Lindqvist method (PV)

The approach proposed by Lindqvist is currently the semi-empirical prediction method, which considers the most hull shape and ice parameters (chapter 2). At the same time it provides practical advantages by its relatively quick and easy applicability. Within this thesis the Lindqvist approach is adapted to the ship type of ice breaking offshore supply vessels, anchor handling tugs and rescue and salvage vessels. In particular, the speed and ice thickness dependencies, which are based on empirical investigations in the original Lindqvist approach, are evaluated in detail for the mentioned ship type. For a more precise analysis of the complex influence of ship speed and ice thickness of the defined ship type on the total resistance in ice, an optimization algorithm is applied to the Lindqvist approach with a total of 16 ice model tests as a recent empirical data set.

Four variables are introduced to the refined Lindqvist approach (see chapter 6.1) in such a way that the influence of the ship speed and the ice thickness can be evaluated. The objective of the optimization algorithm is to determine a valid set of variables which provides the minimum deviation of the total resistance in ice resulting from the optimized prediction method to the total resistance in ice resulting from model tests. The latter are scaled by Froude scaling law without application of further correction methods.

The optimization process makes use of a Particle Swarm Optimization (PSO) algorithm. PSO is a population-based heuristic optimization technique developed by Kennedy and Eberhart (1995). A fitness value is used to evaluate a group of randomly composed population. The population particles which have an in-built memory are then updated with the internal velocity. As a result, the best particle of the population forwards its information to the other particles. Hence, it is a one-way sharing mechanism which only looks for the best solution. The advantages of the PSO are that it converges relatively fast and that it can be implemented with relatively few parameters to adjust.

Based on the newly gained insights of the aforementioned studies (PII – PVI), two modifications are considered for the prediction method during the optimization process: The bottom ice coverage is set to 33 percent (see chapter 5.4, PIV) and the breaking resistance is constrained to be between 30 and 60 percent of the total resistance in ice (see chapter 4.1).

The presented solution of the design objective found by the optimization algorithm lies within the given constraints and none of the defined boundary values is reached. For the investigated ship type the set of variables resulting from the optimization process gives a slightly higher dependency of the breaking resistance on the ice thickness than considered in the original Lindqvist approach. The speed dependency of the breaking resistance seems to be less than in the original Lindqvist approach for the analyzed ships whereas the speed dependency of the submersion resistance seems to be remarkably higher than in the

original Lindqvist approach. The overall influence of speed on the total resistance, i.e. on the combination of breaking and submersion resistance is roughly linear. Thus, the optimized variables seem to be physically reasonable.

From application of the optimized method it can be seen that with respect to the original Lindqvist approach a clear improvement can be achieved in general. The maximum of the absolute deviation to the model test results is reduced from 35.9 or 39.4 percent for the original or refined approach, respectively to 27.3 percent for the optimized approach. The average of the absolute deviation is reduced from 17.7 or 11.9 percent for the original or refined approach, respectively to 10.8 percent for the optimized approach. The standard deviation is reduced from 9.8 or 10.9 percent for the original or refined approach, respectively to 9.4 percent for the optimized approach. Although some individual results of the optimized approach show a higher deviation to the model test results than the original Lindqvist approach, the results are less scattered, meaning that the reliability of the approach is increased. With respect to the refined Lindqvist approach the optimization process still leads to an improvement of accuracy and reliability of the prediction method.

The formulas of the optimized prediction method are given in equation (15) to Eq. (25). Thereby, the variables resulting from the optimization process are written as bold numbers.

$$R_{ice} = R_{Br} + R_S \tag{15}$$

$$R_{Br} = (\mathbf{-0.212 + 1.408} * h_{ice}) * (R_c + R_B) * \left(1 + 1.4 * \frac{v}{\left(g * h_{ice}\right)^{0.5}}\right)^{\mathbf{0.682}} \tag{16}$$

$$R_C = \frac{0.5\sigma_f h_{ice}^{\mathbf{1}}\left(tan(\phi) + \mu\frac{cos(\phi)}{cos(\psi)}\right)}{\left(1 - \mu\frac{sin(\phi)}{\cos(\psi)}\right)} \tag{17}$$

$$R_B = R_{B1} + R_{B2} + R_{B3} + R_{B4} \tag{18}$$

$$R_{B1} = \left(\frac{27}{64}\right)\sigma_f\left(\frac{\sigma_f}{\tau}\right)\frac{B}{4}\frac{h_{ice}^{\mathbf{0.5}}}{\left(\frac{E}{12*(1-\nu^2)*g*\rho_W}\right)^{0.5}}\left(tan(\psi_1) + \mu\frac{cos(\varphi 1)}{cos(\psi 1)\,sin(\alpha 1)}\right)\left(1 + \frac{1}{cos(\psi_1)}\right) \tag{19}$$

$$R_{B2} = \left(\frac{27}{64}\right)\sigma_f\left(\frac{\sigma_f}{\tau}\right)\frac{B}{4}\frac{h_{ice}^{\mathbf{0.5}}}{\left(\frac{E}{12*(1-\nu^2)*g*\rho_W}\right)^{0.5}}\left(tan(\psi_2) + \mu\frac{cos(\varphi_2)}{cos(\psi_2)\,sin(\alpha_2)}\right)\left(1 + \frac{1}{cos(\psi_2)}\right) \tag{20}$$

$$R_{B3} = \left(\frac{27}{64}\right)\sigma_f\left(\frac{\sigma_f}{\tau}\right)\frac{B}{4}\frac{h_{ice}^{0.5}}{\left(\frac{E}{12*(1-\nu^2)*g*\rho_W}\right)^{0.5}}\left(tan(\psi_3) + \mu\frac{cos(\varphi_3)}{cos(\psi_3)\,sin(\alpha_3)}\right)\left(1 + \frac{1}{cos(\psi_3)}\right) \tag{21}$$

$$R_{B4} = \left(\frac{27}{64}\right)\sigma_f\left(\frac{\sigma_f}{\tau}\right)\frac{B}{4}\frac{h_{ice}^{0.5}}{\left(\frac{E}{12*(1-\nu^2)*g*\rho_W}\right)^{0.5}}\left(tan(\psi_4) + \mu\frac{cos(\varphi_4)}{cos(\psi_4)\,sin(\alpha_4)}\right)\left(1 + \frac{1}{cos(\psi_4)}\right) \quad (22)$$

$$R_S = (R_p + R_f) * \left(1 + 9.4 * \frac{v}{\left(g*L_{pp}\right)^{0.5}}\right)^{\mathbf{1.8}} \quad (23)$$

$$R_p = \Delta\rho g h_{ice} * B * T * \frac{(B+T)}{(B+2*T)} \quad (24)$$

$$R_f = \Delta\rho g h_{ice} * B * \mu * \left(0.33 * L_{pp} - \frac{T}{tan(\phi)} - 0.25 * \frac{B}{tan(\alpha)} + T * cos(\phi) * cos(\psi) * \left(\frac{1}{sin(\phi)^2} + \frac{1}{tan(\alpha)^2}\right)^{0.5}\right) \quad (25)$$

Thereby, the ice thickness is to be used in meters and the speed in meters per second. The formulas are only valid for the investigated speed and ice thickness range, i.e. 1.0 to 1.8 m/s and 0.6 to 1.0 m.

In order to distinguish how much of the improvement is attributable to the optimization process itself and how much is attributable to the adaption of the bottom ice coverage, the optimization is also conducted with a bottom ice coverage value of 0.7 as stated in the original Lindqvist. The results, i.e. 11.6 percent mean deviation and 30.0 percent maximum deviation to model test results, show that both, the application of the optimization algorithm as well as the adaption of the bottom ice coverage value from 0.7 to 0.33 lead to significant improvements of the results. With a different bottom ice coverage a different set of variables is found by the algorithm to deliver the best results. Thus, all four variables are affected by the specified bottom ice coverage value.

This page is intentionally left blank.

7 Concluding remarks

7.1 Discussion

Both, model tests and theoretical ice prediction methods have their uncertainties. Due to the complexity of the ice breaking process, all theoretical approaches necessarily make use of assumptions and simplifications resulting in estimations of the physical effects. However, model tests naturally cover the majority of the physical effects of the ice breaking process. Uncertainties may result from scaling methods and the modeled ice structure. Thus, this thesis mainly makes use of up-scaled, but uncorrected values for development of the enhanced prediction formula. Theoretical methods are essential tools during the early design stage of a ship, whereas model tests are still the most reliable prediction method for the total resistance of ships in ice and thus, are to be applied in a later design stage. Finally, both methods have their advantages and thus, their reason for existence.

The breaking resistance portions presented in this thesis are derived from model tests in pre-sawn ice. Thereby, influences of the ice thickness and ship speed on the breaking pattern are neglected. Occasionally, it was observed that pre-sawn ice floes were broken once again by the advancing model. However, these aspects are considered to have only little effect on the determined breaking resistance portions. The influence of the hull friction coefficient on the sliding resistance was not considered.

The skeg resistance portions presented in this thesis appear as an additional resistance component at the first glance. However, a well-designed skeg also induces beneficial effects with regard to the bottom ice coverage. This effect reduces the sliding resistance and may even counterbalance the skeg resistance. Nevertheless, the design of a skeg in the bow area is usually also affected by further aspects than the total resistance in ice.

The developed image analysis procedure contains a number of small uncertainties. Among these are the manual ice floe tracing, the handling of crushed ice and the approximately corrected size of tilted ice floes in the bow region.

The evaluation of the breaking patterns and the ice floe characteristics within this thesis did not result in a valuable contribution to the enhanced resistance prediction method. Although the results indicated tending correlations between the breaking patterns, the ice floe characteristics, the ice properties, ship hull parameters and the ice resistance, no quantitative correlations could be obtained on a sufficiently sound basis. For other found but not presented trends further evaluations are necessary to check how far they are influenced by other parameters. Both aspects require further analysis on the basis of an expanded data set.

One of the findings of the analysis of ice floe creation and distribution is that the bottom ice coverage of the investigated ship type amounts to approximately 33 percent, whereas Lindqvist originally stated 70 percent. One reason could be that all ship models evaluated in this publication are equipped with a skeg in the bow area. A well-designed skeg improves the ability of the bow shape to clear broken ice floes off the ship's hull.

Although the coefficients and exponents resulting from the optimization algorithm for the investigated ship type turn out to meet approximately the general dependencies originally defined by Lindqvist, the accuracy and reliability of the approach could be improved. Individual outliers may be the result of additional and unconsidered phenomena during the ice breaking process, such as shoulder crushing.

It is to be noted that the resulting coefficients and exponents are the results of a numerical optimization process. Although the definition of boundary values and constraints seek to direct the solution to a realistic and physically sound set of variables, the resulting variables remain based on the selected expression of the objective function and in particular the used data sets, i.e. scaled model test results.

The findings described in this thesis are determined on a limited data set and only for one ship type. As numerous physical effects occur during the ice breaking process of a ship advancing in level ice which are linked in a complex manner, the various influences of hull shape and ice properties may turn out to differ for other ship types. Furthermore, an extension of the data set to other ship types and thus, an extension of the range of hull shape parameters may deliver other relationships.

7.2 Summary and conclusion

This thesis focused on the resistance of a ship advancing continuously in level ice. Different aspects of the ice resistance were analyzed for the ice breaking ship type of ice breaking supply vessels, anchor handling tugs and rescue and salvage vessels. Thereby, newly developed methods and techniques were used in the course of ice model tests and a semi-empirical resistance prediction method was enhanced with the gained insight.

At the beginning, a systematic comparison of existing, representative ice resistance prediction methods was carried out. Based on the insights gained during ice model tests and evaluation of the influence of hull shape parameters and ice conditions, the assumptions and simplifications of the prediction methods were assessed. From comparison and analysis of the available prediction methods it was concluded that further research is required to predict the resistance and its components more precisely. The simple physical sound formulas given by Lindqvist form a valuable basis for the

development of an enhanced ice resistance prediction method. However, one of the major issues which have a large influence on the prediction of ice resistance is the precision with which the hull shape of the ship is considered. Furthermore, the empirical basis of the Lindqvist approach may be outdated since the typical hull shapes and dimensions may have changed in the past. Consequently, three aspects of a ship advancing in level ice were analyzed in more detail:

Firstly, different portions and contributions to the total resistance in ice were evaluated by ice model tests which were executed in a special manner. In particular, ice model tests in pre-sawn ice at considerable ice breaking speeds were conducted. By comparison of the resistance values of the pre-sawn ice tests to the resistance values of ice tests in the same but intact ice sheet, the breaking portion of the total resistance in ice could be determined. For the investigated ship type, it was found that the breaking portion amounts to approximately 30 to 60 percent of the total resistance in ice. Dependencies of the ice resistance portions on the ship speed, the ice thickness and the ship hull shape could be found. Furthermore, ice model tests with an instrumented skeg were conducted to evaluate the possibly additional resistance which is induced by the presence of a skeg in the bow area. It was found that the presence of a skeg in the bow area can be responsible for approximately 7 to 11 percent of the total resistance in ice.

Secondly, the ice floe creation and distribution and its influences on the total resistance in ice were analyzed. A systematic comparison of breaking patterns showed tending correlations to the total resistance in ice. A regular shaped breaking pattern with a relatively small number of cusps (breaking pattern class 1) seems to be advantageous for the total resistance in ice. Furthermore, an image analysis procedure including a number of semi-automated MATLAB-scripts was developed to evaluate underwater images of ice model tests. The application of this procedure to a number of ice model tests and analysis of the corresponding test results support the developed hypothesis that the ice resistance is generally of smaller amount if larger ice floes are broken in the bow area compared to smaller ice floes. Furthermore, it was found that the bottom ice coverage of the investigated ship type amounts to approximately 33 percent and that thinner ice can be better cleared off the hull than thicker ice.

Thirdly, the semi-empirical prediction method of Lindqvist was enhanced by two aspects: By means of a subdivision of the bending resistance into four longitudinal sections per ship's half, the precision with which the hull shape is considered can be increased what leads to an improved prediction accuracy. Based on this refined prediction method and on the insights gained in the aforementioned analyses, a numerical particle swarm optimization algorithm was employed to evaluate the dependencies of ice thickness and ship speed on the total resistance in ice. Four variables were introduced to the formulas which were then optimized with regard to a minimum difference between the predicted

total resistance in ice and the corresponding ice model test value. Thereby, the selected models of the underlying ice model tests formed a recent empirical data set of ice breaking ships of the investigated ship type. The coefficients and exponents resulting from the optimization process indicate an ice thickness dependency of the breaking resistance only slightly higher than assumed by Lindqvist. The speed dependency resulting from the optimization process is lower for the breaking resistance and higher for the submersion resistance than assumed by Lindqvist. By consideration of all applied coefficients and exponents as well as the adapted bottom ice coverage, the accuracy and reliability of the approach could be improved.

Assuming that a sufficient amount of model test data is available, the proposed optimization algorithm forms a tool that can be used for modification of the Lindqivst formula related to other ship types and conditions as well. Thus, the tool serves as a good basis for further development of semi-empirical ice resistance prediction methods used in early design stages.

7.3 Future work

In the course of this thesis ice model test results were used from HSVA's data base as well as results of recently conducted tests with the use of specifically designed methods and techniques. Since the precision and reliability of (semi-)empirical methods strongly depend on the underlying data set, the enhanced prediction method presented in this thesis could be further improved by an increased data set. In particular, the results of model tests performed in level ice sheets of a third ice thickness could improve the results of the algorithm since this would enable the use of a polynomial expression instead of a linear one for the ice thickness dependency of the breaking resistance. Thereby, it is essential that the data is of the same or of a comparable origin, i.e. based on ice model tests ideally conducted as towed propulsion tests in model ice comprising a top layer of fine grained ice and a bottom layer of columnar ice.

By means of an extended data set, the trending correlations between ice floe characteristics, the ice resistance, characteristic values of the ship hull and ice properties could be further evaluated to develop quantitative dependencies. Furthermore, it may be possible to determine correlations for the ship's mid-ship and stern region and thus correlations to other resistance components. Based on such data, possibly further resistance terms could be added to the prediction method, e.g. a skeg related term. In order to enable judgment on the advantageousness of a skeg, model tests with a detachable skeg would deliver valuable numbers.

The analysis of the breaking resistance separately from the remaining resistance components by means of pre-sawn ice tests could be enhanced by application of e.g. segmented models. Therefrom deeper insight could be gained on the physical process of ice breaking to improve prediction of the individual resistance components. Additionally, tests in pre-sawn ice with different size of ice floes would provide further insight on the influence of the ice floes size in the bow region on the ice resistance.

With respect to the image analysis procedure, the employment of multiple cameras for capturing the bow region from different positions would provide a basis for replacing the ice floe size correction algorithm in the bow region by a more accurate 3D algorithm.

In order to cope with the uncertainties related to model testing, full scale data would deliver valuable input, although a strictly quantitative evaluation could fall at a lack of homogeneous ice or ideal ship conditions.

This page is intentionally left blank.

8 References

Carter, D. (1983). Ship Resistance to Continuous Motion in Level Ice. Transportation Development Centre, Transport Canada, Montreal, Canada, Report No. TP3679E.

Cho, S.-R., Lee, S., Jeong, S.-Y., Kang, K.-J. (2014). Development of a Prediction Formula for Ship Resistance in Level Ice. Proc. of the 33rd International Conference on Ocean, Offshore and Arctic Engineering (OMAE), June 8-13, 2014, San Francisco, California, USA.

Cho, S.-R., Lee, S. (2015). A Prediction Method of Ice Breaking Resistance Using a Multiple Regression Analysis. International Journal of Architecture and Ocean Engineering, 2015, 7:708-719.

Colbourne, D.B., Lever, J.H. (1992). Development of a Component Based Scaling System for Ship-Ice Model Tests. Journal of Ship Research, SNAME, Vol. 36, No. 1 March 1992.

Crago, W.A., Dix, P.J., German, J.G. (1971). Model Ice Breaking Experiments and their Correlation with Full-Scale Data. Transactions of RINA, Vol. 113, p. 83-108.

Edwards, R.Y., Major, R.A., Kim, J.K., German, J.G., Lewis, J.W., Miller, D.R. (1976). Influence of Major Characteristics of Icebreaker Hulls on Their Powering Requirements and Maneuverability in Ice. Transactions of SNAME, Vol. 8.

Elisejev, V.K. (1968). On the Influence of the Principal Dimensions of an Icebreaker Hull on Ice Resistance. Transactions of AARI, 1968, p. 496-500.

Enkvist, E. (1972). On the Ice Resistance Encountered by Ships Operating in the Continuous Mode of Ice Breaking, The Swedish Academy of Engineering Sciences in Finland, Helsinki, Report No. 24, pp. 181.

Enkvist, E. (1983). A Survey of Experimental Indications of the Relation Between the Submersion and Breaking Components of Level Ice Resistance to Ships. Proceedings of POAC, 1983, p. 484-493.

Enkvist, E., Mustamäki, E. (1986). Model and Full-Scale Tests with an Innovative Icebreaker Bow. Transations of SNAME, Vol. 94, p. 325-351.

Erceg, S., Ehlers, S. (2017). Semi-Empirical Level Ice Resistance Prediction Methods. Journal of Ship Technology Research (Schiffstechnik), 2017, 64:1, p. 1-14.

Ettema, R., Stern, F., Lazaro, J. (1989). Dynamic of Continuous Model Icebreaking by a Polar Class Hull – Part I: Mean Response. Journal of Ship Research, Vol. 33, No. 2, June 1989, SNAME.

Evers, K.-U., Jochmann, P. (1993). An Advanced Technique to Improve the Mechanical Properties of Model Ice Developed at HSVA Ice Tank. The Hamburg Ship Model Basin, HSVA, Hamburg, Germany, Publication.

Hellmann, J.H: (1982). Model and Full-Scale Tests in Ice With the Icebreaker Max Waldeck. Proceedings of Intermaritec, 1982, Hamburg.

HSVA (1996). Appendix C – Data Analysis, Internal Appendix of Standard Report for Industry Projects, Hamburg Ship Model Basin, HSVA, Hamburg, Germany.

Ionov, B.P. (1988). Ice Resistance and its Composition. Transactions of AARI, Gidrometeoiztat, Leningrad, pp. 81.

ITTC (2002). Report of Resistance Tests in Level Ice. Section 7.5-02-04-02.1, ITTC 2002.

Jansson, J.E. (1956). Ice-Breakers and their Design. European Shipbuilding, No. 5-6, Vol. 5, 1956, p 112-128 and p. 143-151.

Jeong, S.-Y., Lee, C.J., Cho, S.R. (2010). Ice Resistance Prediction for Standard Icebreaker Model Ship. Proceedings of 20th International Conference on Offshore and Polar Engineering, Beijing, China, June 20-25, 2010, p. 1300-1304.

Jeong, S.-Y., Choi, K., Kang, K.-J., Ha, J.-S. (2017). Prediction of Ship Resistance in Level Ice Based on Empirical Approach. International Journal of Naval Architecture and Ocean Engineering, 2017, 9:613-623.

Johansson, B.M., Mäkinen, E. (1973). Icebreaking Model Tests; Systematic Variation of Bow Lines and Main Dimensions of Hull Forms Suitable for the Great Lakes. Marine Technology, SNAME, July 1973, Vol. 10, No. 3.

Jones, S.J. (2004). Ships in Ice – A Review. Proc. of 25th Symposium on Naval Hydrodynamics, St. John's, Newfoundland and Labrador, Canada, 8-13 August 2004.

Kämäräinen, J. (1993). Evaluation of Ship Ice Resistance Calculation Methods. Licentiate's Thesis, Helsinki University of Technology, Faculty of Mechanical Engineering, 1993.

Kämäräinen, J. (2007). Theoretical Investigation on the Effect of Fluid Flow Between the Hull of a Ship and Ice Floes on Ice Resistance in Level Ice. Doctoral Dissertation, Helsinki University of Technology, Faculty of Mechanical Engineering, 2007.

Kaminski, M.L., Rigo, P. (2018). Proceedings of the 20th International Ship and Offshore Structures Congress (ISSC), Vol. 1.

Kari, A. (1921). The Design of Icebreakers. Shipbuilding and Shipping Record, No. 18, 22nd December 1921, p. 802-804.

Kashtelyan, V.I., Poznyac, I.I., Ryvlin A.Ya. (1968). Ice Resistance to Motion of a Ship. Sudostroenie, Leningrad.

Keinonen, A.J., Browne, R.P., Revill, C.R. (1991). Icebreaker Design Synthesis – Phase 2 – Analysis of Contemporary Icebreaker Performance. AKAC Inc. Report for Transportation Development Centre, Transport Canada, TP 10923E, September 1991.

Keinonen, A.J., Browne, R.P., Revill, C.R., Reynolds, A. (1996). Icebreaker Characteristics Synthesis. AKAC Inc. Report for Transportation Development Centre, Transport Canada, TP 12812E, July 1996.

Kennedy, J., Eberhart, R. (1995). Particle Swarm Optimization. Proceedings of International Conference of Neural Networks. Piscataway. 1942–1948.

Kitagawa, H., et al. (1982). Vessel Performance in Ice. General Meeting of S.I.R., Report No. 1, December 1982, p. 14-24.

Kitagawa, H., et al. (1983). Vessel Performance in Ice. General Meeting of S.I.R., Report No. 2, December 1983, p. 25-32.

Kotras, T.V., Baird, A.V., Naegle, J.W. (1983). Predicting Ship Performance in Level Ice. Transactions of SNAME, Vol. 91, p. 329-349.

Lee, C.-J., Koh, C.-D., Lee, Y.-Y., Park, I.-R. (2006). A Development of Icebreaking Hull Form for Antarctic Research Vessel. Proceedings of 16th International Offshore and Polar Engineering Conference, ISOPE, San Francisco, California, USA, May 28-June 2, 2006.

Lewis, J.W., Edwards, R.Y. Jr. (1970). Methods for Predicting Icebreaking and Ice Resistance Characteristics of Icebreakers. Transactions of SNAME, Vol. 78, p. 213-249.

Lewis, J.W., DeBord, F.W., Bulat, V.A. (1982). Resistance and Propulsion of Ice-Worthy Ships. Transactions of SNAME, Vol. 90, p. 249-276.

Lindqvist, G. (1989). A Straightforward Method for Calculation of Ice Resistance of Ships, Proc. of 10th Port and Ocean Engineering Conference under Arctic Conditions (POAC), Lulea, Sweden Vol 2, pp 722.

Lindström, C.-A. (1990). Numerical Estimation of Ice Forces Acting on Inclined Structures and Ships in Level Ice, OTC 6445. Offshore Technology Conference, Houston, TX, USA, 1990.

Liukkonen, S., Nortala-Hoikkanen, A. (1992). Ice Resistance on Segmented Icebreaker Model. IAHR Symposium, 1992, Banff, Alberta.

Luk, C.H. (1986). A Two-Dimensional Plasticity and Moment Model for Ship Resistance in Level Ice. Proc. of the IAHR Ice Symposium 1986, Iowa City, Iowa, p. 101-112.

Luk, C.H. (1988). A Three-Dimensional Plasticity and Moment Model for Ship Resistance in Level Ice. Proceedings of the 7th International Conference on Offshore Mechanics and Arctic Engineering (OMAE), Houston Texas, USA, February 7-12, 1988, p. 307-315.

Maksutov, D.D. (1973). Resistance to the Motion of Transport Vessels in Solid Ice; Ice Navigating Qualities of Ships (transl.). CRREL Report No. TL 417, Hanover, New Hampshire, USA, 1973.

Milano, V.R. (1973). Ship Resistance to Continuous Motion in Ice. Transactions of SNAME, Vol. 81, p. 247-306.

Milano, V.R. (1975). Variation of Ship/Ice parameters on Ship Resistance to Continuous Motion in Ice. Proc. of SNAME Ice Tech. Symposium, Montreal, Paper B, pp. 30.

Milano, V.R. (1980). A Re-Analysis of Ship Resistance when in Continuous Motion through Solid Ice. Proc. of Intermaritec Symposium, Hamburg, p. 456-475.

Milano, V.R. (1982). Correlation of Analytical Prediction of Ship Resistance in Ice with Model and Full-Scale test results. Proc. of Intermaritec Symposium, Hamburg, p. 350-372.

Myland, D., Ehlers, S. (2014). Theoretical Investigation on Ice Resistance Prediction Methods for Ships in Level Ice. Proceedings of the 33rd International Conference on Ocean, Offshore and Arctic Engineering, OMAE 2014-23304, June 8-13, 2014, San Francisco, USA.

Myland D., Ehlers S. (2016). Influence of Bow Design on Ice Breaking Resistance. Journal of Ocean Engineering, 119 (2016), p. 217-232.

Myland D., Ehlers S. (2017). Methodology to Assess the Floe Size and Distribution Along a Ship Hull during Model Scale Ice Tests for a Self-Propelled Ship Sailing Ahead in Level Ice. Journal of Ships and Offshore Structures, 12:sup1, p.100-p.108.

Myland D., Ehlers S. (2019). Model Scale Investigation of Aspects Influencing the Ice Resistance of Ships Sailing Ahead in Level Ice. Journal of Ship Technology Research, DOI: 10.1080/09377255.2019.1576390.

Myland D., Ehlers S. (2019). Investigation on Semi-Empirical Coefficients and Exponents of a Resistance Prediction Method for Ships Sailing Ahead in Level Ice. Journal of Ships and Offshore Structures, DOI: 10.1080/17445302.2018.1564535.

Myland D. (2019). Experimental and Theoretical Investigations on the Characteristics of Ice Floes Broken by Ships Sailing Ahead in Level Ice. 38th International Conference on Ocean, Offshore and Arctic Engineering, OMAE 2019-95936, June 4-19, 2019, Glasgow, Scotland (final paper submitted).

Naegle, J.N. (1980). Ice-Resistance Prediction and Motion Simulation for Ships Operating in the Continuous Mode of Icebreaking. Thesis, University of Michigan, 1980, pp. 223.

Narita, S., Yamaguchi, M. (1981). Some Experimental Study on Hull Forms for the New Japanese Antarctic Research Ship, Proceedings of 6th STAR Symposium, SNAME, New York, p. 253-271.

Nozawa, K. (2009). A Consideration on Bow Design of Artic Tanker Transiting in Thin Level Ice and in Broken Ice Channel. Proceedings of the 19th International Offshore and Polar Engineering Conference, ISOPE, Osaka, Japan, June 21-26, 2009.

Nyman, T. (1986). On the Ice-breaking Component in the Level Ice Resistance. Proceedings of IAHR, Ice Symposium, 1986.

Poznyak, I.I., Ionov, B.P. (1981). The Division of Icebreaking Resistance into Components. Proc. of 6th STAR Symposium, SNAME, New York, p. 249-252.

Puntigliano, F. (1995a). On the Resistance Components Below the Waterline in the Continuous Model of Icebreaking – Model Tests. HSVA-Report No. E253/95, Vol. 1, Hamburg.

Puntigliano, F. (1995b). Review of Ship Resistance in Level Ice. HSVA-Report No. E253/95, Vol. 1, Supplement, Hamburg.

Puntigliano, F. (2003). Experimental and Numerical Research on the Interaction Between Ice Floes and a Ship's Hull During Icebreaking. Doctoral Dissertation, Technical University Hamburg-Harburg, 2003.

Riska, K., Wilhelmson, M., Englund, K., Leiviskä, T. (1997). Performance of Merchant Vessels in the Baltic. Research Report No. 52, December 2007, Helsinki University of Technology, Ship Laboratory, Espoo.

Riska, K. (2006a). Ship-Ice Interaction in Ship Design: Theory and Practice, ILS Oy, Helsinki, Finland and University of Science and Technology, Trondheim, Norway, p. 15.

Riska, K. (2006b). Design of Ice Breaking Ships, ILS Oy, Helsinki, Finland and University of Science and Technology, Trondheim, Norway, p. 12.

Runeberg, R. (1889). On Streamers for Winter Navigation and Ice-Breaking. Proceedings of Institution of Civil Engineers, Vol. 97, Session 1888-1889, p. 277-301.

Sawamura, J. (2012). Numerical Investigation of Ice Bending Failure and Ice Submerging Force for Ship Maneuvering in Level Ice. Proceedings of 21st International Symposium on Ice, Dalian, IAHR.

Schwarz, J., Jochmann, P., Hoffmann, L. (1981). Prediction of the Icebreaking Performance of the German Polar Research Vessel. Proceedings of 6th STAR Symposium, SNAME, Ottawa, Ontario, June 17-19.

Segal, Z.B. (1982). Determination of the Icebreaking Capability of River Icebreakers and Cargo Vessels. Sudostroenie, No. 7, 1982, p. 8-10.

Segal, Z.B., Levit, B. (1972). Trafficability of River Icebreakers in ice. Vodnyi Transport, No. 1, 1972, p. 47.

Shimansky, Ju.A. (1939). Conditional Standards of Ice Qualities of a Ship. Transactions of Arctic Institute of Chief Administrator of the Northern Sea Route, Vol. 130, Leningrad, pp. 59.

Shodi, D.S. (1995). Northern Sea Route Reconnaissance Study, A Summary of Icebreaking Technology. CRREL, Special Report No. 95-17, 1995.

Simonson, D.R. (1936). Bow Characteristics for Icebreaking. Journal of American Society of Naval Engineers, Vol. 48, No. 2, p. 249-254.

Spencer, D. (1992). A Standard Method for the Conduct and Analysis of Ice Resistance Model Tests. Proc. of the 23rd ATTC Symposium, p. 301-307.

Spencer, D., Jones, S.J. (2001). Model-Scale/Full-Scale Correlation in Open Water and Ice for Canadian Coast Guard "R-Class" Icebreakers. Journal of Ship Research, Vol 45, No 4, p. 249-261.

Su, B. (2011). Numerical Predictions of Global and Local Ice Loads on Ships. Doctoral Dissertation, Norwegian University of Science and Technology, 2011.

Tan, X., Su, B., Riska, K., Moan, T. (2013). A Six-Degrees-of-Freedom Numerical Model for Level Ice-Ship Interaction, Journal of Cold Regions Science and Technology, 92:1-16.

Tarshis M.K. (1959). Ice Resistance of Ships. Transactions of Murmansk Highest Navigational School, Murmansk, 1959, Issue 1.

Uemura, H.Y.O, Kato, Y.S.H., Izumiyama, K. (1997). Influence of Bow Shape on Icebreaking Resistance in Low Speed Range. Proceedings of 16th International Conference on Offshore Mechanics and Arctic Engineering/ 14th International Conference on Port and Ocean Engineering under Arctic Conditions (Joint OMAE/ POAC Conference), Yokohama, Japan, 13-18 April, 1997.

Valanto, P. (1989). Experimental and Theoretical Investigation of the Icebreaking Cycle in Two Dimensions, Doctoral Thesis, University of California, Berkeley, 1989.

Valanto, P. (1993). Investigation of the Icebreaking Pattern at the Bow of the IB Kapitan Sorokin on the Yenisei River Estuary in May 1991. Proceedings of 12th International Conference on Offshore Mechanics and Arctic Engineering, 1993.

Valanto, P. (2001). The Resistance of Ships in Level Ice. Transactions of SNAME, Vol. 109, 2001, p. 53-83.

Valanto, P. (2015). Icebreakers and Ice Strengthened Ships. In Compendium of Ship Hydrodynamics, Practical Tools and Applications, Chapter 18, L'ENSTA, 2015, ISBN 978-2-7225-0949-8, p. 451-469.

Vance, G.P. (1980). Analysis of the Performance of a 140-ft Great Lake Icebreaker: USCGC Katmai Bay. Report No. 80-8, CRREL, U.S. Army.

von Bock und Polach, R., Ehlers, S. (2011). Heave and Pitch Motions of a Ship in Model Ice: An Experimental Study on Ship Resistance and Ice Breaking Pattern. Journal of Cold Regions Science and Technology, 2011, 68:49-59.

Virtanen et al. (1975). Great Lakes Ore Carrier Series Ice Resistance Model Tests – Draft variation. Wärtsilä Icebreaking Model Basin, Test Report No. A-34 to U.S. Department of Commerce, Maritime Administration.

White, R.M. (1970). Prediction of Icebreaker Capability. Transactions of RINA, Vol. 112, No. 2, p. 225-251.

Yamaguchi, H., Kato, H. (1994). Hydrodynamic Effect of Ship Advance on Ice Flexural Failure. Proceedings of the 4th International Offshore and Polar Engineering Conference, ISPOE, Osaka, Japan, April 10-15, 1994.

Yamaguchi, H., Uemura, O., Suzuki, Y., Kato, H., Izumiyama, K. (1997). Influence of Bow Shape on Icebreaking Resistance in Low Speed Range. Proceedings of the International Conference on Ocean, Offshore and Arctic Engineering, OMAE 1997, Vol. IV.

Zahn, P.B., Phillips, L. (1987). Towed Resistance Trials in Ice of the USCGC Mobile Bay (WTGB103). Montreal, Canada: Transport Canada, Transportation Development Centre.

Zahn, P.B., Humphreys, D., Phillips, L. (1987). Full-Scale Towed Resistance Trials of the USCGC Mobile Bay in Uniform Level Ice. Transactions of SNAME, Vol. 95, 1987, pp. 45-77.

Zhou, Q., Peng, H. (2014). Numerical Simulation of a Dynamically Controlled Ship in Level Ice. Journal of Offshore and Polar Engineering, 2014, 24:184-191.

Zhou, Q., Peng, H., Qiu, W. (2016). Numerical Investigations of Ship-Ice Interaction and Maneuvering Performance in Level Ice. Journal of Cold Regions Science and Technology, 2016, 122:36-49.

This page is intentionally left blank.

Part II – Publications

This page is intentionally left blank.

Publication 1

Myland, D., Ehlers, S. (2014). Theoretical Investigation on Ice Resistance Prediction Methods for Ships in Level Ice. Proceedings of the 33rd International Conference on Ocean, Offshore and Arctic Engineering, OMAE 2014-23304, June 8-13, 2014, San Francisco, USA.

This page is intentionally left blank.

Publication 2

Myland D., Ehlers S. (2016). Influence of Bow Design on Ice Breaking Resistance. Journal of Ocean Engineering, 119 (2016), p. 217-232.

This page is intentionally left blank.

Ocean Engineering 119 (2016) 217–232

Contents lists available at ScienceDirect

Ocean Engineering

journal homepage: www.elsevier.com/locate/oceaneng

Influence of bow design on ice breaking resistance

Daniela Myland [a,b,*], Sören Ehlers [b,c]

[a] Hamburgische Schiffbau-Versuchsanstalt GmbH, HSVA, Bramfelder Str. 164, 22305 Hamburg, Germany
[b] Technische Universität Hamburg-Harburg, TUHH, Schwarzenbergstraße 95, 21073 Hamburg, Germany
[c] Norwegian University of Science and Technology, NTNU, NO-7491 Trondheim, Norway

ARTICLE INFO

Article history:
Received 11 March 2015
Accepted 6 February 2016
Available online 22 February 2016

Keywords:
Ice breaking resistance
Resistance prediction method
Bow shape
Ice breaking ships
Level ice

ABSTRACT

One of the main contributions to the resistance in level ice is the breaking force which is mainly influenced by the bow shape, beside ice properties and the ship's speed. Understanding the influence of the bow shape on the ice breaking resistance is essential for the assessment of the hull form in an early design stage. However, at a first glance the bow shapes of modern ice breaking vessels seem to be quite similar. Thus, a need exists to evaluate the contribution of the ice breaking force to the resistance in ice methodically for different bow shapes. Since model tests are still the most reliable resistance prediction method, they form the basis for the analysis of the ice breaking process at the bow. Specifically, breaking patterns and geometric bow parameters are investigated. The findings are compared with the selected semi-empirical method of Lindqvist. On this basis the Lindqvist approach is evaluated with further model test results and theoretical considerations. Finally, refinements of the Lindqvist formula are suggested where appropriate based on the analysis.

1. Introduction

The major requirement for ice breaking ships is a good performance in level ice. Good performance means low ice resistance, high propulsive efficiency and guaranteed continuity in ice breaking. This paper focuses on the resistance in ice, which can be subdivided into the following categories according to the different forces acting on the ship hull: Breaking, rotary, submersion and sliding forces (Puntigliano, 2003). This subdivision of the resistance in ice is the result of creation and advance of ice floes caused by the ship hull proceeding through the ice.

In practical ship design empirical or semi-empirical formulas are used to approximate the resistance in the early design stage. After one or more promising designs have developed, a numerical resistance prediction method based on Computational Fluid Dynamics (CFD) or other advanced numerical methods may be used. But up to now the available CFD-methods for ice resistance prediction are not sufficiently reliable to give a valuable contribution to the design process. Thus, in a later design stage model tests have to be used to evaluate one or few specific designs.

One of the main contributions to the resistance in level ice is the breaking force (Puntigliano, 2003; Riska, 2006; Valanto, 2001), which is mainly influenced by the bow shape, beside ice properties and the ship's speed. Although the bow shapes of modern ice breaking vessels seem to be quite similar at a first glance the breaking resistance may show significant differences. In order to save costs and time during the design process it is of great advantage to be able to evaluate the ice breaking resistance of a vessel in an early design stage as precisely as possible. However, there may be constraints for the bow geometry due to ice class requirements. Important ice class rules are given by the Finnish Transport Safety Agency, TraFi (TraFi, 2010), and the Russian classification society RMRS (Russian Maritime Register of Shipping, 2013). Specifically, TraFi requires a certain engine power depending on the ice class resulting from an approximation formula. The formula is based on the bow geometry and the main dimensions of the ship. The Russian rules require certain angles of the bow depending on the ice class. Beside the existing regulations, a need exists to evaluate the contribution of the ice breaking force to the total resistance methodically for different bow shapes.

As a consequence, a detailed analysis of different bow shapes based on ice model test results from HSVA's database from 1996 to 2014 is carried out. The analysis is based on current ice breaking ships such as Ice Breaking Supply Vessels, Anchor Handling Tugs as well as Salvage or Rescue Vessels. Especially in recent years the demand for such ice breaking ships increased strongly, which is why the majority of the available test data originates from this group of ships. The analysis focuses in particular on the breaking patterns formed in level ice (Fig. A15) with regard to relevant hull shape parameters as identified by Myland and Ehlers (2014). The main hull data of the ships are presented in Table A1. The ship models chosen for test analysis have similar scaling factors leading to model ice conditions, model speed values and ship model dimensions in the same range. In order to

* Corresponding author at: Hamburgische Schiffbau-Versuchsanstalt GmbH, HSVA, Bramfelder Str. 164, 22305 Hamburg, Germany.
E-mail addresses: myland@hsva.de (D. Myland), ehlers@tuhh.de (S. Ehlers).

http://dx.doi.org/10.1016/j.oceaneng.2016.02.021
0029-8018/

Nomenclature

B	ship breadth
E	modulus of elasticity
FP	pull force
g	gravitational acceleration
h_{ice}	level ice thickness
l	length of cusp
l_c	characteristic length of ice
L, L_{pp}	ship length between perpendiculars
L_{bow}	ship bow length
n	number of cusps
n_{idling}	rate of revolution at idling condition
n_{max}	maximum rate of revolution
R_B	bending resistance
R_{B1}	bending resistance at 1/8 B
R_{B2}	bending resistance at 2/8 B
R_{B3}	bending resistance at 3/8 B
R_{B4}	bending resistance at 4/8 B
R_{BR}	breaking resistance
R_C	crushing resistance
R_{ice}	ice resistance
R_{OW}	open water resistance
R_S	submersion resistance
RIT, R_{tot}	total resistance
T	ship draught
THDF	trust deduction fraction
TT	thrust
v	ship velocity
α	waterline (entrance) angle
α_{avg}	average waterline angle at center line of hull
$\alpha 1$	waterline angle at 1/8 B
$\alpha 2$	waterline angle at 2/8 B
$\alpha 3$	waterline angle at 3/8 B
$\alpha 4$	waterline angle at 4/8 B
$\Delta\rho$, ρ_g	density difference
μ	friction coefficient between ship hull and ice
ν	Poisson's ratio
ρ_w	density of water
σ_f, σ_{flex}	flexural strength
φ	buttock angle
ϕ	stem angle
ψ	normal angle – angle between normal to the bow plate and vertical
ψ_{avg}	average normal angle

obtain a certain friction coefficient between ice and hull ($\mu = 0.1$) the tested ship models were painted with a special paint composition.

The actual ice and ship property values of the selected ice model tests were measured during the testing and extrapolated to their target values in full scale as listed in Table A2. The extrapolation was done according to HSVA's standard correction methods (Appendix C – Data Analysis). The methods were set up in the past by comparison of full scale trials with corresponding model test results. These correction methods have been validated against full scale data several times. Using the target ice and ship property values improves the precision of the analysis since the range of considered ice properties is reduced. Thus, the ice and ship property values as listed in Table A2 can be kept almost constant throughout the analysis. As a consequence the analysis can be mainly focused on the bow shape. Due to the fact that the selected model tests were carried out as towed propulsion tests the target value of the ship speed is equal to the measured value. The model test conditions of ice and investigated ships correspond to typical design values of the chosen group of ships.

Understanding the influence of the bow shape on the total resistance is essential for the assessment of the hull form in an early design stage. Several theoretical ice prediction methods may be applied here, e.g. Su et al. (2010), Sawamura (2012), Lindström (1990), Valanto (2001) and Lindqvist (1989), which take into account the physical effects of the ice breaking process by different approaches. In Table A3 a systematic comparison of the mentioned methods is given.

Another issue, which has a large influence on the prediction of the resistance in ice, is the precision with which the hull shape of the ship is considered. Provided that the hull shape is taken into account, only a limited number of characteristic values are used for its description. The same applies for the ice conditions. Thus, from comparison of the presented theoretical ice prediction methods it can be concluded that the relevant resistance contributions are considered differently for each method by means of generalizing assumptions, strong simplifications, or are even neglected in the existing approaches. Thus, further research is required to predict the resistance and its components more precisely as stated in Myland and Ehlers (2014).

From theoretical considerations the obvious difference between model tests and all presented methods in Table A3 is that model tests seek to cover major physical effects of full scale ship-ice interaction, whereas almost every analytical or empirical method is the result of the author's judgment about the significance and influence of each physical effect by setting up equations to describe them. However, some of the formulas include physical effects of full scale ship-ice interaction by taking into account model test results. Nevertheless, also these methods lead to only rough estimations of the resistance, since the present ship design, i.e. the bow shape, is not fully considered in the applied prediction method. Consequently, the aim of this paper is to analyze the ice breaking process at the bow in more detail, compare the findings with a selected semi-empirical method, evaluate the semi-empirical method with further model test results and theoretical considerations and finally suggest adjustments where appropriate based on the analysis. The prediction method is chosen on the basis of Table A3 with the objective to identify the influence of geometric changes on the resistance rapidly in the conceptual design phase. Table A3 reveals that the Lindqvist method is the most advanced empirical prediction method for calculation of the ship`s resistance in level ice by taking into account the most hull shape and ice parameters.

2. Presentation of applied methods

Brief descriptions of two resistance prediction methods are given in this chapter – Lindqvist approach and ice model tests.

Since model tests are still the most reliable resistance prediction method, they form the basis for the analysis of the ice breaking process at the bow. The findings are finally used to suggest adjustments for the semi-empirical method of Lindqvist where appropriate. Table A3 reveals that the approach of Lindqvist forms a valuable basis for revision, because it takes into account most relevant hull shape and ice parameters.

2.1. Lindqvist approach

Lindqvist (1989) approximated the ice resistance by simple but physically sound formulas. The considered hull parameters are presented in Fig. A7.

Lindqvist divided the ice resistance into two main components- ice breaking and submersion of the ice floes. The submersion component includes the resistance due to ice floes sliding along the ship hull, whereas the rotation of the ice floes is not taken into account by Lindqvist. The breaking component is further divided into a bending (Eq. (1)) and a crushing (Eq. (2)) component.

$$R_B = \left(\frac{27}{64}\right)\sigma_f B \frac{\left(h_{ice}^{1.5}\right)}{\sqrt{\frac{E}{12(1-\nu^2)\rho_w g}}}\left(\tan(\psi)+\mu\frac{\cos(\phi)}{\cos(\psi)\sin(\alpha)}\right)\left(1+\frac{1}{\cos(\psi)}\right) \quad (1)$$

$$R_C = 0.5\sigma_f h_{ice}^2\left(\tan(\phi)+\mu\frac{\cos(\phi)}{\cos(\psi)}\right)\Big/\left(1-\mu\frac{\sin(\phi)}{\cos(\psi)}\right) \quad (2)$$

where R_B is the bending resistance, σ_f the flexural strength, B the ship breadth, h_{ice} the ice thickness, ν the Poisson's ratio, ρ_w the density of water, g the gravitational acceleration, ψ the normal angle, μ the friction coefficient between ship hull and ice, ϕ the stem angle, α the waterline entrance angle and R_C the crushing resistance. The normal angle is calculated from the waterline entrance angle and the stem angle according to Eq. (3).

$$\psi = \text{atan}(\tan(\phi)/\sin(\alpha)) \quad (3)$$

Both, Eqs. (1) and (2) were derived from semi-empirical approximation of the physical process of ice breaking. The formulas consider only roughly the mechanical and geometrical parameters.

The submersion component was estimated by application of full scale experiments and experience gained from model testing. From observations Lindqvist knew that the underwater part of the bow is more or less completely covered by ice pieces. This knowledge led to the calculation of the submersion resistance as the sum of the loss of potential energy and the frictional forces that are acting between the ship hull and the ice floes (Eq. (4)).

$$R_S = \rho_g g h_{ice} B\left(\frac{T(B+T)}{B+2T}+\mu\left(0.7L-\frac{T}{\tan(\phi)}-\frac{B}{4\tan(\alpha)}+T\cos(\phi)\cos(\psi)\sqrt{\frac{1}{\sin(\phi)^2}+\frac{1}{\tan(\alpha)^2}}\right)\right) \quad (4)$$

where R_S is the submersion resistance, ρ_g the density difference, T the ship draught and L the ship length between perpendiculars.

The influence of a plough is not considered in the formula, whereas the ship's draft and the density difference between ice and water are taken into account. The total estimated bottom coverage of the vessel is 70%, since the stern of the vessel is in general not completely covered by ice.

The main resistance components are extended by speed dependent components based on empirical constants. Thus, the resulting ice resistance is reported by Lindqvist as given in Eq. (5).

$$R_{ice} = (R_c+R_B)\left(\frac{1+1.4*\nu}{\sqrt{g*h_{ice}}}\right)+R_S\left(\frac{1+9.4*\nu}{\sqrt{g*L}}\right) \quad (5)$$

where R_{ice} is the ice resistance and ν the ship velocity.

2.2. Ice model tests at HSVA

In order to understand the influence of the bow shape on the ice breaking resistance model test results from HSVA's database are used. Almost all ship model tests at HSVA, which serve for determination of the resistance in level ice, were performed as towed propulsion tests. Provided that the rate of revolution is varied within a sufficient wide range the towed propulsion test is a favorable alternative to the pure towing test for determination of the total resistance in ice. From pure towing tests only the resistance in ice can be obtained whereas much more information can be gained by towed propulsion tests, such as information about thrust deduction, propulsion efficiency and required propulsive power. Thus, the test data for the analysis are taken from towed propulsion tests which provide both, suitable underwater videos to evaluate the bow shapes as well as the total resistance values.

2.2.1. Ship model preparation

The following equipment, partly installed in the ship model itself, was used to perform towed propulsion tests in level ice: Propulsion system; In case of pods six component scales or in case of conventional propulsion systems dynamometers to measure thrust of the ship model; Load cell at the bow to measure the towing force; Speed wheel to measure carriage speed and position; Data acquisition and storage system and power supply system.

Fig. A8 shows exemplarily a ship's propulsor (left) and presents the load cell mounted at the bow to measure the pull force FP during a towed propulsion test (right).

2.2.2. Model ice preparation

According to Evers and Jochmann (1993) HSVA's current model ice preparation starts with freezing the ice from a 0.7% sodium chloride solution, where the ice surface is exposed to pre-cooled air of about −18° C. By spraying water into the cold air of the ice tank (Fig. A9) the droplets freeze in the air and form small ice crystals, which settle on the water surface such that the growth of a fine-grained ice of primarily columnar crystal structure is initiated.

Highly pressure-saturated air in the tank water leads to formation of air bubbles with a diameter of 200–500 μm embedded in the model ice. Due to the air content in the ice it is appearing white. This side effect is beneficial for the analysis of photos and videos of ice tests.

Before reaching the target ice thickness the cooling system is switched off and the air temperature is raised to a point slightly above the freezing point (Fig. A10). This temperature is kept until the target flexural strength is reached. Then, the heat transfer into the tank is reduced to a minimum in order to keep the flexural strength almost constant for the duration of the test.

2.2.3. Test execution – towed propulsion test

During a towed propulsion test (Fig. A11) the ship model is towed at a constant speed value and the propeller rate is raised in steps from idling propeller condition up to a rate above the self-propulsion point. During this procedure the pull force and the total thrust are measured as shown in Fig. A12. The pull force is recorded by the load cell mounted at the ship bow (Fig. A8, right), whereby the system thrust is determined by a six component scale located at the top of the propulsor's shaft line in case of pods and by a dynamometer at the shaft line in case of conventional propulsion systems. The data are measured with 50 Hz.

2.2.4. Test results – total resistance in ice

Assuming that for a constant speed the thrust deduction fraction, THDF, is independent of the rate of revolution or the propulsor load, respectively, a linear regression is employed to the data of pull force vs. developed propulsor thrust. Using this regression function the towing force for vanishing thrust is determined. The value obtained in equilibrium is the total resistance, RIT, see Fig. A12.

2.2.5. Test results – breaking pattern

One of the most important results for the following analysis is the video recording made below the water surface of the breaking process of the ice sheet at the ship bow. Snapshots are generated from those underwater videos showing the breaking patterns of the bow segments as shown in Appendix A. As an example, a series of snapshots from different breaking cycles for one ship model within one test run (constant speed and almost constant ice

conditions) is presented in Fig. A14. From all of the snapshots belonging to the shown series just minimal differences between the images can be identified. Since these differences are within the required accuracy for the following analysis all of them are considered to be representative for a certain ship under the given conditions as presented in Table A2. As a consequence, only one characteristic snapshot per test run is used for the analysis.

3. Review of Lindqvist method

In order to identify possible improvements of Lindqvist's approach for the prediction of the ice breaking resistance, the total resistance values from model testing are compared to the ice resistance values from Lindqvist's approach. The resistance values gained by model testing are calculated according to the procedure described in Chapter 2.2.4. Table A4 summarizes the results, which are normalized by the mean length of all ships due to confidentiality reasons. Therein, a much narrower scatter of resistance values for the Lindqvist approach compared to the model test results are shown. Additionally, the ice resistance values estimated on the basis of the Lindqvist approach are mostly smaller than the ones from model testing. Both aspects indicate that Lindqvist does not take into account all physical effects related to the ice breaking process.

Considering the above mentioned points the approach of Lindqvist is reviewed by the help of further model test results as well as theoretical considerations. In particular the consideration of the following aspects concerning the breaking force as a part of the ice resistance (Eq. (1)) is further investigated and refined in the following subchapters: Open water resistance; Ship shape parameters and number of cusps/breaking pattern.

3.1. Open water resistance

The resistance due to the water flow around the hull is not taken into account in Lindqvist's approach. It is commonly known that the influence of this water flow to the total resistance is small. Nevertheless, this portion should be considered as a part of it. The open water resistance can be subdivided into the following parts: frictional resistance, wave resistance, eddy resistance and air resistance. The wave and the eddy resistance may be reduced due to the presence of ice. Since both portions are small under Froude numbers of 0.1, the resistance due to the water flow around the hull in ice is assumed to be equal to the open water resistance (Eq. (6)).

$$R_{tot} = R_{ice} + R_{ow} \tag{6}$$

where R_{tot} is the total resistance.

The ice resistance R_{ice} is given in Eq. (5) by Lindqvist (1989). Thus, the total resistance R_{tot} can be expressed by Eq. (7).

$$R_{tot} = (R_c + R_B)\left(\frac{1+1.4*\nu}{\sqrt{g*h_{ice}}}\right) + R_S\left(\frac{1+9.4*\nu}{\sqrt{g*L}}\right) + R_{ow} \tag{7}$$

3.2. Selection of ship shape parameters

For predicting the ice breaking force, Lindqvist considers the bow geometry by means of four ship shape parameters as stated in Chapter 2.1, i.e. ship breadth, stem angle, waterline entrance angle and normal angle at the stem. In order to evaluate the influence of these parameters the model test results are analyzed regarding correlations between the geometric parameters and the resistance values. These correlations are derived from Table A5 and Fig. A13. In order to use the total resistance values taken from HSVA's data base in a confidential way, they are parameterized by the mean length of all investigated ships.

Fig. A13 reveals a clear influence of the stem angle on the total resistance in ice, meaning the total resistance in ice tends to be higher for increasing stem angles. None of the other parameters, i.e. the waterline entrance angle, the normal angle at the stem and the ship breadth respectively shows any clear dependency between the total resistance in ice and the according ship shape parameters. One possible reason is that the study is based on a specific type of ship and thus, the considered parameters are within a narrow range. However, the breaking pattern and the total resistance values from model testing show significant differences. Hence, it seems that the ship shape parameters selected by Lindqvist may have to be extended or the mathematical expressions within the formulas may have to be modified.

3.3. Refinement of ship shape parameters

As already concluded from Table A4 and Chapter 3.1.2 minor changes in the hull shape are not considered for the resistance values according to the Lindqvist approach. In order to be more precise HSVA divided the ship breadth, B, into four sections: 1/8 B, 2/8 B, 3/8 B and 4/8 B from the centerline as shown in Fig. A21. Accordingly, the buttock angle and the waterline angle are determined. Each normal angle is calculated from the waterline (entrance) angle as well as the stem or buttock angle φ according to Eqs. (3) or (8) respectively.

$$\psi = \mathrm{atan}(\tan(\varphi)/\sin(\alpha)) \tag{8}$$

Finally, the formula for calculation of the bending resistance is extended by the resistance contributions resulting from the different sections as shown in Eqs. (9)–(13).

$$R_{B1} = \left(\frac{27}{64}\right)\sigma_f \frac{B}{4}\frac{\left(h_{ice}^{1.5}\right)}{\sqrt{\frac{E}{12(1-\nu^2)\rho_w g}}}\left(\tan(\psi_1) + \mu\frac{\cos(\varphi_1)}{\cos(\psi_1)\sin(\alpha_1)}\right)\left(1+\frac{1}{\cos(\psi_1)}\right) \tag{9}$$

$$R_{B2} = \left(\frac{27}{64}\right)\sigma_f \frac{B}{4}\frac{\left(h_{ice}^{1.5}\right)}{\sqrt{\frac{E}{12(1-\nu^2)\rho_w g}}}\left(\tan(\psi_2) + \mu\frac{\cos(\varphi_2)}{\cos(\psi_2)\sin(\alpha_2)}\right)\left(1+\frac{1}{\cos(\psi_2)}\right) \tag{10}$$

$$R_{B3} = \left(\frac{27}{64}\right)\sigma_f \frac{B}{4}\frac{\left(h_{ice}^{1.5}\right)}{\sqrt{\frac{E}{12(1-\nu^2)\rho_w g}}}\left(\tan(\psi_3) + \mu\frac{\cos(\varphi_3)}{\cos(\psi_3)\sin(\alpha_3)}\right)\left(1+\frac{1}{\cos(\psi_3)}\right) \tag{11}$$

$$R_{B4} = \left(\frac{27}{64}\right)\sigma_f \frac{B}{4}\frac{\left(h_{ice}^{1.5}\right)}{\sqrt{\frac{E}{12(1-\nu^2)\rho_w g}}}\left(\tan(\psi_4) + \mu\frac{\cos(\varphi_4)}{\cos(\psi_4)\sin(\alpha_4)}\right) \times \left(1+\frac{1}{\cos(\psi_4)}\right) \tag{12}$$

$$R_B = R_{B1} + R_{B2} + R_{B3} + R_{B4} \tag{13}$$

where R_{B1} is the bending resistance at 1/8 B, R_{B2} the bending resistance at 2/8 B, R_{B3} the bending resistance at 3/8 B and R_{B4} the bending resistance at 4/8 B.

3.4. Number of cusps

The ice is broken at the ships's bow into a certain number of cusps. The number of cusps n is obtained according to Lindqvist by Eq. (14).

$$n = B/(l * \sin(\alpha)) \tag{14}$$

Lindqvist assumes that the length of the cusps, l, broken during sailing through ice is one third of the characteristic length of ice, l_c (Eq. (15)).

$$l = 1/3 l_c \tag{15}$$

where by the characteristic length of ice, which is a measure for the deformation of ice, is determined as stated in Eq. (16).

$$l_c = \left(E * \frac{h_{ice}^3}{(12 * (1-\nu^2) * \rho_w * g)} \right)^{0.25} \tag{16}$$

where E is the modulus of elasticity.

The publication of Lindqvist (1989) does not reveal in detail where and when during the breaking process this number of cusps, n, is reached. However, it can be derived from Eq. (14) that n is the number of cusps which is broken within one breaking cycle at the waterline at the bow. The submersion part of the total resistance as defined by Lindqvist does not take into account any further breaking within the breaking process. From the underwater videos (Figs. A1–A6) further breaking of the cusps in the bow region can be identified. Since further breaking induces additional forces at the bow, it can be assumed that this is at least one reason for deviating total resistance values between model tests and Lindqvist.

In order to consider further breaking in the bow region in addition to the initially broken ice floes the number of cusps is determined at the end of the bow region. This is done for each of the ships studied in this paper on the basis of underwater video recording of model tests as presented in Appendix A. Finally, the determined number of cusps is compared to the number of cusps resulting from Lindqvist's approach. Table A6 summarizes the values of both methods.

Although the number of cusps is strongly affected by the complete bow geometry, Lindqvist considers only a limited number of hull shape parameters for its calculation. For the investigated ships these parameters are in a very narrow range. In contrast, the model tests consider the complete bow geometry including special design features such as the forward skeg. The number of cusps determined from model tests show a wider scatter than the number of cusps calculated on the basis of Lindqvist's approach, as it can be seen in Table A6.

Furthermore, the number of cusps determined from model tests is in most cases slightly lower than the number of cusps according to Lindqvist. This is noteworthy especially, when realizing that the number of cusps determined from model tests is considered at the end of the bow region, whereas the Lindqvist approach is supposed to give the number of cusps during the initial breaking process at the waterline. But since the relation of bending strength to compressive strength cannot be modeled correctly and thus, natural sea ice is more brittle than the model ice, it is usual that fewer cusps are broken during model testing compared to ice breaking in reality. Consequently, the cusp number defined by Lindqvist may have the correct range for ice breaking in natural sea ice. The deviation related to the more ductile model ice is usually being compensated when scaling the total resistance and other model test results to full scale by applying the correction methods as stated in Chapter 1.

4. Further investigation on ice breaking resistance

On the basis of the gained knowledge by review of the Lindqvist approach (Chapter 3) the influence of the ship geometry on the total resistance is investigated in more detail. For the investigation model test results are used, i.e. snapshots and geometric parameters. Snapshots of the bow area of the studied ships are prepared from underwater videos (Appendix A) and subdivided into two breaking pattern classes. Moreover, selected geometric parameters of each ship bow are analyzed in order to identify correlations between the ship's hull shape and the total resistance in ice specific for each breaking pattern class. The analysis findings are compared to the results obtained from the review of Lindqvist's semi-empirical method. Table A8 summarizes the investigated ship data and test conditions.

4.1. Breaking pattern classes

To evaluate the influence of bow shapes on the total resistance in ice the chosen ships are divided into two breaking pattern classes by visual assessment of the ice breaking pattern they create, see Table A7. Examples for both breaking pattern classes are given in Fig. A15. Breaking pattern class 1 is characterized by large ice floes covering the ship hull in a regular pattern. Mostly, one ice floe covers half of the ship's breadth. Breaking pattern class 2 shows smaller sized floes and consequently an increased amount of floes with different shapes. While the ice floes of breaking pattern class 1 are shaped like bars, which are arranged in a regular pattern, the ones of breaking pattern class 2 are shaped and arranged more individually. A further subdivision of the breaking pattern classes may be possible with a significantly larger set of ships, which is, however, beyond the scope of this analysis.

Based on the defined breaking pattern classes it can be concluded from Table A6 that the number of cusps determined from the underwater video recording seems to be slightly higher for breaking pattern class 2 than the cusp numbers for breaking pattern class 1. Nevertheless, the clarity with which the ships of the study could be divided into breaking pattern classes based on the initial breaking pattern at the bow has diminished at the beginning of the parallel midship. For consolidating the dependency the data basis may have to be extended or the quality of investigated snapshots may have to be improved. In contrary, the values resulting from Lindqvist's approach do not outline any dependency to the breaking pattern classes.

4.2. Geometric parameter analysis

Understanding the influence of the bow geometry on the total resistance in ice is essential for development or assessment of a preliminary bow shape in an early design stage. The review of Lindqvist's approach revealed that the selection of bow shape parameters may have to be extended or the mathematical expressions within the formulas may have to be modified. Thus, the correlations between selected geometric parameters and the resistance values specific to each breaking pattern class are analyzed. The parameters comprise the ones selected by Lindqvist and further bow parameters as identified by Myland and Ehlers (2014) and listed in Table A8.

The average waterline angle in Table A8 is calculated as given in Eq. (17).

$$\alpha_{avg} = (\alpha + \alpha_1 + \alpha_2 + \alpha_3 + \alpha_4)/5 \tag{17}$$

where α_{avg} is the average waterline angle, α_1 the waterline angle at 1/8 B, α_2 the waterline angle at 2/8 B, α_3 the waterline angle at 3/8 B and α_4 the waterline angle at 4/8 B.

For determination of the average buttock and normal angles Eq. (17) has to be adjusted accordingly.

In order to plot the total resistance values taken from HSVA's data base in a confidential way, they are parameterized by the mean length of all investigated ships. The ship bow length is defined as the waterline length between the ship bow and the parallel midship (Fig. A16).

In general Table A8 reveals smaller resistance values for breaking pattern class 1 than for breaking pattern class 2. Furthermore, the values indicate a correlation of the bow length, the average buttock angle and the average normal angle to the total

resistance, RIT, and at the same time to the breaking pattern classes as shown in Figs. A17–A20. However, these parameters are geometrically related to the stem angle, especially the bow length and the average buttock angle. Thus, their dependency might be a result of this relation. The average normal angle considers additionally the waterline entrance angle. However, a modification of the mathematical expressions even with respect to the average normal angle does not seem to be feasible.

By reviewing the waterlines of the different ships basically two characteristics can be developed. Some waterlines are straight or even concave and have a small shoulder radius, whereas other waterlines are smoothly rounded with a large radius at the shoulder, as shown exemplarily in Figs. A22 and A23. But the characteristics are often too weakly pronounced to allow a clear distribution into groups. In addition, the characteristics cannot be assigned to the breaking pattern classes.

5. Results of refined method

In this section the results of the refined Lindqvist formula for common ice breaking ships as defined in Chapter 1 are compared to both, values calculated by application of Lindqvist's original approach and model test results. Since the execution of model tests is still the most reliable method to determine the total resistance in ice, the model test results are used as a basis to evaluate the suitability of the other two approaches. Thus, Fig. A24 shows the results of both formulas in relation to the corresponding model test result for each ship.

As it can be seen in Fig. A24 the deviations of the original semi-empirical method from the model test results could be reduced for most of the investigated ships by application of the refined method. Specifically, for ship models 4, 5 and 8 the refined method resulted in slightly increased deviations compared to the original method. For all other investigated models the deviation was reduced, for both over and under estimated values of the original Lindqvist approach. For ship model No. 3 the refined method leads to a slight over estimation of the total resistance in ice, whereas the original method resulted in an under estimation. By means of the prediction formulas the total resistance in ice seems to be under estimated for ship models belonging to breaking pattern class 2. Whereas the predicted total resistance in ice is partly under estimated and partly over estimated for the ship models of breaking pattern class 1. However, the scatter of deviations of resistance values according to both Lindqvist formulas from model test results is in the same range for both breaking pattern classes, when neglecting the outlier, i.e. the resistance of ship model 5.

6. Summary and conclusions

This paper evaluates the influences of different bow shapes on the resistance caused by a ship advancing in level ice. Model test results and theoretical considerations are used for identification of inconsistencies and subsequent refinement of a semi-empirical resistance prediction method, i.e. the approach of Lindqvist. The evaluation of the Lindqvist approach focuses on the component of the resistance which is related to ice breaking. By means of snapshots from underwater video recording the considered ships were divided into two breaking pattern classes. Based on the gained knowledge further model test results were used to find a possible correlation between bow shape parameters or two dimensional characteristics and the total resistance in ice with relation to the defined breaking pattern classes. Finally, the resistance values resulting from the developed refinements of the Lindqvist approach are compared to the resistance values of the original Lindqvist method and the values from model testing.

Lindqvist only considers a certain number of hull shape parameters instead of the complete bow geometry. An evaluation of the ship shape parameters selected by Lindqvist as well as further usual ship shape parameters shows that the ship shape parameters selected by Lindqvist already represent the main influences, i.e. basically the stem angle, but neglect at least geometry details which have a certain contribution to the total resistance in ice. From further analysis of model test results a dependency of the breaking pattern classes to the total resistance in ice is determined. A breaking pattern consisting of small and irregular-shaped ice floes (breaking pattern class 2) seems to induce a higher resistance than a more regular shaped breaking pattern consisting of large ice floes only (breaking pattern class 1). However, with the available data base it does not seem to be feasible to obtain sound correlations between ship shape parameters and the total resistance in ice related to the breaking pattern classes. Neither an analysis of the waterline characteristics reveals a valuable correlation.

A comparison of the number of cusps considered in the Lindqvist approach and determined from underwater video recording revealed a significant difference. It is assumed that the number of cusps in Lindqvist's method is supposed to indicate the amount of ice floes in one broken row at the waterline. The underwater video recording from the model tests show significantly less floes even when taking into account that the number of cusps in one row at the beginning of the parallel midship should be the governing parameter related to ice breaking. However, the number of cusps strongly depends on the type of model ice preparation and resulting model ice properties. The latter, and consequently the breaking pattern, may deviate from the ice properties in reality.

By a refinement of the considered bow angles, i.e. normal angle, stem angle and buttock angle, Lindqvist's formula could be improved slightly. Further slight improvements may be possible with an extended data base or video material of better quality.

In order to further investigate possible causes for the wide scatter of resistance values in ice with respect to the defined common ice breaking ships, special design features such as geometric dimensions of the forward skeg and its influence on the ice breaking process may have to be evaluated. In addition the distribution of ships into breaking pattern classes may contribute to the investigation of the bow geometry influence on ice breaking resistance, although no precise correlation could be determined within this analysis.

As stated in the introduction both model tests and theoretical ice prediction methods have their uncertainties. Due to the complexity of the ice breaking process, all theoretical approaches necessarily make use of assumptions and simplifications resulting in rough estimations of the physical effects. However, model tests seek to cover major physical effects of the ice breaking process. Uncertainties may result from scaling methods and the modeled ice structure, especially the ratio between compressive and flexural strength. Finally, both methods have their advantages and thus, their reason for existence. Theoretical methods are essential tools during the early design stage of a ship, whereas model tests are still the most reliable prediction method for the total resistance of ships in ice and thus, are to be applied in a later design stage.

Acknowledgment

The authors are grateful to HSVA and NTNU for financial support of the paper.

Appendix A. Snapshots of breaking patterns for investigated ship models

See Figs. A1–A24.

Fig. A1. Breaking pattern of ship model 1 (left) and ship model 2 (right).

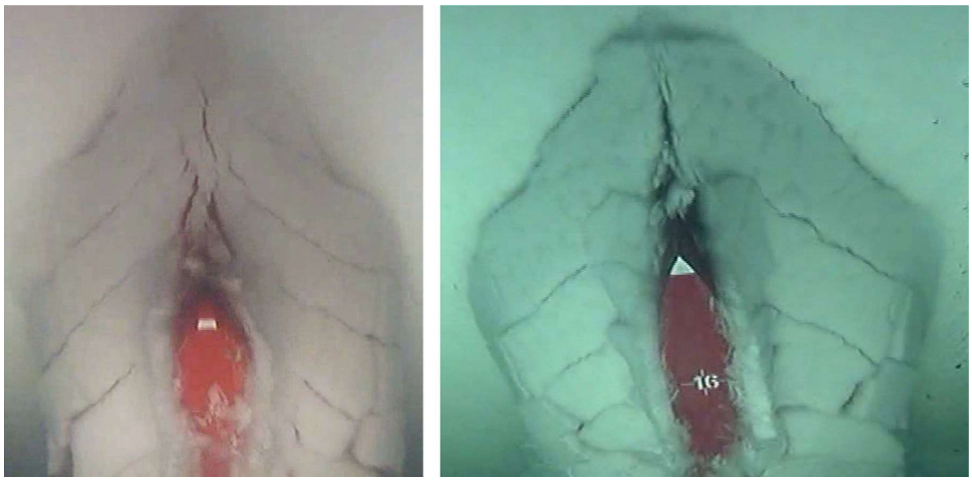

Fig. A2. Breaking pattern of ship model 3 (left) and ship model 4 (right).

Fig. A3. Breaking pattern of ship model 5.

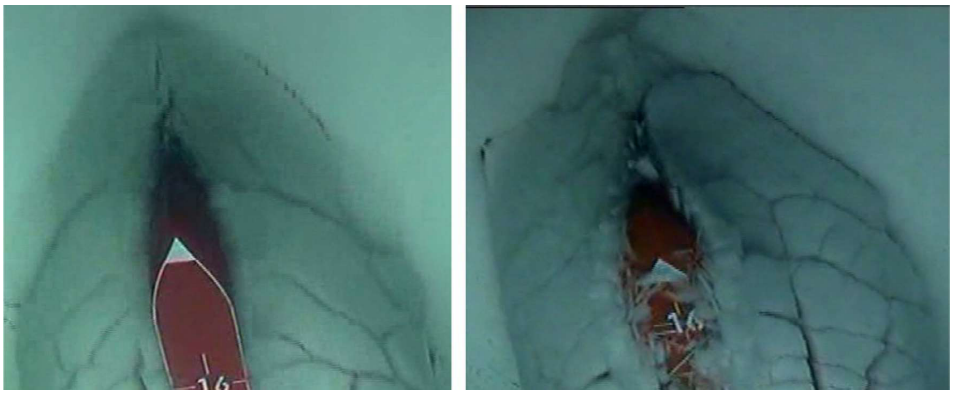

Fig. A4. Breaking pattern of ship model 6 (left) and ship model 7 (right).

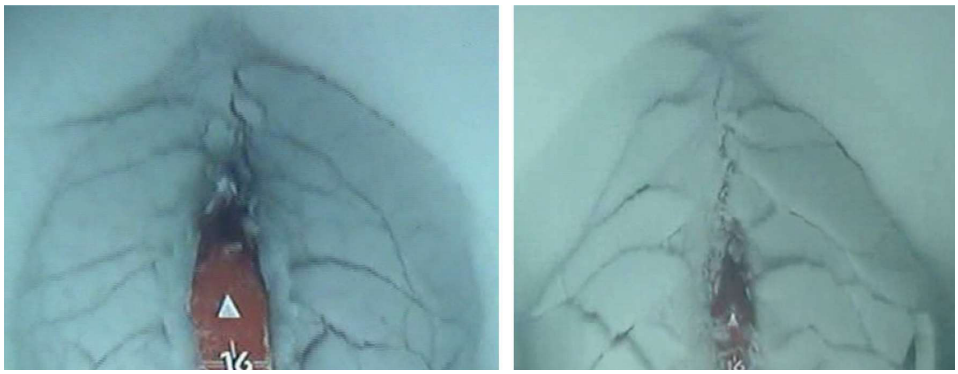

Fig. A5. Breaking pattern of ship model 8 (left) and ship model 9 (right).

Fig. A6. Breaking pattern of ship model 10 (left) and ship model 11 (right).

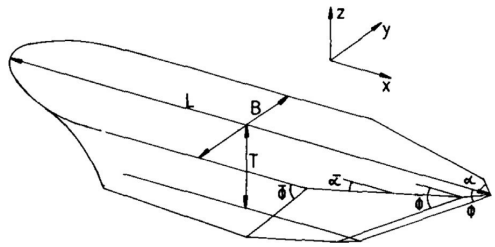

Fig. A7. Considered hull parameters by Lindqvist (1989).

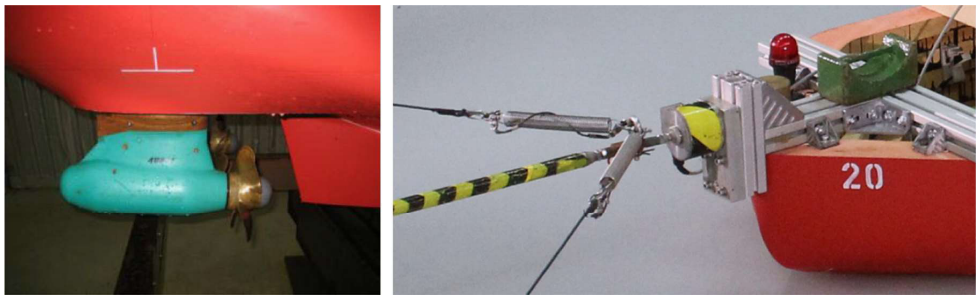

Fig. A8. Left: azimuth thruster of tested ship model, right: load cell at bow.

Fig. A9. Water is sprayed into the air of the pre-cooled ice tank at HSVA forming small ice crystals which settle on the water surface.

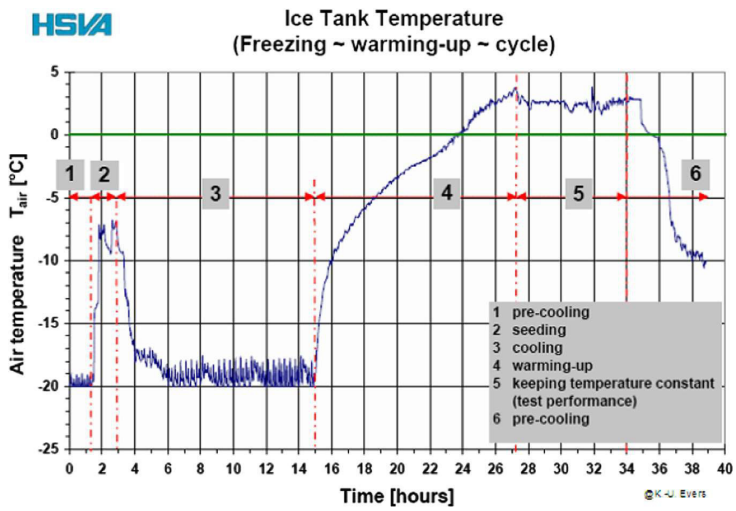

Fig. A10. History of temperature during freezing–warming-cycle in the ice tank (Sutherland and Evers, 2013).

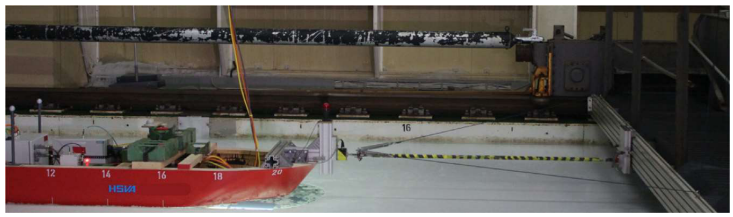

Fig. A11. Execution of towed propulsion test.

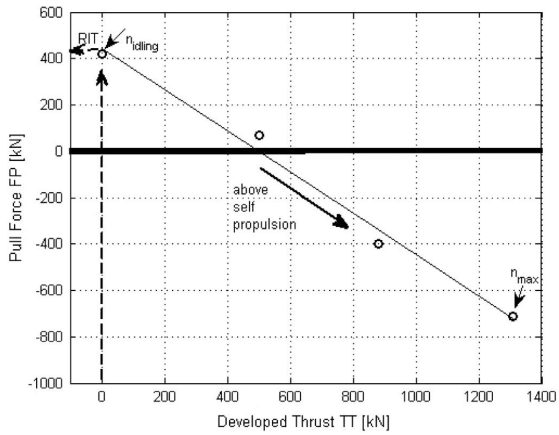

Fig. A12. Test analysis of towed propulsion test in ice.

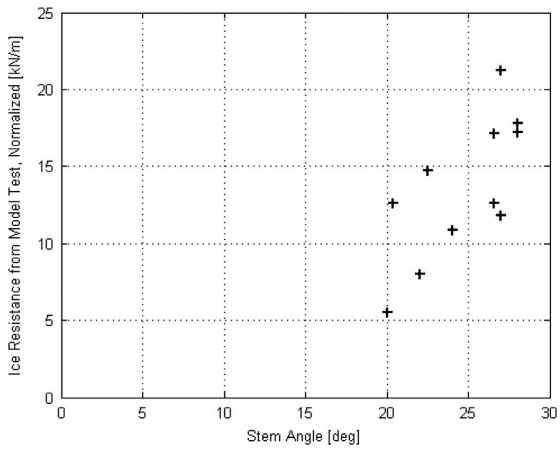

Fig. A13. Total resistance from model testing vs. stem angle.

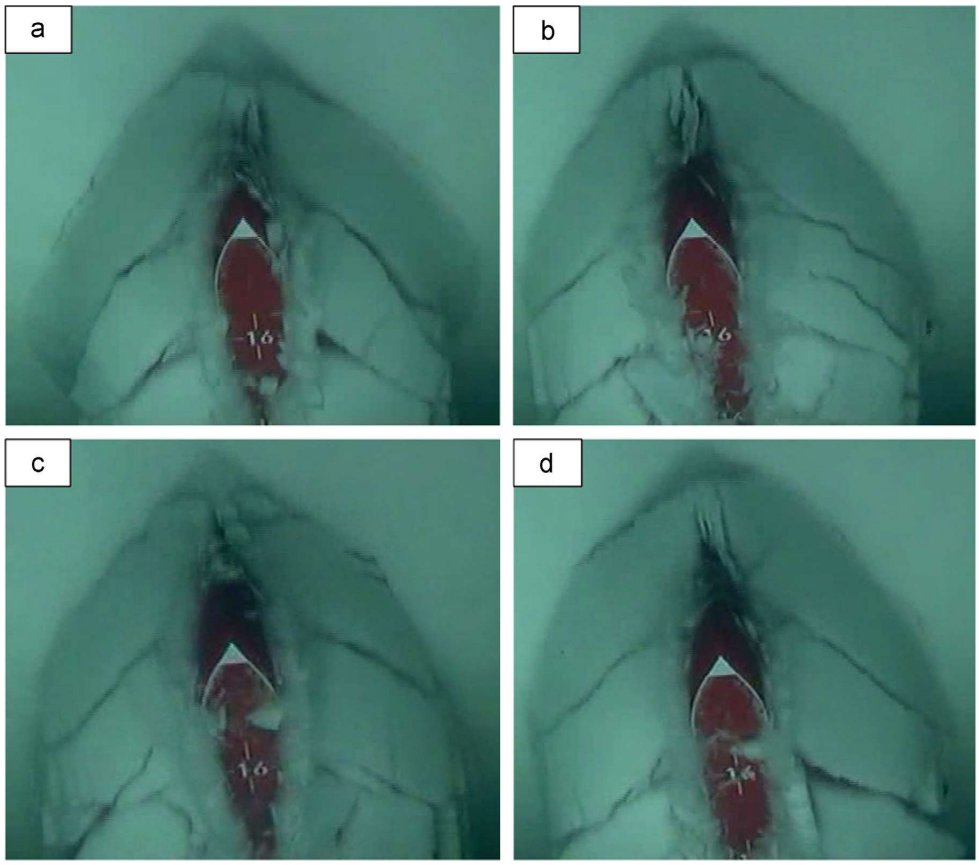

Fig. A14. Series of snapshots for different breaking cycles within one test run.

Fig. A15. Left: example for breaking pattern class 1, right: example for breaking pattern class 2.

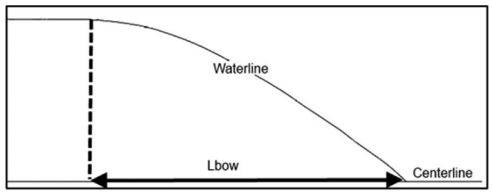

Fig. A16. Definition of bow length L_{bow}.

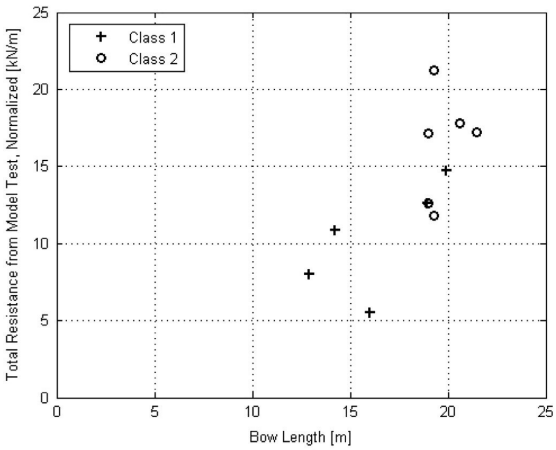

Fig. A17. Total resistance from model testing vs. ship bow length.

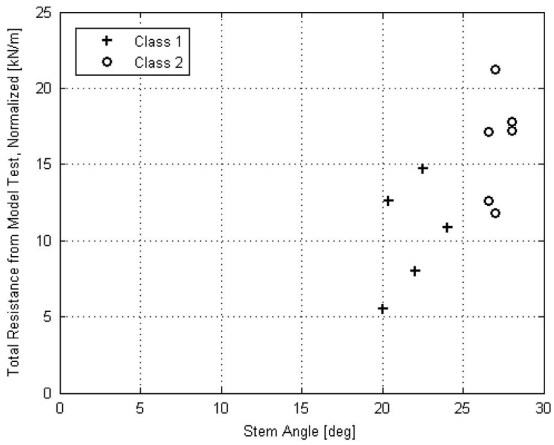

Fig. A18. Total resistance from model testing vs. ship stem angle.

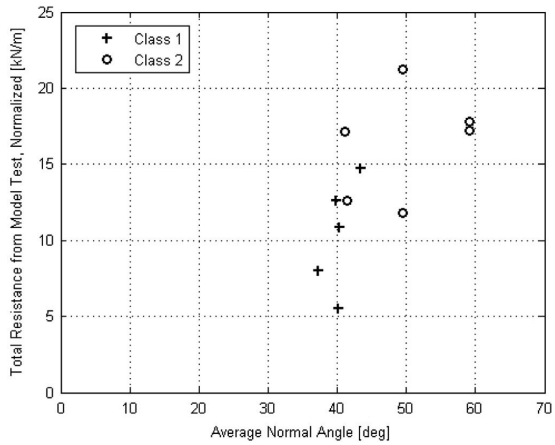

Fig. A19. Total resistance from model testing vs. average normal angle of ship.

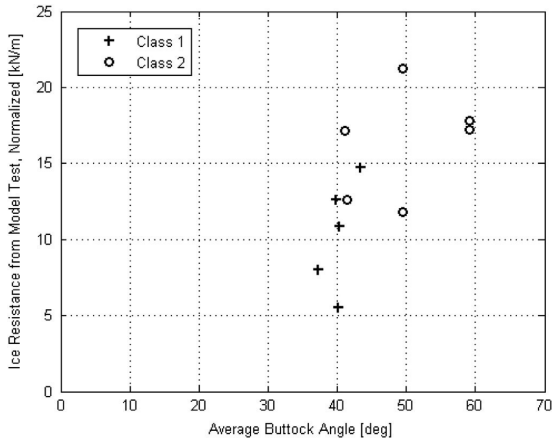

Fig. A20. Total resistance from model testing vs. average buttock angle.

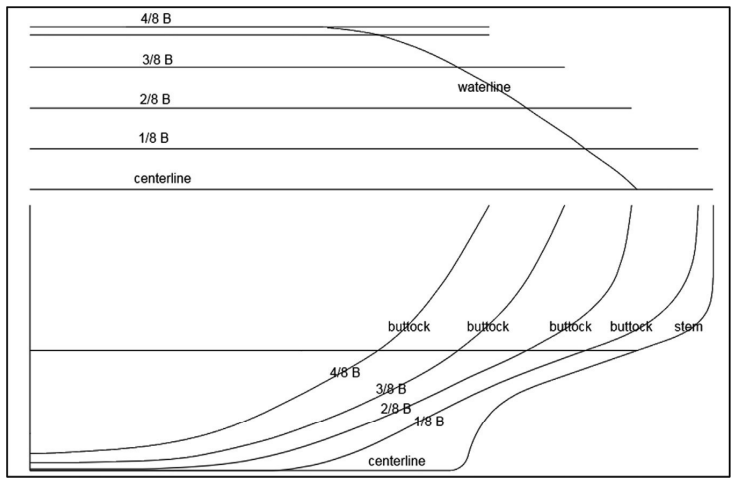

Fig. A21. Definition of waterline and buttock angles.

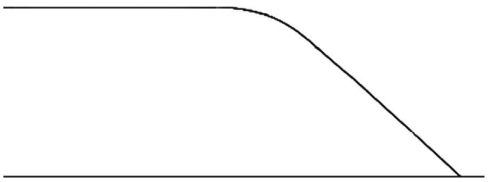

Fig. A22. Example of waterline characteristic 1.

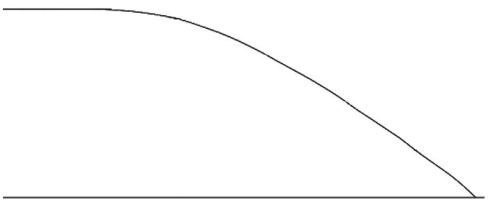

Fig. A23. Example of waterline characteristic 2.

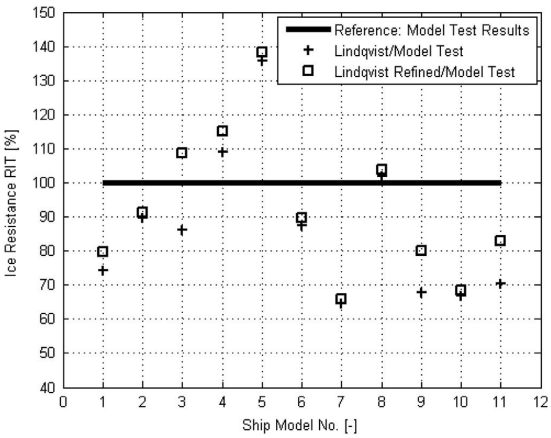

Fig. A24. Total resistance from model testing (line), Lindqvist (plus), adjusted refined approach (squares) vs. ship model no.

See Tables A1–A8.

Table A1
Main hull data of investigated ships and scaling factors.

Property	Abbreviation	Value
Length	L_{pp} [m]	Between 70 and 90
Breadth	B [m]	Between 18 and 23
Draught	T [m]	Between 6.5 and 9.0
Fore foot	–	Present
Lambda	λ [−]	Between 17.14 and 26.25

Table A2
Model test parameters.

Property	Abbreviation	Target value	Mean	Standard deviation
Ice thickness	h_{ice} [m]	Between 0.9 and 1.2	1.01	0.08
Ship speed	v [m/s]	Between 2.0 and 3.5	2.55	0.58
Ice flexural strength	σ_{flex} [kPa]	500	–	–
Ice-hull friction coefficient	μ [−]	0.1	–	–

Table A3
Comparison of theoretical ice breaking prediction methods with regard to relevant ship and ice parameters.

Parameter	Author				
	Su (2011)	Sawamura (2012)	Lindström (1990)	Valanto (2001)	Lindqvist (1989)
Stem angle ϕ [deg]	No	No	No	Yes	Yes
Waterline entrance angle α [deg]	No	No	Yes	Yes	Yes
Buttock angle φ [deg]	No	No	Yes	Yes	Yes
Ship breadth B [m]	Yes	Yes	Yes	Yes	Yes
Ship speed v [kN]	Yes	Yes	Yes	Yes	Yes
Ice thickness h_{ice} [m]	Yes	Yes	Yes	Yes	Yes
Number of broken cusps n [–]	No	No	No	No	Yes
Friction coefficient μ [–]	Yes	Yes	Yes	Yes	Yes
Flexural strength σ_{flex} [kPa]	Yes	Yes	Yes	Yes	Yes
Density difference of ice and water $\Delta\rho$ [kg/m^3]	No	No	No	Yes	Yes

Table A4
Resistance values resulting from model tests and Lindqvist formula.

Ship model no.	Applied method		
	Ice model test at HSVA: RIT [kN/m]	Lindqvist approach: R_{ice} [kN/m]	Deviation: Lindqvist/ ice model test [%]
1	14.72	10.93	74.25
2	12.58	11.28	89.67
3	5.50	8.97	163.09
4	10.86	9.03	83.15
5	7.97	10.83	135.88
6	11.84	10.36	87.50
7	17.15	11.10	64.72
8	12.63	12.88	101.98
9	17.79	12.07	67.85
10	21.23	14.18	66.79
11	17.18	12.07	70.26

Table A5
Main hull parameters of investigated ships related to breaking pattern classes.

Ship model no.* [–]	Stem angle ϕ [deg]	Waterline entrance angle α [deg]	Normal angle at stem [deg]	Total resistance from model tests RIT (normalized) [kN/m]
1	22.5	44.7	31.1	31.1
2	20.4	90	20.4	14.72
3	20	90	20.0	12.58
4	24	42.3	33.5	5.5
5	22	42.2	31.0	10.86
6	27	98.8	27.3	7.97
7	26.6	101.3	27.0	11.84
8	26.6	101.3	27.0	17.15
9	28	55	33.0	12.63
10	27	98.8	27.3	17.79
11	28	55	33.0	21.23

Table A6
Number of cusps resulting from model tests and Lindqvist formula.

Ship model no. [–]	Number of cusps from model testing	Number of cusps from Lindqvist formula
1	8.5	10.54
2	8.5	9.09
3	6.0	7.96
4	7.0	7.89
5	5.5	9.05
6	7.0	9.18
7	9.5	9.57
8	10.0	9.57
9	9.0	10.09
10	10.0	7.40
11	7.5	10.09

Table A7
Ship models assigned to breaking pattern classes.

Breaking pattern class [–]	Ship model no. [–]
1	1–5
2	6–11

Table A8
Ship and ice parameters of investigated ships.

Ship model no.	Parameter								
	Ice thickness [m]	Ship speed [kN]	Stem angle [deg]	Water-line entrance angle [deg]	Normal angle at stem [deg]	Bow length L_{bow} [m]	Avg. buttock angle [deg]	Avg. waterline angle [deg]	Avg. normal angle [deg]
1	1.0	2.5	22.5	44.7	31.1	19.9	28.4	20.6	43.4
2	1.1	2.0	20.4	90.0	20.4	18.9	23.8	24.9	39.8
3	1.0	2.5	20.0	90.0	20.0	16.0	23.3	21.1	40.1
4	1.0	1.0	24.0	42.3	33.5	14.2	26.2	24.2	40.3
5	0.9	3.5	22.0	42.2	31.0	12.9	25.7	13.3	37.2
6	1.0	2.0	27.0	98.8	27.3	19.3	31.3	18.7	49.5
7	1.0	3.0	26.6	101.3	27.0	19.0	26.6	25.2	41.1
8	1.0	3.0	26.6	101.3	27.0	19.0	26.7	26.6	41.4
9	1.0	2.0	28.0	55.0	33.0	20.6	41.3	16.1	59.2
10	1.2	3.5	27.0	98.8	27.3	19.3	31.3	18.7	49.5
11	1.0	2.0	28.0	55.0	33.0	21.5	41.3	16.1	59.2

Appendix B. Supplementary material

Supplementary data associated with this article can be found in the online version at http://dx.doi.org/10.1016/j.oceaneng.2016.02.021.

References

Appendix C – Data Analysis. Appendix of Standard Report for Industry Projects, The Hamburg Ship Model Basin, HSVA, Hamburg, Germany.

Evers, K.-U., Jochmann, P., 1993. An Advanced Technique to Improve the Mechanical Properties of Model Ice Developed at HSVA Ice Tank. Publication.

Lindqvist, G., 1989. A straightforward method for calculation of ice resistance of ships. In: Proceedings of the 10th International Conference on Port and Ocean Engineering under Arctic Conditions, POAC'89, Lulea, Sweden.

Lindström, C.-A., 1990. Numerical estimation of ice forces acting on inclined structures and ships in level ice. In: Proceedings of the 22nd International Offshore Technology Conference, OTC 6445, Houston, Texas, USA, May 7–10, 2014.

Myland, D., Ehlers, S., 2014. Theoretical investigation on ice resistance prediction methods for ships in level ice. In: Proceedings of the 33rd International Conference on Ocean, Offshore and Arctic Engineering, OMAE 2014-23304, San Francisco, USA, June 8–13.

Puntigliano, F., 2003. Experimental and Numerical Research on the Interaction Between Ice Floes and a Ship's Hull During Icebreaking (Dissertation). Technical University Hamburg-Harburg, TUHH, Hamburg, Germany.

Riska, K., 2006. Ship–Ice Interaction in Ship Design: Theory and Practice. Publication, p. 15.

Russian Maritime Register of Shipping, 2013. Rules for the Classification and Construction of Sea-going Ships, Volume 1, ND No. 2-020101-072-E, Saint-Petersburg, Russia.

Sawamura, J., 2012. Numerical investigation of ice bending failure and ice submerging force for ship maneuvering in level ice. In: Proceedings of 20th International Symposium on Ice, IAHR, , Lahti, Finland, June 14–18, 2010.

Su, B., Riska, K., Moan, T., 2010. A numerical method for the prediction of ship performance in level ice. Cold Reg. Sci. Technol. 60, 177–188.

Sutherland, J., Evers, K.-U., 2013. Foresight Study on Laboratory Modeling of Wave and Ice Loads on Coastal and Marine Structures, Deliverable D2.3, EC Contract No. 261520, HYDRALAB-IV.

TraFi, 2010. Maritime Safety Regulations, Finish–Swedish Ice Class Rules 2010, Finland.

Valanto, P., 2001. On the cause and distribution of resistance forces on ship hulls moving in level ice. In: Proceedings of the 16th International Conference on Port and Ocean Engineering Conference under Arctic Conditions, POAC'01, Ottawa, Canada.

Errata

Nomenclature:

R_{B1} bending resistance between stem and 1/8 B
R_{B2} bending resistance between 1/8 B and 2/8 B
R_{B3} bending resistance between 2/8 B and 3/8 B
R_{B4} bending resistance between 3/8 B and near 4/8 B

α_1 average waterline angle between stem and 1/8 B
α_2 average waterline angle between 1/8 B and 2/8 B
α_3 average waterline angle between 2/8 B and 3/8 B
α_4 average waterline angle between 3/8 B and near 4/8 B

3.3 Refinement of ship shape parameters:

In order to be more precise HSVA divided the ship breadth, B, into four sections: 1/8 B, 2/8 B, 3/8 B and near 4/8 B from the centerline as shown in Figure 21.

The last paragraph is to be replaced by:
"where, φ_1 is the average of the stem angle and the buttock angle at 1/8 B, φ_2 is the average of the buttock angle at 1/8 B and the buttock angle at 2/8 B, φ_3 is the average of the buttock angle at 2/8 B and the buttock angle at 3/8 B and φ_4 is the average of the buttock angle at 3/8 B and the buttock angle near 4/8 B. The average waterline and the average normal angles are determined accordingly."

Table 5: Main hull parameters of investigated ships related to breaking pattern classes

Ship Model No. [-]	Waterline entrance angle α [deg]	Total resistance from model tests RIT (normalized) [kN/m]
1	44.7	14.72
2	90.0	12.58
3	90.0	5.50
4	42.3	10.86
5	42.2	7.97
6	90.0	11.84
7	90.0	17.15
8	90.0	12.63
9	55.0	17.79
10	90.0	21.23
11	55.0	17.18

Table 8: Ship and ice parameters of investigated ships

Parameter / Ship Model No.	Water-line entrance angle [deg]
6	90.0
7	90.0
8	90.0
10	90.0

Publication 3

Myland D., Ehlers S. (2017). Methodology to Assess the Floe Size and Distribution Along a Ship Hull during Model Scale Ice Tests for a Self-Propelled Ship Sailing Ahead in Level Ice. Journal of Ships and Offshore Structures, 12:sup1, p.100-p.108.

This page is intentionally left blank.

Publication 4

Myland D., Ehlers S. (2019). Model Scale Investigation of Aspects Influencing the Ice Resistance of Ships Sailing Ahead in Level Ice. Journal of Ship Technology Research, DOI: 10.1080/09377255.2019.1576390.

This page is intentionally left blank.

Publication 5

Myland D., Ehlers S. (2019). Investigation on Semi-Empirical Coefficients and Exponents of a Resistance Prediction Method for Ships Sailing Ahead in Level Ice. Journal of Ships and Offshore Structures, DOI: 10.1080/17445302.2018.1564535.

This page is intentionally left blank.

Publication 6

Myland D. (2019). Experimental and Theoretical Investigations on the Characteristics of Ice Floes Broken by Ships Sailing Ahead in Level Ice. 38th International Conference on Ocean, Offshore and Arctic Engineering, OMAE 2019-95936, June 4-19, 2019, Glasgow, Scotland (final paper submitted).

Is not include due to copyright

This page is intentionally left blank.

Part III – Previous PhD Theses Published at the Department of Marine Technology

This page is intentionally left blank.

Previous PhD theses published at the Department of Marine Technology (earlier: Faculty of Marine Technology) NORWEGIAN UNIVERSITY OF SCIENCE AND TECHNOLOGY

Report No.	Author	Title
	Kavlie, Dag	Optimization of Plane Elastic Grillages, 1967
	Hansen, Hans R.	Man-Machine Communication and Data-Storage Methods in Ship Structural Design, 1971
	Gisvold, Kaare M.	A Method for non-linear mixed -integer programming and its Application to Design Problems, 1971
	Lund, Sverre	Tanker Frame Optimalization by means of SUMT-Transformation and Behaviour Models, 1971
	Vinje, Tor	On Vibration of Spherical Shells Interacting with Fluid, 1972
	Lorentz, Jan D.	Tank Arrangement for Crude Oil Carriers in Accordance with the new Anti-Pollution Regulations, 1975
	Carlsen, Carl A.	Computer-Aided Design of Tanker Structures, 1975
	Larsen, Carl M.	Static and Dynamic Analysis of Offshore Pipelines during Installation, 1976
UR-79-01	Brigt Hatlestad, MK	The finite element method used in a fatigue evaluation of fixed offshore platforms. (Dr.Ing. Thesis)
UR-79-02	Erik Pettersen, MK	Analysis and design of cellular structures. (Dr.Ing. Thesis)
UR-79-03	Sverre Valsgård, MK	Finite difference and finite element methods applied to nonlinear analysis of plated structures. (Dr.Ing. Thesis)
UR-79-04	Nils T. Nordsve, MK	Finite element collapse analysis of structural members considering imperfections and stresses due to fabrication. (Dr.Ing. Thesis)
UR-79-05	Ivar J. Fylling, MK	Analysis of towline forces in ocean towing systems. (Dr.Ing. Thesis)
UR-80-06	Nils Sandsmark, MM	Analysis of Stationary and Transient Heat Conduction by the Use of the Finite Element Method. (Dr.Ing. Thesis)
UR-80-09	Sverre Haver, MK	Analysis of uncertainties related to the stochastic modeling of ocean waves. (Dr.Ing. Thesis)
UR-81-15	Odland, Jonas	On the Strength of welded Ring stiffened cylindrical Shells primarily subjected to axial Compression
UR-82-17	Engesvik, Knut	Analysis of Uncertainties in the fatigue Capacity of Welded Joints
UR-82-18	Rye, Henrik	Ocean wave groups
UR-83-30	Eide, Oddvar Inge	On Cumulative Fatigue Damage in Steel Welded Joints
UR-83-33	Mo, Olav	Stochastic Time Domain Analysis of Slender Offshore Structures
UR-83-34	Amdahl, Jørgen	Energy absorption in Ship-platform impacts
UR-84-37	Mørch, Morten	Motions and mooring forces of semi submersibles as determined by full-scale measurements and theoretical analysis
UR-84-38	Soares, C. Guedes	Probabilistic models for load effects in ship structures

UR-84-39	Aarsnes, Jan V.	Current forces on ships
UR-84-40	Czujko, Jerzy	Collapse Analysis of Plates subjected to Biaxial Compression and Lateral Load
UR-85-46	Alf G. Engseth, MK	Finite element collapse analysis of tubular steel offshore structures. (Dr.Ing. Thesis)
UR-86-47	Dengody Sheshappa, MP	A Computer Design Model for Optimizing Fishing Vessel Designs Based on Techno-Economic Analysis. (Dr.Ing. Thesis)
UR-86-48	Vidar Aanesland, MH	A Theoretical and Numerical Study of Ship Wave Resistance. (Dr.Ing. Thesis)
UR-86-49	Heinz-Joachim Wessel, MK	Fracture Mechanics Analysis of Crack Growth in Plate Girders. (Dr.Ing. Thesis)
UR-86-50	Jon Taby, MK	Ultimate and Post-ultimate Strength of Dented Tubular Members. (Dr.Ing. Thesis)
UR-86-51	Walter Lian, MH	A Numerical Study of Two-Dimensional Separated Flow Past Bluff Bodies at Moderate KC-Numbers. (Dr.Ing. Thesis)
UR-86-52	Bjørn Sortland, MH	Force Measurements in Oscillating Flow on Ship Sections and Circular Cylinders in a U-Tube Water Tank. (Dr.Ing. Thesis)
UR-86-53	Kurt Strand, MM	A System Dynamic Approach to One-dimensional Fluid Flow. (Dr.Ing. Thesis)
UR-86-54	Arne Edvin Løken, MH	Three Dimensional Second Order Hydrodynamic Effects on Ocean Structures in Waves. (Dr.Ing. Thesis)
UR-86-55	Sigurd Falch, MH	A Numerical Study of Slamming of Two-Dimensional Bodies. (Dr.Ing. Thesis)
UR-87-56	Arne Braathen, MH	Application of a Vortex Tracking Method to the Prediction of Roll Damping of a Two-Dimension Floating Body. (Dr.Ing. Thesis)
UR-87-57	Bernt Leira, MK	Gaussian Vector Processes for Reliability Analysis involving Wave-Induced Load Effects. (Dr.Ing. Thesis)
UR-87-58	Magnus Småvik, MM	Thermal Load and Process Characteristics in a Two-Stroke Diesel Engine with Thermal Barriers (in Norwegian). (Dr.Ing. Thesis)
MTA-88-59	Bernt Arild Bremdal, MP	An Investigation of Marine Installation Processes – A Knowledge - Based Planning Approach. (Dr.Ing. Thesis)
MTA-88-60	Xu Jun, MK	Non-linear Dynamic Analysis of Space-framed Offshore Structures. (Dr.Ing. Thesis)
MTA-89-61	Gang Miao, MH	Hydrodynamic Forces and Dynamic Responses of Circular Cylinders in Wave Zones. (Dr.Ing. Thesis)
MTA-89-62	Martin Greenhow, MH	Linear and Non-Linear Studies of Waves and Floating Bodies. Part I and Part II. (Dr.Techn. Thesis)
MTA-89-63	Chang Li, MH	Force Coefficients of Spheres and Cubes in Oscillatory Flow with and without Current. (Dr.Ing. Thesis
MTA-89-64	Hu Ying, MP	A Study of Marketing and Design in Development of Marine Transport Systems. (Dr.Ing. Thesis)
MTA-89-65	Arild Jæger, MH	Seakeeping, Dynamic Stability and Performance of a Wedge Shaped Planing Hull. (Dr.Ing. Thesis)
MTA-89-66	Chan Siu Hung, MM	The dynamic characteristics of tilting-pad bearings

MTA-89-67	Kim Wikstrøm, MP	Analysis av projekteringen for ett offshore projekt. (Licenciat-avhandling)
MTA-89-68	Jiao Guoyang, MK	Reliability Analysis of Crack Growth under Random Loading, considering Model Updating. (Dr.Ing. Thesis)
MTA-89-69	Arnt Olufsen, MK	Uncertainty and Reliability Analysis of Fixed Offshore Structures. (Dr.Ing. Thesis)
MTA-89-70	Wu Yu-Lin, MR	System Reliability Analyses of Offshore Structures using improved Truss and Beam Models. (Dr.Ing. Thesis)
MTA-90-71	Jan Roger Hoff, MH	Three-dimensional Green function of a vessel with forward speed in waves. (Dr.Ing. Thesis)
MTA-90-72	Rong Zhao, MH	Slow-Drift Motions of a Moored Two-Dimensional Body in Irregular Waves. (Dr.Ing. Thesis)
MTA-90-73	Atle Minsaas, MP	Economical Risk Analysis. (Dr.Ing. Thesis)
MTA-90-74	Knut-Aril Farnes, MK	Long-term Statistics of Response in Non-linear Marine Structures. (Dr.Ing. Thesis)
MTA-90-75	Torbjørn Sotberg, MK	Application of Reliability Methods for Safety Assessment of Submarine Pipelines. (Dr.Ing. Thesis)
MTA-90-76	Zeuthen, Steffen, MP	SEAMAID. A computational model of the design process in a constraint-based logic programming environment. An example from the offshore domain. (Dr.Ing. Thesis)
MTA-91-77	Haagensen, Sven, MM	Fuel Dependant Cyclic Variability in a Spark Ignition Engine - An Optical Approach. (Dr.Ing. Thesis)
MTA-91-78	Løland, Geir, MH	Current forces on and flow through fish farms. (Dr.Ing. Thesis)
MTA-91-79	Hoen, Christopher, MK	System Identification of Structures Excited by Stochastic Load Processes. (Dr.Ing. Thesis)
MTA-91-80	Haugen, Stein, MK	Probabilistic Evaluation of Frequency of Collision between Ships and Offshore Platforms. (Dr.Ing. Thesis)
MTA-91-81	Sødahl, Nils, MK	Methods for Design and Analysis of Flexible Risers. (Dr.Ing. Thesis)
MTA-91-82	Ormberg, Harald, MK	Non-linear Response Analysis of Floating Fish Farm Systems. (Dr.Ing. Thesis)
MTA-91-83	Marley, Mark J., MK	Time Variant Reliability under Fatigue Degradation. (Dr.Ing. Thesis)
MTA-91-84	Krokstad, Jørgen R., MH	Second-order Loads in Multidirectional Seas. (Dr.Ing. Thesis)
MTA-91-85	Molteberg, Gunnar A., MM	The Application of System Identification Techniques to Performance Monitoring of Four Stroke Turbocharged Diesel Engines. (Dr.Ing. Thesis)
MTA-92-86	Mørch, Hans Jørgen Bjelke, MH	Aspects of Hydrofoil Design: with Emphasis on Hydrofoil Interaction in Calm Water. (Dr.Ing. Thesis)
MTA-92-87	Chan Siu Hung, MM	Nonlinear Analysis of Rotordynamic Instabilities in Highspeed Turbomachinery. (Dr.Ing. Thesis)
MTA-92-88	Bessason, Bjarni, MK	Assessment of Earthquake Loading and Response of Seismically Isolated Bridges. (Dr.Ing. Thesis)
MTA-92-89	Langli, Geir, MP	Improving Operational Safety through exploitation of Design Knowledge - an investigation of offshore platform safety. (Dr.Ing. Thesis)
MTA-92-90	Sævik, Svein, MK	On Stresses and Fatigue in Flexible Pipes. (Dr.Ing. Thesis)

MTA-92-91	Ask, Tor Ø., MM	Ignition and Flame Growth in Lean Gas-Air Mixtures. An Experimental Study with a Schlieren System. (Dr.Ing. Thesis)
MTA-86-92	Hessen, Gunnar, MK	Fracture Mechanics Analysis of Stiffened Tubular Members. (Dr.Ing. Thesis)
MTA-93-93	Steinebach, Christian, MM	Knowledge Based Systems for Diagnosis of Rotating Machinery. (Dr.Ing. Thesis)
MTA-93-94	Dalane, Jan Inge, MK	System Reliability in Design and Maintenance of Fixed Offshore Structures. (Dr.Ing. Thesis)
MTA-93-95	Steen, Sverre, MH	Cobblestone Effect on SES. (Dr.Ing. Thesis)
MTA-93-96	Karunakaran, Daniel, MK	Nonlinear Dynamic Response and Reliability Analysis of Drag-dominated Offshore Platforms. (Dr.Ing. Thesis)
MTA-93-97	Hagen, Arnulf, MP	The Framework of a Design Process Language. (Dr.Ing. Thesis)
MTA-93-98	Nordrik, Rune, MM	Investigation of Spark Ignition and Autoignition in Methane and Air Using Computational Fluid Dynamics and Chemical Reaction Kinetics. A Numerical Study of Ignition Processes in Internal Combustion Engines. (Dr.Ing. Thesis)
MTA-94-99	Passano, Elizabeth, MK	Efficient Analysis of Nonlinear Slender Marine Structures. (Dr.Ing. Thesis)
MTA-94-100	Kvålsvold, Jan, MH	Hydroelastic Modelling of Wetdeck Slamming on Multihull Vessels. (Dr.Ing. Thesis)
MTA-94-102	Bech, Sidsel M., MK	Experimental and Numerical Determination of Stiffness and Strength of GRP/PVC Sandwich Structures. (Dr.Ing. Thesis)
MTA-95-103	Paulsen, Hallvard, MM	A Study of Transient Jet and Spray using a Schlieren Method and Digital Image Processing. (Dr.Ing. Thesis)
MTA-95-104	Hovde, Geir Olav, MK	Fatigue and Overload Reliability of Offshore Structural Systems, Considering the Effect of Inspection and Repair. (Dr.Ing. Thesis)
MTA-95-105	Wang, Xiaozhi, MK	Reliability Analysis of Production Ships with Emphasis on Load Combination and Ultimate Strength. (Dr.Ing. Thesis)
MTA-95-106	Ulstein, Tore, MH	Nonlinear Effects of a Flexible Stern Seal Bag on Cobblestone Oscillations of an SES. (Dr.Ing. Thesis)
MTA-95-107	Solaas, Frøydis, MH	Analytical and Numerical Studies of Sloshing in Tanks. (Dr.Ing. Thesis)
MTA-95-108	Hellan, Øyvind, MK	Nonlinear Pushover and Cyclic Analyses in Ultimate Limit State Design and Reassessment of Tubular Steel Offshore Structures. (Dr.Ing. Thesis)
MTA-95-109	Hermundstad, Ole A., MK	Theoretical and Experimental Hydroelastic Analysis of High Speed Vessels. (Dr.Ing. Thesis)
MTA-96-110	Bratland, Anne K., MH	Wave-Current Interaction Effects on Large-Volume Bodies in Water of Finite Depth. (Dr.Ing. Thesis)
MTA-96-111	Herfjord, Kjell, MH	A Study of Two-dimensional Separated Flow by a Combination of the Finite Element Method and Navier-Stokes Equations. (Dr.Ing. Thesis)
MTA-96-112	Æsøy, Vilmar, MM	Hot Surface Assisted Compression Ignition in a Direct Injection Natural Gas Engine. (Dr.Ing. Thesis)
MTA-96-113	Eknes, Monika L., MK	Escalation Scenarios Initiated by Gas Explosions on

		Offshore Installations. (Dr.Ing. Thesis)
MTA-96-114	Erikstad, Stein O., MP	A Decision Support Model for Preliminary Ship Design. (Dr.Ing. Thesis)
MTA-96-115	Pedersen, Egil, MH	A Nautical Study of Towed Marine Seismic Streamer Cable Configurations. (Dr.Ing. Thesis)
MTA-97-116	Moksnes, Paul O., MM	Modelling Two-Phase Thermo-Fluid Systems Using Bond Graphs. (Dr.Ing. Thesis)
MTA-97-117	Halse, Karl H., MK	On Vortex Shedding and Prediction of Vortex-Induced Vibrations of Circular Cylinders. (Dr.Ing. Thesis)
MTA-97-118	Igland, Ragnar T., MK	Reliability Analysis of Pipelines during Laying, considering Ultimate Strength under Combined Loads. (Dr.Ing. Thesis)
MTA-97-119	Pedersen, Hans-P., MP	Levendefiskteknologi for fiskefartøy. (Dr.Ing. Thesis)
MTA-98-120	Vikestad, Kyrre, MK	Multi-Frequency Response of a Cylinder Subjected to Vortex Shedding and Support Motions. (Dr.Ing. Thesis)
MTA-98-121	Azadi, Mohammad R. E., MK	Analysis of Static and Dynamic Pile-Soil-Jacket Behaviour. (Dr.Ing. Thesis)
MTA-98-122	Ulltang, Terje, MP	A Communication Model for Product Information. (Dr.Ing. Thesis)
MTA-98-123	Torbergsen, Erik, MM	Impeller/Diffuser Interaction Forces in Centrifugal Pumps. (Dr.Ing. Thesis)
MTA-98-124	Hansen, Edmond, MH	A Discrete Element Model to Study Marginal Ice Zone Dynamics and the Behaviour of Vessels Moored in Broken Ice. (Dr.Ing. Thesis)
MTA-98-125	Videiro, Paulo M., MK	Reliability Based Design of Marine Structures. (Dr.Ing. Thesis)
MTA-99-126	Mainçon, Philippe, MK	Fatigue Reliability of Long Welds Application to Titanium Risers. (Dr.Ing. Thesis)
MTA-99-127	Haugen, Elin M., MH	Hydroelastic Analysis of Slamming on Stiffened Plates with Application to Catamaran Wetdecks. (Dr.Ing. Thesis)
MTA-99-128	Langhelle, Nina K., MK	Experimental Validation and Calibration of Nonlinear Finite Element Models for Use in Design of Aluminium Structures Exposed to Fire. (Dr.Ing. Thesis)
MTA-99-129	Berstad, Are J., MK	Calculation of Fatigue Damage in Ship Structures. (Dr.Ing. Thesis)
MTA-99-130	Andersen, Trond M., MM	Short Term Maintenance Planning. (Dr.Ing. Thesis)
MTA-99-131	Tveiten, Bård Wathne, MK	Fatigue Assessment of Welded Aluminium Ship Details. (Dr.Ing. Thesis)
MTA-99-132	Søreide, Fredrik, MP	Applications of underwater technology in deep water archaeology. Principles and practice. (Dr.Ing. Thesis)
MTA-99-133	Tønnessen, Rune, MH	A Finite Element Method Applied to Unsteady Viscous Flow Around 2D Blunt Bodies With Sharp Corners. (Dr.Ing. Thesis)
MTA-99-134	Elvekrok, Dag R., MP	Engineering Integration in Field Development Projects in the Norwegian Oil and Gas Industry. The Supplier Management of Norne. (Dr.Ing. Thesis)
MTA-99-135	Fagerholt, Kjetil, MP	Optimeringsbaserte Metoder for Ruteplanlegging innen skipsfart. (Dr.Ing. Thesis)
MTA-99-136	Bysveen, Marie, MM	Visualization in Two Directions on a Dynamic Combustion Rig for Studies of Fuel Quality. (Dr.Ing.

		Thesis)
MTA-2000-137	Storteig, Eskild, MM	Dynamic characteristics and leakage performance of liquid annular seals in centrifugal pumps. (Dr.Ing. Thesis)
MTA-2000-138	Sagli, Gro, MK	Model uncertainty and simplified estimates of long term extremes of hull girder loads in ships. (Dr.Ing. Thesis)
MTA-2000-139	Tronstad, Harald, MK	Nonlinear analysis and design of cable net structures like fishing gear based on the finite element method. (Dr.Ing. Thesis)
MTA-2000-140	Kroneberg, André, MP	Innovation in shipping by using scenarios. (Dr.Ing. Thesis)
MTA-2000-141	Haslum, Herbjørn Alf, MH	Simplified methods applied to nonlinear motion of spar platforms. (Dr.Ing. Thesis)
MTA-2001-142	Samdal, Ole Johan, MM	Modelling of Degradation Mechanisms and Stressor Interaction on Static Mechanical Equipment Residual Lifetime. (Dr.Ing. Thesis)
MTA-2001-143	Baarholm, Rolf Jarle, MH	Theoretical and experimental studies of wave impact underneath decks of offshore platforms. (Dr.Ing. Thesis)
MTA-2001-144	Wang, Lihua, MK	Probabilistic Analysis of Nonlinear Wave-induced Loads on Ships. (Dr.Ing. Thesis)
MTA-2001-145	Kristensen, Odd H. Holt, MK	Ultimate Capacity of Aluminium Plates under Multiple Loads, Considering HAZ Properties. (Dr.Ing. Thesis)
MTA-2001-146	Greco, Marilena, MH	A Two-Dimensional Study of Green-Water Loading. (Dr.Ing. Thesis)
MTA-2001-147	Heggelund, Svein E., MK	Calculation of Global Design Loads and Load Effects in Large High Speed Catamarans. (Dr.Ing. Thesis)
MTA-2001-148	Babalola, Olusegun T., MK	Fatigue Strength of Titanium Risers – Defect Sensitivity. (Dr.Ing. Thesis)
MTA-2001-149	Mohammed, Abuu K., MK	Nonlinear Shell Finite Elements for Ultimate Strength and Collapse Analysis of Ship Structures. (Dr.Ing. Thesis)
MTA-2002-150	Holmedal, Lars E., MH	Wave-current interactions in the vicinity of the sea bed. (Dr.Ing. Thesis)
MTA-2002-151	Rognebakke, Olav F., MH	Sloshing in rectangular tanks and interaction with ship motions. (Dr.Ing. Thesis)
MTA-2002-152	Lader, Pål Furset, MH	Geometry and Kinematics of Breaking Waves. (Dr.Ing. Thesis)
MTA-2002-153	Yang, Qinzheng, MH	Wash and wave resistance of ships in finite water depth. (Dr.Ing. Thesis)
MTA-2002-154	Melhus, Øyvin, MM	Utilization of VOC in Diesel Engines. Ignition and combustion of VOC released by crude oil tankers. (Dr.Ing. Thesis)
MTA-2002-155	Ronæss, Marit, MH	Wave Induced Motions of Two Ships Advancing on Parallel Course. (Dr.Ing. Thesis)
MTA-2002-156	Økland, Ole D., MK	Numerical and experimental investigation of whipping in twin hull vessels exposed to severe wet deck slamming. (Dr.Ing. Thesis)
MTA-2002-157	Ge, Chunhua, MK	Global Hydroelastic Response of Catamarans due to Wet Deck Slamming. (Dr.Ing. Thesis)
MTA-2002-158	Byklum, Eirik, MK	Nonlinear Shell Finite Elements for Ultimate Strength and Collapse Analysis of Ship Structures. (Dr.Ing. Thesis)
IMT-2003-1	Chen, Haibo, MK	Probabilistic Evaluation of FPSO-Tanker Collision in

		Tandem Offloading Operation. (Dr.Ing. Thesis)
IMT-2003-2	Skaugset, Kjetil Bjørn, MK	On the Suppression of Vortex Induced Vibrations of Circular Cylinders by Radial Water Jets. (Dr.Ing. Thesis)
IMT-2003-3	Chezhian, Muthu	Three-Dimensional Analysis of Slamming. (Dr.Ing. Thesis)
IMT-2003-4	Buhaug, Øyvind	Deposit Formation on Cylinder Liner Surfaces in Medium Speed Engines. (Dr.Ing. Thesis)
IMT-2003-5	Tregde, Vidar	Aspects of Ship Design: Optimization of Aft Hull with Inverse Geometry Design. (Dr.Ing. Thesis)
IMT-2003-6	Wist, Hanne Therese	Statistical Properties of Successive Ocean Wave Parameters. (Dr.Ing. Thesis)
IMT-2004-7	Ransau, Samuel	Numerical Methods for Flows with Evolving Interfaces. (Dr.Ing. Thesis)
IMT-2004-8	Soma, Torkel	Blue-Chip or Sub-Standard. A data interrogation approach of identity safety characteristics of shipping organization. (Dr.Ing. Thesis)
IMT-2004-9	Ersdal, Svein	An experimental study of hydrodynamic forces on cylinders and cables in near axial flow. (Dr.Ing. Thesis)
IMT-2005-10	Brodtkorb, Per Andreas	The Probability of Occurrence of Dangerous Wave Situations at Sea. (Dr.Ing. Thesis)
IMT-2005-11	Yttervik, Rune	Ocean current variability in relation to offshore engineering. (Dr.Ing. Thesis)
IMT-2005-12	Fredheim, Arne	Current Forces on Net-Structures. (Dr.Ing. Thesis)
IMT-2005-13	Heggernes, Kjetil	Flow around marine structures. (Dr.Ing. Thesis
IMT-2005-14	Fouques, Sebastien	Lagrangian Modelling of Ocean Surface Waves and Synthetic Aperture Radar Wave Measurements. (Dr.Ing. Thesis)
IMT-2006-15	Holm, Håvard	Numerical calculation of viscous free surface flow around marine structures. (Dr.Ing. Thesis)
IMT-2006-16	Bjørheim, Lars G.	Failure Assessment of Long Through Thickness Fatigue Cracks in Ship Hulls. (Dr.Ing. Thesis)
IMT-2006-17	Hansson, Lisbeth	Safety Management for Prevention of Occupational Accidents. (Dr.Ing. Thesis)
IMT-2006-18	Zhu, Xinying	Application of the CIP Method to Strongly Nonlinear Wave-Body Interaction Problems. (Dr.Ing. Thesis)
IMT-2006-19	Reite, Karl Johan	Modelling and Control of Trawl Systems. (Dr.Ing. Thesis)
IMT-2006-20	Smogeli, Øyvind Notland	Control of Marine Propellers. From Normal to Extreme Conditions. (Dr.Ing. Thesis)
IMT-2007-21	Storhaug, Gaute	Experimental Investigation of Wave Induced Vibrations and Their Effect on the Fatigue Loading of Ships. (Dr.Ing. Thesis)
IMT-2007-22	Sun, Hui	A Boundary Element Method Applied to Strongly Nonlinear Wave-Body Interaction Problems. (PhD Thesis, CeSOS)
IMT-2007-23	Rustad, Anne Marthine	Modelling and Control of Top Tensioned Risers. (PhD Thesis, CeSOS)
IMT-2007-24	Johansen, Vegar	Modelling flexible slender system for real-time simulations and control applications
IMT-2007-25	Wroldsen, Anders Sunde	Modelling and control of tensegrity structures. (PhD

		Thesis, CeSOS)
IMT-2007-26	Aronsen, Kristoffer Høye	An experimental investigation of in-line and combined inline and cross flow vortex induced vibrations. (Dr. avhandling, IMT)
IMT-2007-27	Gao, Zhen	Stochastic Response Analysis of Mooring Systems with Emphasis on Frequency-domain Analysis of Fatigue due to Wide-band Response Processes (PhD Thesis, CeSOS)
IMT-2007-28	Thorstensen, Tom Anders	Lifetime Profit Modelling of Ageing Systems Utilizing Information about Technical Condition. (Dr.ing. thesis, IMT)
IMT-2008-29	Refsnes, Jon Erling Gorset	Nonlinear Model-Based Control of Slender Body AUVs (PhD Thesis, IMT)
IMT-2008-30	Berntsen, Per Ivar B.	Structural Reliability Based Position Mooring. (PhD-Thesis, IMT)
IMT-2008-31	Ye, Naiquan	Fatigue Assessment of Aluminium Welded Box-stiffener Joints in Ships (Dr.ing. thesis, IMT)
IMT-2008-32	Radan, Damir	Integrated Control of Marine Electrical Power Systems. (PhD-Thesis, IMT)
IMT-2008-33	Thomassen, Paul	Methods for Dynamic Response Analysis and Fatigue Life Estimation of Floating Fish Cages. (Dr.ing. thesis, IMT)
IMT-2008-34	Pákozdi, Csaba	A Smoothed Particle Hydrodynamics Study of Two-dimensional Nonlinear Sloshing in Rectangular Tanks. (Dr.ing.thesis, IMT/ CeSOS)
IMT-2007-35	Grytøyr, Guttorm	A Higher-Order Boundary Element Method and Applications to Marine Hydrodynamics. (Dr.ing.thesis, IMT)
IMT-2008-36	Drummen, Ingo	Experimental and Numerical Investigation of Nonlinear Wave-Induced Load Effects in Containerships considering Hydroelasticity. (PhD thesis, CeSOS)
IMT-2008-37	Skejic, Renato	Maneuvering and Seakeeping of a Singel Ship and of Two Ships in Interaction. (PhD-Thesis, CeSOS)
IMT-2008-38	Harlem, Alf	An Age-Based Replacement Model for Repairable Systems with Attention to High-Speed Marine Diesel Engines. (PhD-Thesis, IMT)
IMT-2008-39	Alsos, Hagbart S.	Ship Grounding. Analysis of Ductile Fracture, Bottom Damage and Hull Girder Response. (PhD-thesis, IMT)
IMT-2008-40	Graczyk, Mateusz	Experimental Investigation of Sloshing Loading and Load Effects in Membrane LNG Tanks Subjected to Random Excitation. (PhD-thesis, CeSOS)
IMT-2008-41	Taghipour, Reza	Efficient Prediction of Dynamic Response for Flexible amd Multi-body Marine Structures. (PhD-thesis, CeSOS)
IMT-2008-42	Ruth, Eivind	Propulsion control and thrust allocation on marine vessels. (PhD thesis, CeSOS)
IMT-2008-43	Nystad, Bent Helge	Technical Condition Indexes and Remaining Useful Life of Aggregated Systems. PhD thesis, IMT
IMT-2008-44	Soni, Prashant Kumar	Hydrodynamic Coefficients for Vortex Induced Vibrations of Flexible Beams, PhD thesis, CeSOS
IMT-2009-45	Amlashi, Hadi K.K.	Ultimate Strength and Reliability-based Design of Ship Hulls with Emphasis on Combined Global and Local Loads. PhD Thesis, IMT

IMT-2009-46	Pedersen, Tom Arne	Bond Graph Modelling of Marine Power Systems. PhD Thesis, IMT
IMT-2009-47	Kristiansen, Trygve	Two-Dimensional Numerical and Experimental Studies of Piston-Mode Resonance. PhD-Thesis, CeSOS
IMT-2009-48	Ong, Muk Chen	Applications of a Standard High Reynolds Number Model and a Stochastic Scour Prediction Model for Marine Structures. PhD-thesis, IMT
IMT-2009-49	Hong, Lin	Simplified Analysis and Design of Ships subjected to Collision and Grounding. PhD-thesis, IMT
IMT-2009-50	Koushan, Kamran	Vortex Induced Vibrations of Free Span Pipelines, PhD thesis, IMT
IMT-2009-51	Korsvik, Jarl Eirik	Heuristic Methods for Ship Routing and Scheduling. PhD-thesis, IMT
IMT-2009-52	Lee, Jihoon	Experimental Investigation and Numerical in Analyzing the Ocean Current Displacement of Longlines. Ph.d.-Thesis, IMT.
IMT-2009-53	Vestbøstad, Tone Gran	A Numerical Study of Wave-in-Deck Impact usin a Two-Dimensional Constrained Interpolation Profile Method, Ph.d.thesis, CeSOS.
IMT-2009-54	Bruun, Kristine	Bond Graph Modelling of Fuel Cells for Marine Power Plants. Ph.d.-thesis, IMT
IMT 2009-55	Holstad, Anders	Numerical Investigation of Turbulence in a Sekwed Three-Dimensional Channel Flow, Ph.d.-thesis, IMT.
IMT 2009-56	Ayala-Uraga, Efren	Reliability-Based Assessment of Deteriorating Ship-shaped Offshore Structures, Ph.d.-thesis, IMT
IMT2009-57	Kong, Xiangjun	A Numerical Study of a Damaged Ship in Beam Sea Waves. Ph.d.-thesis, IMT/CeSOS.
IMT 2010-58	Kristiansen, David	Wave Induced Effects on Floaters of Aquaculture Plants, Ph.d.-thesis, CeSOS.
IMT 2010-59	Ludvigsen, Martin	An ROV-Toolbox for Optical and Acoustic Scientific Seabed Investigation. Ph.d.-thesis IMT.
IMT2010-60	Hals, Jørgen	Modelling and Phase Control of Wave-Energy Converters. Ph.d.thesis, CeSOS.
IMT2010- 61	Shu, Zhi	Uncertainty Assessment of Wave Loads and Ultimate Strength of Tankers and Bulk Carriers in a Reliability Framework. Ph.d. Thesis, IMT/ CeSOS
IMT2010-62	Shao, Yanlin	Numerical Potential-Flow Studies on Weakly-Nonlinear Wave-Body Interactions with/without Small Forward Speed, Ph.d.thesis,CeSOS.
IMT2010-63	Califano, Andrea	Dynamic Loads on Marine Propellers due to Intermittent Ventilation. Ph.d.thesis, IMT.
IMT2010-64	El Khoury, George	Numerical Simulations of Massively Separated Turbulent Flows, Ph.d.-thesis, IMT
IMT 2010-65	Seim, Knut Sponheim	Mixing Process in Dense Overflows with Emphasis on the Faroe Bank Channel Overflow. Ph.d.thesis, IMT
IMT 2010-66	Jia, Huirong	Structural Analysis of Intect and Damaged Ships in a Collission Risk Analysis Perspective. Ph.d.thesis CeSoS.
IMT 2010-67	Jiao, Linlin	Wave-Induced Effects on a Pontoon-type Very Large Floating Structures (VLFS). Ph.D.-thesis, CeSOS.
IMT 2010-68	Abrahamsen, Bjørn Christian	Sloshing Induced Tank Roof with Entrapped Air Pocket.

		Ph.d.thesis, CeSOS.
IMT 2011-69	Karimirad, Madjid	Stochastic Dynamic Response Analysis of Spar-Type Wind Turbines with Catenary or Taut Mooring Systems. Ph.d.-thesis, CeSOS.
IMT -2011-70	Erlend Meland	Condition Monitoring of Safety Critical Valves. Ph.d.-thesis, IMT.
IMT – 2011-71	Yang, Limin	Stochastic Dynamic System Analysis of Wave Energy Converter with Hydraulic Power Take-Off, with Particular Reference to Wear Damage Analysis, Ph.d. Thesis, CeSOS.
IMT – 2011-72	Visscher, Jan	Application of Particla Image Velocimetry on Turbulent Marine Flows, Ph.d.Thesis, IMT.
IMT – 2011-73	Su, Biao	Numerical Predictions of Global and Local Ice Loads on Ships. Ph.d.Thesis, CeSOS.
IMT – 2011-74	Liu, Zhenhui	Analytical and Numerical Analysis of Iceberg Collision with Ship Structures. Ph.d.Thesis, IMT.
IMT – 2011-75	Aarsæther, Karl Gunnar	Modeling and Analysis of Ship Traffic by Observation and Numerical Simulation. Ph.d.Thesis, IMT.
Imt – 2011-76	Wu, Jie	Hydrodynamic Force Identification from Stochastic Vortex Induced Vibration Experiments with Slender Beams. Ph.d.Thesis, IMT.
Imt – 2011-77	Amini, Hamid	Azimuth Propulsors in Off-design Conditions. Ph.d.Thesis, IMT.
IMT –2011-78	Nguyen, Tan-Hoi	Toward a System of Real-Time Prediction and Monitoring of Bottom Damage Conditions During Ship Grounding. Ph.d.thesis, IMT.
IMT- 2011-79	Tavakoli, Mohammad T.	Assessment of Oil Spill in Ship Collision and Grounding, Ph.d.thesis, IMT.
IMT- 2011-80	Guo, Bingjie	Numerical and Experimental Investigation of Added Resistance in Waves. Ph.d.Thesis, IMT.
IMT- 2011-81	Chen, Qiaofeng	Ultimate Strength of Aluminium Panels, considering HAZ Effects, IMT
IMT-2012-82	Kota, Ravikiran S.	Wave Loads on Decks of Offshore Structures in Random Seas, CeSOS.
IMT-2012-83	Sten, Ronny	Dynamic Simulation of Deep Water Drilling Risers with Heave Compensating System, IMT.
IMT-2012-84	Berle, Øyvind	Risk and resilience in global maritime supply chains, IMT.
IMT-2012-85	Fang, Shaoji	Fault Tolerant Position Mooring Control Based on Structural Reliability, CeSOS.
IMT-2012-86	You, Jikun	Numerical studies on wave forces and moored ship motions in intermediate and shallow water, CeSOS.
IMT-2012-87	Xiang ,Xu	Maneuvering of two interacting ships in waves, CeSOS
IMT-2012-88	Dong, Wenbin	Time-domain fatigue response and reliability analysis of offshore wind turbines with emphasis on welded tubular joints and gear components, CeSOS
IMT-2012-89	Zhu, Suji	Investigation of Wave-Induced Nonlinear Load Effects in Open Ships considering Hull Girder Vibrations in Bending and Torsion, CeSOS
IMT-2012-90	Zhou, Li	Numerical and Experimental Investigation of Station-keeping in Level Ice, CeSOS

IMT-2012-91	Ushakov, Sergey	Particulate matter emission characteristics from diesel enignes operating on conventional and alternative marine fuels, IMT
IMT-2013-1	Yin, Decao	Experimental and Numerical Analysis of Combined In-line and Cross-flow Vortex Induced Vibrations, CeSOS
IMT-2013-2	Kurniawan, Adi	Modelling and geometry optimisation of wave energy converters, CeSOS
IMT- 2013-3	Al Ryati, Nabil	Technical condition indexes doe auxiliary marine diesel engines, IMT
IMT-2013-4	Firoozkoohi, Reza	Experimental, numerical and analytical investigation of the effect of screens on sloshing, CeSOS
IMT-2013-5	Ommani, Babak	Potential-Flow Predictions of a Semi-Displacement Vessel Including Applications to Calm Water Broaching, CeSOS
IMT- 2013-6	Xing, Yihan	Modelling and analysis of the gearbox in a floating spar-type wind turbine, CeSOS
IMT-7-2013	Balland, Océane	Optimization models for reducing air emissions from ships, IMT
IMT-8-2013	Yang, Dan	Transitional wake flow behind an inclined flat plate----- Computation and analysis, IMT
IMT-9-2013	Abdillah, Suyuthi	Prediction of Extreme Loads and Fatigue Damage for a Ship Hull due to Ice Action, IMT
IMT-10-2013	Ramìrez, Pedro Agustìn Pèrez	Ageing management and life extension of technical systems- Concepts and methods applied to oil and gas facilities, IMT
IMT-11-2013	Chuang, Zhenju	Experimental and Numerical Investigation of Speed Loss due to Seakeeping and Maneuvering. IMT
IMT-12-2013	Etemaddar, Mahmoud	Load and Response Analysis of Wind Turbines under Atmospheric Icing and Controller System Faults with Emphasis on Spar Type Floating Wind Turbines, IMT
IMT-13-2013	Lindstad, Haakon	Strategies and measures for reducing maritime CO2 emissons, IMT
IMT-14-2013	Haris, Sabril	Damage interaction analysis of ship collisions, IMT
IMT-15-2013	Shainee, Mohamed	Conceptual Design, Numerical and Experimental Investigation of a SPM Cage Concept for Offshore Mariculture, IMT
IMT-16-2013	Gansel, Lars	Flow past porous cylinders and effects of biofouling and fish behavior on the flow in and around Atlantic salmon net cages, IMT
IMT-17-2013	Gaspar, Henrique	Handling Aspects of Complexity in Conceptual Ship Design, IMT
IMT-18-2013	Thys, Maxime	Theoretical and Experimental Investigation of a Free Running Fishing Vessel at Small Frequency of Encounter, CeSOS
IMT-19-2013	Aglen, Ida	VIV in Free Spanning Pipelines, CeSOS
IMT-1-2014	Song, An	Theoretical and experimental studies of wave diffraction and radiation loads on a horizontally submerged perforated plate, CeSOS
IMT-2-2014	Rogne, Øyvind Ygre	Numerical and Experimental Investigation of a Hinged 5-body Wave Energy Converter, CeSOS

IMT-3-2014	Dai, Lijuan	Safe and efficient operation and maintenance of offshore wind farms ,IMT
IMT-4-2014	Bachynski, Erin Elizabeth	Design and Dynamic Analysis of Tension Leg Platform Wind Turbines, CeSOS
IMT-5-2014	Wang, Jingbo	Water Entry of Freefall Wedged – Wedge motions and Cavity Dynamics, CeSOS
IMT-6-2014	Kim, Ekaterina	Experimental and numerical studies related to the coupled behavior of ice mass and steel structures during accidental collisions, IMT
IMT-7-2014	Tan, Xiang	Numerical investigation of ship's continuous- mode icebreaking in leverl ice, CeSOS
IMT-8-2014	Muliawan, Made Jaya	Design and Analysis of Combined Floating Wave and Wind Power Facilities, with Emphasis on Extreme Load Effects of the Mooring System, CeSOS
IMT-9-2014	Jiang, Zhiyu	Long-term response analysis of wind turbines with an emphasis on fault and shutdown conditions, IMT
IMT-10-2014	Dukan, Fredrik	ROV Motion Control Systems, IMT
IMT-11-2014	Grimsmo, Nils I.	Dynamic simulations of hydraulic cylinder for heave compensation of deep water drilling risers, IMT
IMT-12-2014	Kvittem, Marit I.	Modelling and response analysis for fatigue design of a semisubmersible wind turbine, CeSOS
IMT-13-2014	Akhtar, Juned	The Effects of Human Fatigue on Risk at Sea, IMT
IMT-14-2014	Syahroni, Nur	Fatigue Assessment of Welded Joints Taking into Account Effects of Residual Stress, IMT
IMT-1-2015	Bøckmann, Eirik	Wave Propulsion of ships, IMT
IMT-2-2015	Wang, Kai	Modelling and dynamic analysis of a semi-submersible floating vertical axis wind turbine, CeSOS
IMT-3-2015	Fredriksen, Arnt Gunvald	A numerical and experimental study of a two-dimensional body with moonpool in waves and current, CeSOS
IMT-4-2015	Jose Patricio Gallardo Canabes	Numerical studies of viscous flow around bluff bodies, IMT
IMT-5-2015	Vegard Longva	Formulation and application of finite element techniques for slender marine structures subjected to contact interactions, IMT
IMT-6-2015	Jacobus De Vaal	Aerodynamic modelling of floating wind turbines, CeSOS
IMT-7-2015	Fachri Nasution	Fatigue Performance of Copper Power Conductors, IMT
IMT-8-2015	Oleh I Karpa	Development of bivariate extreme value distributions for applications in marine technology,CeSOS
IMT-9-2015	Daniel de Almeida Fernandes	An output feedback motion control system for ROVs, AMOS
IMT-10-2015	Bo Zhao	Particle Filter for Fault Diagnosis: Application to Dynamic Positioning Vessel and Underwater Robotics, CeSOS
IMT-11-2015	Wenting Zhu	Impact of emission allocation in maritime transportation, IMT
IMT-12-2015	Amir Rasekhi Nejad	Dynamic Analysis and Design of Gearboxes in Offshore Wind Turbines in a Structural Reliability Perspective, CeSOS
IMT-13-2015	Arturo Jesùs Ortega Malca	Dynamic Response of Flexibles Risers due to Unsteady Slug Flow, CeSOS

IMT-14-2015	Dagfinn Husjord	Guidance and decision-support system for safe navigation of ships operating in close proximity, IMT
IMT-15-2015	Anirban Bhattacharyya	Ducted Propellers: Behaviour in Waves and Scale Effects, IMT
IMT-16-2015	Qin Zhang	Image Processing for Ice Parameter Identification in Ice Management, IMT
IMT-1-2016	Vincentius Rumawas	Human Factors in Ship Design and Operation: An Experiential Learning, IMT
IMT-2-2016	Martin Storheim	Structural response in ship-platform and ship-ice collisions, IMT
IMT-3-2016	Mia Abrahamsen Prsic	Numerical Simulations of the Flow around single and Tandem Circular Cylinders Close to a Plane Wall, IMT
IMT-4-2016	Tufan Arslan	Large-eddy simulations of cross-flow around ship sections, IMT
IMT-5-2016	Pierre Yves-Henry	Parametrisation of aquatic vegetation in hydraulic and coastal research,IMT
IMT-6-2016	Lin Li	Dynamic Analysis of the Instalation of Monopiles for Offshore Wind Turbines, CeSOS
IMT-7-2016	Øivind Kåre Kjerstad	Dynamic Positioning of Marine Vessels in Ice, IMT
IMT-8-2016	Xiaopeng Wu	Numerical Analysis of Anchor Handling and Fish Trawling Operations in a Safety Perspective, CeSOS
IMT-9-2016	Zhengshun Cheng	Integrated Dynamic Analysis of Floating Vertical Axis Wind Turbines, CeSOS
IMT-10-2016	Ling Wan	Experimental and Numerical Study of a Combined Offshore Wind and Wave Energy Converter Concept
IMT-11-2016	Wei Chai	Stochastic dynamic analysis and reliability evaluation of the roll motion for ships in random seas, CeSOS
IMT-12-2016	Øyvind Selnes Patricksson	Decision support for conceptual ship design with focus on a changing life cycle and future uncertainty, IMT
IMT-13-2016	Mats Jørgen Thorsen	Time domain analysis of vortex-induced vibrations, IMT
IMT-14-2016	Edgar McGuinness	Safety in the Norwegian Fishing Fleet – Analysis and measures for improvement, IMT
IMT-15-2016	Sepideh Jafarzadeh	Energy effiency and emission abatement in the fishing fleet, IMT
IMT-16-2016	Wilson Ivan Guachamin Acero	Assessment of marine operations for offshore wind turbine installation with emphasis on response-based operational limits, IMT
IMT-17-2016	Mauro Candeloro	Tools and Methods for Autonomous Operations on Seabed and Water Coumn using Underwater Vehicles, IMT
IMT-18-2016	Valentin Chabaud	Real-Time Hybrid Model Testing of Floating Wind Tubines, IMT
IMT-1-2017	Mohammad Saud Afzal	Three-dimensional streaming in a sea bed boundary layer
IMT-2-2017	Peng Li	A Theoretical and Experimental Study of Wave-induced Hydroelastic Response of a Circular Floating Collar
IMT-3-2017	Martin Bergström	A simulation-based design method for arctic maritime transport systems
IMT-4-2017	Bhushan Taskar	The effect of waves on marine propellers and propulsion

IMT-5-2017	Mohsen Bardestani	A two-dimensional numerical and experimental study of a floater with net and sinker tube in waves and current
IMT-6-2017	Fatemeh Hoseini Dadmarzi	Direct Numerical Simualtion of turbulent wakes behind different plate configurations
IMT-7-2017	Michel R. Miyazaki	Modeling and control of hybrid marine power plants
IMT-8-2017	Giri Rajasekhar Gunnu	Safety and effiency enhancement of anchor handling operations with particular emphasis on the stability of anchor handling vessels
IMT-9-2017	Kevin Koosup Yum	Transient Performance and Emissions of a Turbocharged Diesel Engine for Marine Power Plants
IMT-10-2017	Zhaolong Yu	Hydrodynamic and structural aspects of ship collisions
IMT-11-2017	Martin Hassel	Risk Analysis and Modelling of Allisions between Passing Vessels and Offshore Installations
IMT-12-2017	Astrid H. Brodtkorb	Hybrid Control of Marine Vessels – Dynamic Positioning in Varying Conditions
IMT-13-2017	Kjersti Bruserud	Simultaneous stochastic model of waves and current for prediction of structural design loads
IMT-14-2017	Finn-Idar Grøtta Giske	Long-Term Extreme Response Analysis of Marine Structures Using Inverse Reliability Methods
IMT-15-2017	Stian Skjong	Modeling and Simulation of Maritime Systems and Operations for Virtual Prototyping using co-Simulations
IMT-1-2018	Yingguang Chu	Virtual Prototyping for Marine Crane Design and Operations
IMT-2-2018	Sergey Gavrilin	Validation of ship manoeuvring simulation models
IMT-3-2018	Jeevith Hegde	Tools and methods to manage risk in autonomous subsea inspection,maintenance and repair operations
IMT-4-2018	Ida M. Strand	Sea Loads on Closed Flexible Fish Cages
IMT-5-2018	Erlend Kvinge Jørgensen	Navigation and Control of Underwater Robotic Vehicles
IMT-6-2018	Bård Stovner	Aided Intertial Navigation of Underwater Vehicles
IMT-7-2018	Erlend Liavåg Grotle	Thermodynamic Response Enhanced by Sloshing in Marine LNG Fuel Tanks
IMT-8-2018	Børge Rokseth	Safety and Verification of Advanced Maritime Vessels
IMT-9-2018	Jan Vidar Ulveseter	Advances in Semi-Empirical Time Domain Modelling of Vortex-Induced Vibrations
IMT-10-2018	Chenyu Luan	Design and analysis for a steel braceless semi-submersible hull for supporting a 5-MW horizontal axis wind turbine
IMT-11-2018	Carl Fredrik Rehn	Ship Design under Uncertainty
IMT-12-2018	Øyvind Ødegård	Towards Autonomous Operations and Systems in Marine Archaeology
IMT-13- 2018	Stein Melvær Nornes	Guidance and Control of Marine Robotics for Ocean Mapping and Monitoring
IMT-14-2018	Petter Norgren	Autonomous Underwater Vehicles in Arctic Marine Operations: Arctic marine research and ice monitoring
IMT-15-2018	Minjoo Choi	Modular Adaptable Ship Design for Handling Uncertainty in the Future Operating Context
MT-16-2018	Ole Alexander Eidsvik	Dynamics of Remotely Operated Underwater Vehicle Systems

IMT-17-2018	Mahdi Ghane	Fault Diagnosis of Floating Wind Turbine Drivetrain-Methodologies and Applications
IMT-18-2018	Christoph Alexander Thieme	Risk Analysis and Modelling of Autonomous Marine Systems
IMT-19-2018	Yugao Shen	Operational limits for floating-collar fish farms in waves and current, without and with well-boat presence
IMT-20-2018	Tianjiao Dai	Investigations of Shear Interaction and Stresses in Flexible Pipes and Umbilicals
IMT-21-2018	Sigurd Solheim Pettersen	Resilience by Latent Capabilities in Marine Systems
IMT-22-2018	Thomas Sauder	Fidelity of Cyber-physical Empirical Methods. Application to the Active Truncation of Slender Marine Structures
IMT-23-2018	Jan-Tore Horn	Statistical and Modelling Uncertainties in the Design of Offshore Wind Turbines
IMT-24-2018	Anna Swider	Data Mining Methods for the Analysis of Power Systems of Vessels
IMT-1-2019	Zhao He	Hydrodynamic study of a moored fish farming cage with fish influence
IMT-2-2019	Isar Ghamari	Numerical and Experimental Study on the Ship Parametric Roll Resonance and the Effect of Anti-Roll Tank
IMT-3-2019	Håkon Strandenes	Turbulent Flow Simulations at Higher Reynolds Numbers
IMT-4-2019	Siri Mariane Holen	Safety in Norwegian Fish Farming – Concepts and Methods for Improvement
IMT-5-2019	Ping Fu	Reliability Analysis of Wake-Induced Riser Collision
IMT-6-2019	Vladimir Krivopolianskii	Experimental Investigation of Injection and Combustion Processes in Marine Gas Engines using Constant Volume Rig
IMT-7-2019	Anna Maria Kozlowska	Hydrodynamic Loads on Marine Propellers Subject to Ventilation and out of Water Condition.
IMT-8-2019	Hans-Martin Heyn	Motion Sensing on Vessels Operating in Sea Ice: A Local Ice Monitoring System for Transit and Stationkeeping Operations under the Influence of Sea Ice
IMT-9-2019	Stefan Vilsen	Method for Real-Time Hybrid Model Testing of Ocean Structures – Case on Slender Marine Systems
IMT-10-2019	Finn-Christian W. Hanssen	Non-Linear Wave-Body Interaction in Severe Waves
IMT-11-2019	Trygve Fossum	Adaptive Sampling for Marine Robotics
IMT-12-2019	Jørgen Bremnes Nielsen	Modeling and Simulation for Design Evaluation
IMT-13-2019	Yuna Zhao	Numerical modelling and dyncamic analysis of offshore wind turbine blade installation
IMT-14-2019	Daniela Myland	Experimental and Theoretical Investigations on the Ship Resistance in Level Ice